TOG Proteins: Essential +TIPs Regulators of Interphase Microtubule Dynamics

Joshua D. Currie

A dissertation submitted to the faculty of the University of North Carolina at Chapel Hill in partial fulfillment of the requirements for the degree of Doctor of Philosophy in the Department of Biology.

Chapel Hill
2011

Approved by:

Stephen Rogers

Kevin Slep

Jim Bear

Mark Peifer

Victoria Bautch

ABSTRACT

Joshua D Currie: TOG Proteins: Essential +TIP Regulators of Interphase Microtubule Dynamics
(Under the direction of Dr. Stephen L. Rogers)

Microtubules exhibit a signature behavior, termed dynamic instability, in which individual microtubules cycle between phases of growth and shrinkage while the total microtubule polymer remains constant. These dynamics are promoted by the conserved XMAP215/Dis1 family of microtubule-associated proteins (MAPs). During my thesis I have conducted an *in vivo* structure-function analysis of the *Drosophila* homologue, Mini spindles (Msps). Msps exhibits EB1-dependent and spatially regulated localization to microtubules, localizing to microtubule plus ends in the cell interior and decorating the lattice of growing and shrinking microtubules in the cell periphery. RNAi rescue experiments revealed that Msps' NH_2-terminal four TOG domains were sufficient to partially restore microtubule dynamics and promote EB1 comet formation and that TOG domains function as paired units. We also identified TOG5 and novel inter-TOG linker motifs that are sufficient for binding to the microtubule lattice. These novel microtubule contact sites are necessary for Msps peripheral lattice association and allow Msps to regulate dynamic instability. Additionally, I have been able to determine the region of Msps that is responsible for plus end tracking in cells. This occurs through a novel interaction with the EB1-binding protein, Sentin, that enhances

Msps accumulation at the plus end and affects the velocity and lifetime of plus end growth. From these results we have learned that Msps is an important microtubule regulator that controls multiple parts of dynamic instability through its unique domain structure.

TABLE OF CONTENTS

LIST OF TABLES

LIST OF FIGURES

Chapter 1

INTRODUCTION

Summary

Microtubules are a dynamic cytoskeleton that is essential for intracellular traffic, cell migration, and chromosome segregation. The dynamic nature of microtubules is regulated in cells by a diverse group of proteins called plus end proteins or +TIPs. It is the function and interplay between these +TIPs that produces the the normal dynamic instability found in vivo. In this chapter, I will outline our current understanding of microtubule dynamics in cells and how this is thought to be regulated by +TIPs. I will briefly introduce the major families of +TIP proteins and how they interact in interphase to regulate microtubule dynamics. Finally, I will examine the role for +TIPs in cell migration using a novel *Drosophila* cell line called D17.

The Dynamic Microtubule Cytoskeleton

Microtubules are polymers that form a network of cellular tracks necessary for intracellular transport, cell signaling, chromosome segregation, and establishing and reinforcing specific sub-cellular compartments of protein activity.

The vital property that enables microtubules to participate in all these functions is their dynamic nature. Far from being static paths connecting regions

of the cell, microtubules are able to rapidly switch between phases of growth and shrinkage. This allows them to probe the cellular environment for vesicular cargo, contact sites of cortical signaling that require the delivery of key regulatory factors, or capture sister chromatids at the kinetochore during mitosis, in a process aptly termed microtubule “search and capture” (for review see Odde, 2005). The stochastic switching in microtubule behavior between phases of polymerization, depolymerization, and pause has been termed dynamic instability (Mitchison and Kirschner, 1984).

The rapid assembly and disassembly of microtubules is an inherent characteristic of the polymer that is based on the properties of the tubulin monomer. Tubulin exists as an obligate heterodimer of α and β tubulin. Both subunits have similar structures and bind soluble GTP (Caplow and Reid, 1985), but it is the hydrolysis of GTP to GDP by the β subunit that alters the ability of the tubulin heterodimer to incorporate into microtubules (Weisenberg et al., 1976). Tubulin monomers are added onto microtubules in a head to tail fashion with α tubulin making connections with a previously added β subunit (Amos and Klug, 1974), so that GTP-bound β tubulin is at the distal end of the filament (Figure 1). Strands of tubulin in end-to-end connections, termed protofilaments, also form lateral interactions with other protofilaments to form the characteristic tube of 13 protofilaments (Mandelkow and Mandelkow, 1985). This polarity of tubulin heterodimer addition is also translated into the polymerized microtubule, where addition and subtraction happens preferentially at one end (Allen and Borisy,

1974), termed the plus end, while the other minus end is stable and often anchored at the microtubule organizing center (MTOC) in animal cells.

It is the process of β tubulin GTP hydrolysis that is thought to signal a switch from polymerization to depolymerization. Shortly after incorporation, GTP is hydrolyzed and is thought to change the conformation of the tubulin heterodimer from a “straight” conformation that facilitates lateral interactions between subunits to that of a “kinked” conformation that disrupts lateral interactions between adjacent molecules (Krebs et al., 2005). Polymerization is thought to persist based on the existence of a cap of GTP bound monomers that maintain strong lateral interactions among protofilaments at the growing plus end (Caplow and Shanks, 1996) (Figure 1).

The predominant dogma is that polymerization happens through the addition of heterodimers onto individual protofilaments that elongate together as a sheet and fold into a tubule structure with a seam. Loss of the GTP cap through rapid GTP hydrolysis or a lag in the incorporation of new GTP monomers causes depolymerization by the peeling of “kinked” GDP-bound protofilaments off the microtubule plus end in a “rams head” structure (Zovko et al., 2008). A third, paused microtubule structure is thought to exist where a meta-stable, uniform GTP cap prevents the addition or subtraction of monomers from the microtubule plus end (Tran et al., 1997; Shelden and Wadsworth, 1993)(Figure 1). Although microtubules can clearly be seen to cycle through stages of growth, shrinkage, or pause, it is not clear how a microtubule might transition between these distinct structural states, and it is not known if the paused state exists as an obligate

intermediate structure that microtubules must transition through to progress from growth to shrinkage, termed catastrophe, or from shrinkage toward growth, know as rescue.

Regulation of Microtubule Dynamics by Microtubule Associated Proteins

The intrinsic dynamic instability of microtubules can be observed in the presence of purified tubulin heterodimers below a critical concentration of approximately 15μM and the presence of excess GTP (Mitchison and Kirschner, 1984). Although this in vitro setting can recapitulate many of the behaviors of microtubules in vivo, the rates of transition as well as the rates of growth or shrinkage in-vivo are much higher than what can be reproduced using purified tubulin. This discrepancy between the kinetics of dynamic instability in vitro versus in vivo is due to a diverse set of molecules known as Microtubule Associated Proteins (MAPs). In general, these molecules can be subdivided into three general classes of molecules based on their interactions with tubulin. Classical or neuronal MAPs such as Tau (for review see Nunez and Fischer, 1997) were some of the first MAPs discovered, due to their enrichment in brain tissue, the source of most experimentally purified tubulin. These molecules bind exclusively to the lateral sidewall of the microtubule and increase growth by stabilizing and protecting microtubules from disassembly. Second, molecular motors such as Kinesin family motors and dynein carry out most of the transport roles of microtubules by processively moving across the length of microtubules while tethered to cargo (Gennerich and Vale, 2009). Finally, plus end proteins, or

+TIPs, are a class of MAPs that specifically recognize and bind to the plus end of microtubules to regulate dynamic instability and connect

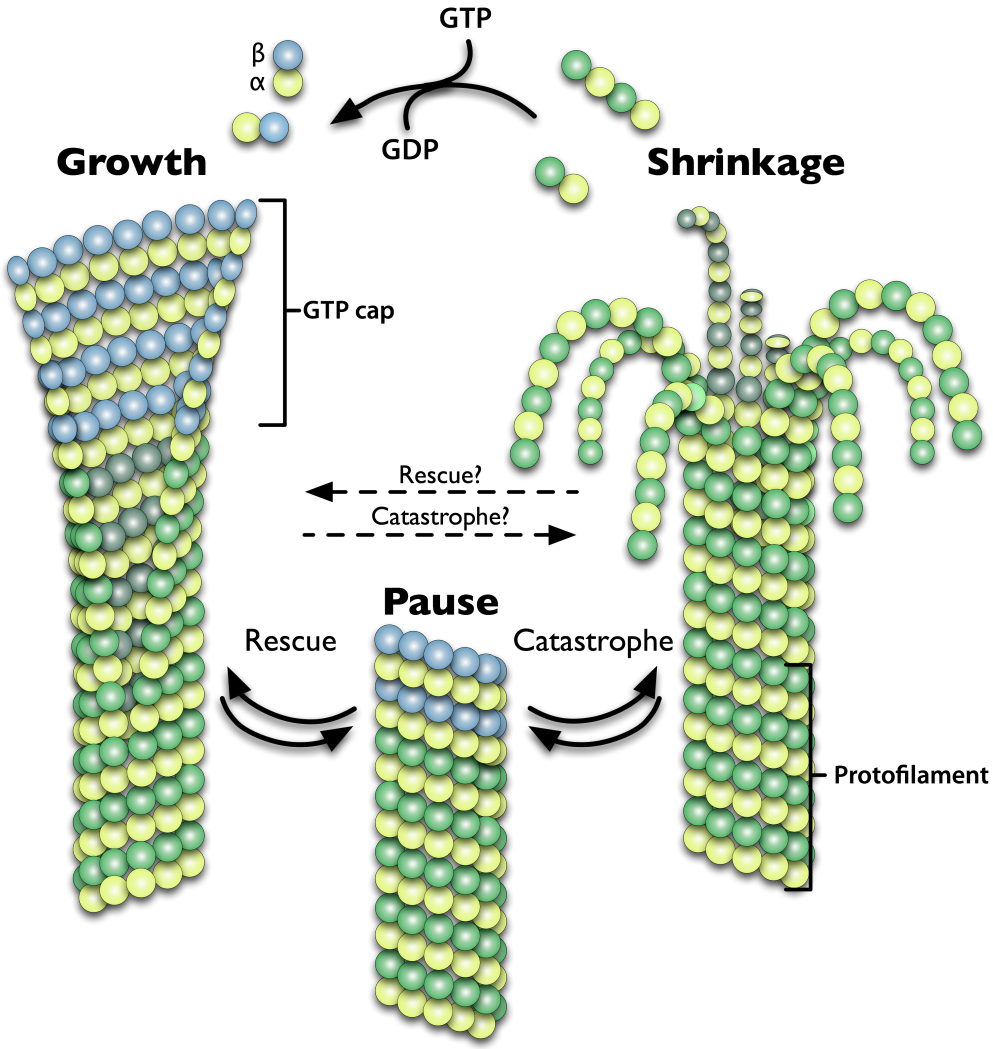

Figure 1. Microtubules Are A Dynamic Polymer Network.

Cartoon schematic of the three states of microtubule dynamic instability. Growth (left) represents the addition of GTP-loaded tubulin heterodimers (represented by blue β-tubulin) forming a protective GTP cap that is predicted to built from a sheet that closes into the characteristic 13 protofilament tube. Shrinkage (right) is the loss of "curved" GDP-bound subunits in a curling "rams head" structure. A protofilament is illustrated (bottom right) as the head-to-tail arrangement of

tubulin heterodimers that form lateral interactions to become a microtubule. The paused state (middle) represent a stable microtubule configuration where there is a stable GTP cap that prevents the addition or loss of subunits. It is thought that microtubules transition through the pause state from growth to shrinkage (termed catastrophe) or from shrinkage to growth (termed rescue).

microtubule ends with relevant cellular sites (Akhmanova and Steinmetz, 2008). +TIPs play a key role in enhancing and regulating microtubule dynamic instability and will be the focus of the rest of this manuscript.

Plus end Proteins (+TIPs)

+TIPs represent an expanding and diverse family of proteins that are loosely categorized by their accumulation at microtubule plus ends. Although often studied in isolation, it has become increasing clear that +TIPs exist in complex milieu of hierarchical interactions. This is also confounded by the fact that many interacting +TIPs produce opposing phenotypes when depleted from cells (Laycock et al., 2006). How seemingly antagonistic +TIPs exist and interact on the common interface of the microtubule plus end to regulate microtubule dynamics is one of the key questions left unanswered. I will now briefly discuss the various classes of +TIPs (Figure 2) that directly regulate microtubule dynamics and how they contribute to the unique hierarchy of plus end protein structure.

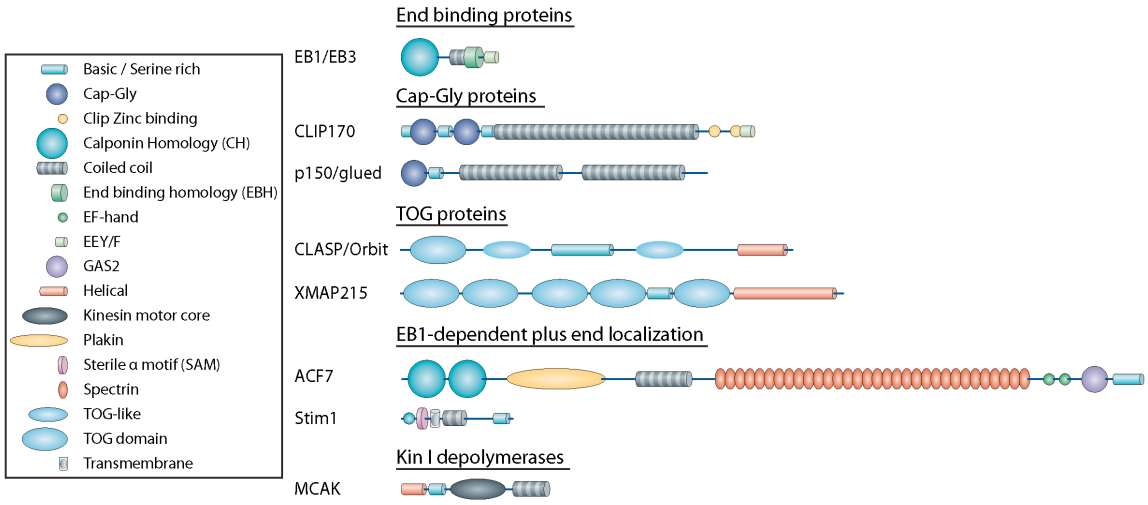

Figure 2. +TIP Families and Their Domain Structure.

Adapted from (Akhmanova and Steinmetz, 2008), this diagram represents the major +TIP families such as the End Binding proteins, Cap-Gly proteins, TOG proteins, +TIPs with MAP or non-MAP function that have EB1-dependent plus end localization, and the Kin I family of microtubule depolymerases. Coil-coil motifs represent known dimerization domains in the case of EB proteins, Cap-Gly proteins, and Kin I motors.

End Binding (EB) Proteins

EB1 and other End Binding family members represent the core plus end protein conserved in all eukaryotic cells. All species possess at least one family member (Akhmanova and Hoogenraad, 2005), and in animals there is a ubiquitous isoform, commonly EB1 or EB3, and several tissue specific isoforms (Komarova et al., 2005). EB1 is thought to form the nucleus of the +TIP protein complex (Akhmanova and Steinmetz, 2008; Vaughan, 2005). Nearly all +TIPs have either a direct or indirect interaction with EB1, and this interaction may represent the primary plus end localization signal for other +TIPs.

EB1 was first isolated as a binding partner for the tumor suppressor Adenamatous Polyposis Coli (APC) (Su et al., 1995). Immunofluorescence of EB1 revealed colocalization at the distal ends of microtubules (Morrison et al., 1998), the first observation of a protein accumulating at plus ends. Since that time, there has been an ever-expanding array of EB1 interacting proteins. These can be generally subdivided between EB1-binding MAPs that utilize other domains to bind tubulin and/or microtubules to regulate microtubule dynamics, and EB1-binding proteins such as RhoGEF2 (Rogers et al., 2004b), which harness tip tracking on plus ends in order to dynamically alter other aspects of cellular behavior. EB1, on the other hand, seems to be one of the few, bonafide plus end proteins that can localize to the plus end in vitro in the absence of any other factors (Bieling et al., 2007).

This highlights a key question: How do +TIPs such as EB1 recognize the plus end? While the exact mechanism remains a mystery several models have arisen to explain the preference for the plus end by +TIPs such as EB1. One model postulates that EB1 recognizes a unique structure at the edges of the plus end sheet and facilitates its closure into a tube. This is based on *in vitro* evidence by cryo-electron microscopy that EB1 was preferentially localized to the microtubule seam where presumably protofilaments converge to close the microtubule (Vitre et al., 2008). This is also consistent with the types of microtubules that form in the presence of EB1. In vitro polymerized microtubules often deviate from the normal 13 protofilament structures found in cells, with tubes containing anywhere from 13-16 protofilaments. Under the same conditions, the addition of EB1 promotes the assembly of 13 protofilament-microtubules with a decrease in the number of higher protofilament tubes (Vitre et al., 2008). Another more prevalent model is that EB1 recognizes a specific conformation of GTP-bound tubulin that specifically labels the plus end.

A recent in vitro study using specific GTP analogs that slow or prevent hydrolysis, thus locking tubulin in a GTP-bound state, revealed that EB1 would then bind the entire length of the polymerized microtubule (Maurer et al., 2011). This was true for GTP analogues such as GTPγS that modify the third or γ-phosphate of GTP. Modification of the β-phosphate using GMPCPP did not lead to any association of EB1 with the microtubule lattice. This suggests that EB1 may recognize not only the unique straight conformation of GTP-tubulin, but may also sense the nucleotide state of tubulin between GTP, GDP-Pi, and GDP-

bound forms. This recognition of tubulin seems to be specific to incorporated tubulin, as EB1 exhibits relatively low affinity for soluble tubulin (Slep and Vale, 2007; Niethammer et al., 2007).

EB1 consists of three domains: a microtubule-binding calponin homology domain, a dimerization domain, and a COOH-terminal interaction domain. EB1's calponin homology (CH) domain represents a divergent line of CH domains also present in other MAPs such as Ndc80 (Wei et al., 2007). They differ from the classically defined CH structures that bind actin when present in pairs (Hayashi and Ikura, 2003). The interaction domain has a terminal EEY motif that mimics the final residues of tubulin's C-terminal E-hooks (also EEY) (Honnappa et al., 2006). These motifs seem to represent a mode for many MAPs to recognize and bind tubulin (Steinmetz and Akhmanova, 2008). Crystal structure complexes of EB1 with +TIPs CLIP170 and p150/Glued demonstrate a conserved mechanism for both binding EB1 and tubulin at these C-terminal regions through interaction with their Cap-Gly domains (more below). A similar ETF motif at the C-terminal end of CLIP170 causes a competitive auto-inhibition in cis and a trans inhibition of the p150 Cap-Gly domain (Hayashi et al., 2007). Posttranslational modification of tubulin can regulate MAP affinities by the cyclic removal and addition of the final tyrosine by tubulin carboxypeptidase and tubulin tyrosine ligase, respectively (Peris et al., 2006). MAP binding to tubulin's E-hooks can also be assayed experimentally in vitro using the protease subtilisin, which selectively removes the E-hooks (Rodionov et al., 1990). It is not yet clear if any of these same

modifications are made in vivo to EB family proteins and if it can affect their function and interaction with other +TIPs.

The majority of EB1's interactions with other +TIPs occur through a recently characterized "SKIP" motif that binds to EB1's dimerization domain (Slep et al., 2005, Honnappa et al., 2009). The inclusion of this motif is sufficient to target proteins to the plus end, and it is found in a wide range of proteins that possess additional microtubule association domains (e.g. CLIP170, CLASP) as well as proteins with no characterized microtubule regulatory function (e.g. RhoGEF2, STIM1). EB1 association via SKIP motifs even exists within +TIPs that antagonize microtubule growth, as in the depolymerizing kinesin 13 member MCAK (Honnappa et al., 2009). It seems that this SKIP motif is a general microtubule plus end localization signal that is a characteristic of almost every +TIP identified to date.

The lynchpin characteristic of EB1 at the center of +TIP hierarchy somewhat confounds systematic investigation of its affect on microtubule dynamics in cells. Because of EB1 can accumulate at microtubule plus ends, in vitro reconstitution seemed to be a excellent reductionist system to study purified tubulin and EB proteins (Bieling et al., 2007). Despite several in vitro studies, no consensus has emerged that completely correlates with the in vivo evidence for EB1's affect on microtubules. In vitro, EB1 consistently increases the rate of microtubule growth (Komarova et al., 2009, Vitre et al., 2008, Bieling et al., 2007). In some in vitro studies, EB1 suppresses catastrophes and promotes rescue, while in other in vitro settings EB proteins increase both catastrophe and

rescue (Komarova et al., 2009, Vitre et al., 2008). The latter agrees the most with in vivo examination of EB proteins. In *Drosophila* S2 cells, depletion of EB1 by RNAi lowers the frequencies of both catastrophe and rescue and results in paused, non-dynamic microtubules (Rogers, 2002). In mammalian cells, depletion of EB proteins results in a loss of persistent microtubule growth and a large increase in catastrophe frequency that is not mediated through EB1's SKIP interacting C-terminal tail (Komarova et al., 2009). Overall, it seems that EB proteins are responsible for promoting growth through their CH domains as well as through interactions with other +TIP binding partners. Whether independently or through interactions with other +TIPs, EB proteins exert an important role in enhancing the normal dynamic instability of microtubules.

Cytoplasmic Linker Proteins (CLIPs)

Cytoplasmic Linker Protein (CLIP170) was first isolated from Hela cells as a MAP essential for coupling endocytic vesicles to microtubules in vitro (Pierre et al., 1992). In the first observation of realtime tip tracking, GFP-CLIP170 labeled the growing ends of microtubules and presented an unprecedented view of microtubule dynamics at the growing end (Perez et al., 1999). Upon cloning the gene, it became clear that it was a part of a conserved family of proteins with multiple isoforms across several taxa. It shared homology in its principle microtubule binding domain with other MAPs like *Drosophila* p150/glued as well as tubulin chaperones (Pierre et al., 1992). Molecular examination of CLIP170's domain structure revealed two N-terminal Cytoskeletal Associate Protein Glycine

Rich (CAP-Gly) domains necessary for binding both EB1 and tubulin's EEY terminus (Steinmetz and Akhmanova, 2008), a serine rich microtubule-lattice binding domain, a homo-dimerizing coil-coil, a zinc-binding regulatory domain, and a C-terminal ETF motif. As mentioned previously, CLIP170, but not the shorter CLIP115 isoform, exhibits a head to tail auto-inhibition by binding of the CAP-Gly domains to the zinc binding domain and ETF motif at the C-terminus (Lansbergen et al., 2004) (Hayashi et al., 2007). It is the CAP-Gly domains that bind tubulin and EB1 and target CLIPs to the plus end (Dixit et al., 2009) (Wittmann, 2008), but the serine-rich domain also seems essential for plus end localization. It is likely that it mediates some form of microtubule lattice diffusion (Hoogenraad et al., 2000). The N-terminal CAP-Gly domains and serine-rich domains also have potent microtubule polymerization-stimulating abilities in bulk in vitro assays (Gupta et al., 2010).

CLIP family proteins display two main functions in regulating interphase microtubule function. As microtubule-vesicle linkers, CLIPs act to efficiently allow microtubule plus ends to "search and capture" endocytic vesicles (Pierre et al., 1992, Lomakin et al., 2009); how exactly they couple cargo microtubule attachment to minus end-directed motor movement is currently unknown. This coupling of capture to minus end movement is most likely linked to CLIP's shared domain structure and association with p150/glued and the dynein/dynactin complex (Coquelle et al., 2002, Lansbergen et al., 2004). CLIP proteins also exert a stabilizing effect on microtubule dynamics. In cells, loss of CLIP170 leads to an increase in catastrophe frequency and a destabilization of microtubules at

the cell's leading edge (Komarova et al., 2002). It is not entirely clear if this is due to the activity of CLIP170 or its ability to recruit CLASPs to the plus end (see below). It seems likely that the multimerization of CAP-Gly domains and a serine rich region allow CLIPs themselves to exert affects on microtubule dynamics. This question has not been definitively answered in vitro to determine the mechanism of CLIP170's affect on dynamic instability.

Cytoplasmic Linker Associated Proteins (CLASPs)

Using either CLIP115 or CLIP170 as bait in a yeast two hybrid screen of embryonic mouse cDNA, Ana Akhmanova and colleagues identified two related protein that bound to a portion of the CLIP coil-coil region (Akhmanova et al., 2001). These novel MAPs were aptly named CLIP associated protein or CLASP1 and CLASP2. They were related to a previously characterized *Drosophila* gene, Chromosome bows/Mast/Orbit, mutation of which had a variety of deleterious effects on the formation of the mitotic spindles during syncytial blastula divisions and later embryogenesis (Inoue et al., 2000, Lemos et al., 2000). In mammalian cells, depletion of CLASP1 and 2 destabilized microtubules that had oriented at the leading edge of migrating fibroblasts (Akhmanova et al., 2001). Without stabilized microtubules to reinforce a polarized front and rear, CLASP2 knockout cells were unable to maintain a persistent direction of cell migration, although the distance cells migrated was unchanged (Drabek et al., 2006).

CLASP1 and CLASP2 are similar in structure and have redundant functions; often represented as a single gene in lower eukaryotes (Yin et al.,

2002, Al-Bassam et al., 2010). At their N-terminus, CLASPs have a series of three domains designated as TOG(1) and TOG-like(2) domains (Slep, 2009). TOG domains bind tubulin (Slep and Vale, 2007) and were first characterized in another family of +TIPs, the Dis1/XMAP215 family of proteins (see below). Between the first and second TOG-like (TOGL) domain is a serine and threonine-rich region that acts as a high affinity microtubule association domain (Wittmann and Waterman-Storer, 2005). Within this region is an EB1-binding “SKIP” motif (Mimori-Kiyosue et al., 2005). Finally, at the extreme C-terminus of the protein is the CLIP interaction domain. Although all of these domains have been elucidated and functionally tested separately, we have little knowledge about how these domains interact to affect CLASP function within the +TIP hierarchy. In mammalian fibroblasts, CLASP localizes at the plus end of leading edge microtubules, where it is associated with a stable, cortical complex of proteins including the microtubule/actin crosslinker MACF7/Shortstop, the posphatidylinositol (3,4,5)-binding (PIP3) protein LL5β, and the scaffolding protein ELKS (Lansbergen et al., 2006). These membrane bound cortical patches appear to be important in anchoring microtubules and preventing their catastrophe away from the leading edge. Additionally, cortical patches often localize near cortical actin and focal adhesions, but do not overlap perfectly. One complication is that cortical patches appear to be cell type specific, as they were observed in Swiss 3T3 fibroblasts and Hela cells, but not epithelial COS7 cells.

The leading edge of a polarized culture cell has discrete zones of actin assembly and remodeling that are established by activation of Rho family

GTPases. Activation of the small GTPase Rac initiates dendritic actin assembly within an outermost three micrometer zone termed the lamellipodia (Hall, 2005). This actin array treadmills rearward, in a process termed retrograde flow, into the lamella sub-compartment where it is disassembled and recycled or remodeled into longer, unbranched filaments that are incorporated into stress fibers. The action of retrograde flow actively opposes the movement of microtubules into the cell periphery, leaving a relative few “pioneer” microtubules able to penetrate to the cell cortex (Waterman-Storer and Salmon, 1997). Although Rac activation increases the forces opposing cortical microtubule growth, Rac activity also positively promotes microtubule growth into the lamella/lamellipodia. This occurs through several means, although all of the molecular mechanisms have yet to be elucidated. One such mechanism is where p21 activated kinase (Pak) downstream of Rac promotes microtubule growth into the lamella/lamellipodia. This net growth in pioneer microtubules could be due in part to both an activation of growth promoting factors and inactivation of microtubule depolymerization factors. Op18/stathmin is a cytosolic tubulin-sequestering phosphoprotein that induces microtubule catastrophe by lowering the available pool of monomers competent to incorporate into protofilaments. Phosphorylation downstream of Rac/Pak, specifically within the lamella/lamellipodia, inactivates Op18/stathmin and frees tubulin monomers, raising the concentration of available tubulin (Wittmann et al., 2004). Finally, modulation of CLASP’s domains downstream of Rac activation results in a preferential stabilization of pioneer microtubules (Wittmann and Waterman-Storer, 2005). In epithelial cells such as Ptk1 cells,

CLASP exhibits a bimodal localization pattern. In the cell body, CLASP labels the plus end of microtubules similar to EB1. In the lamella and lamellipodia, however, CLASP localizes along the length of the microtubule. As mentioned previously, CLASP possesses a serine-threonine rich microtubule lattice-binding domain that overlaps with its EB1 binding SKIP motif. The serine and threonines within this domain include nine phosphorylation motifs for glycogen synthase kinase 3 (GSK3) (Kumar et al., 2009). GSK3β remains active within the cell body and its phosphorylation of CLASP negatively regulates the tip tracking domain. It is the degree of phosphorylation along the stretch of serines that determines either localization: cytosolic in the case of full phosphorylation, plus end tracking when partially phosphorylated, or lamella microtubule lattice- binding when partially phosphorylated, or lamella microtubule binding when completely unphosphorylated. In the lamella, GSK3 is inactivated by Akt phosphorylation downstream of activated PI3K at the leading edge (Wittmann and Waterman-Storer, 2005). This leads to the rapid dephosphorylation of CLASP and lamella association that stabilizes lamella microtubules as they polymerize into the cell periphery. For now, this observation seems limited to certain epithelial cell types, but may reflect a broad regulation of CLASPs that is not as easily discernible in cell types without large lamella which more readily compartmentalize the complex signaling involved. Interestingly, in these same epithelial cells, there is no accumulation of CLASP in cortical patches as observed in fibroblasts, but both pathways accomplish similar affects on microtubules downstream of PIP3 production at the leading edge. This could represent convergent pathways based

on either signaling gradients or cell type specific binding partners to modulate CLASP activity in the periphery to stabilize microtubules.

Dis1/XMAP215 TOG Proteins

The first representative of one of the most highly conserved +TIP families was *Xenopus* XMAP215. It was the first +TIP identified, isolated from a fraction of mitotic extract, this protein accelerated the polymerization of microtubules in vitro by ten fold (Gard and Kirschner, 1987). Because of its effects on microtubules, it appeared that unlike previously described MAPs, XMAP215 acted at the plus end to increase polymerization. Additionally, unlike conventional MAPs such as Tau which promotes growth through microtubule stabilization, XMAP215 not only stimulated microtubule growth, but microtubules were also more dynamic, prone to switch between rapid disassembly and rescue at their plus ends. Shortly thereafter, similar proteins were described in budding and fission yeast, Stu2p and Dis1, respectively (Wang and Huffaker, 1997, Nabeshima et al., 1995). Analysis of secondary structure revealed a common iteration of six helical pairs in an arrangement related to known Armadillo repeats. These domains were named Tumor Overexpressed Gene domains, or TOG domains, after a homologous human protein found to be elevated in colonic and hepatic cancers (Charrasse et al., 1995, Charrasse et al., 1998). These roughly 200 amino acid TOG domains are a hallmark of Dis1/XMAP215 family members and have been used to the identify family members in all species examined thus far (Gard et al., 2004). With the exception of fission yeast which possess two related TOG

proteins, Dis1 and Alp14 (Garcia, 2001), all other species seem to possess only one XMAP215 homolog (Kinoshita et al., 2002). While other proteins also possess TOG domains (e.g. CLASP family members), there is little redundancy in their functions as a core regulators of microtubule dynamics. Dis1/XMAP215 family members interact with the plus end through their TOG domains, which bind tubulin using a tandem pair of TOG domains. It is thought that the TOG domains act to rapidly add or subtract tubulin from the plus end through their TOG domains (Slep and Vale, 2007; Al-Bassam et al., 2007). Several in vitro studies have focused on XMAP215's ability to contribute to individual facets of microtubule dynamics such as growth or disassembly (Popov et al., 2002; Brouhard et al., 2008; Shirasu-Hiza, 2003), but the exact mechanism by which XMAP215 functions to increase overall microtubule dynamics has yet to be fully determined. One model postulates that because TOG domains bind tubulin from solution and facilitate addition to the plus end, and the local concentration of soluble tubulin heterodimer is what dictates whether TOG proteins contribute to growth or shrinkage (Brouhard et al., 2008). When the local concentration of tubulin drops below a certain level, TOG proteins bind to tubulin at the plus end, stripping monomers from the end and promoting depolymerization.

The domain structure of Dis1/XMAP215 family members consists of an N-terminal array of TOG domains followed by a C-terminal protein interaction domain. In yeast TOG proteins there are two TOG domains followed by a serine-rich region and a C-terminal dimerization domain, bringing the functional number of TOG domains to four (Wang and Huffaker, 1997). Animals, plants (Whittington

et al., 2001), and amoeba (Gräf et al., 2003) have arrays of five TOG domains, but lack the dimerization domain of their yeast homologues. As mentioned previously, TOG domains are comprised of six adjacent pairs of α helices connected by inter helical loops (Slep, 2009). By sequence analysis, the most conserved feature between TOG domains of separate species is the inter-helical loops that form a linear interface that is hypothesized to interact with tubulin. Of particular note is a conserved tryptophan (or phenylalanine in the case of TOG5) within the first inter-helical loop. Using a bacterially purified TOG1-2 construct, a binding shift can be observed with purified tubulin using gel filtration. Mutation of the either one or both tryptophans results in a stepwise loss of tubulin interaction in this assay (Slep and Vale, 2007).

Since a minimum of two TOG domains is needed to bind tubulin, it was originally proposed that the array of five TOG domains in XMAP215 would bind oligomers of tubulin in solution, thus templating protofilaments to accelerate microtubule growth (Spittle et al., 2000; Asbury, 2008). Evidence for this has recently come from in vitro examination of microtubule growth using a sensitive optic trap that could detect nanometer changes in microtubule length. In the presence of XMAP215, microtubule growth and disassembly happened in large steps, upward of 64 nanometers or eight tubulin heterodimers (Kerssemakers et al., 2006), although the temporal sensitivity of this assay may have skewed the interpretation of such large growth changes. This suggests that XMAP215 can affect microtubule dynamics by adding or subtracting tubulin en bloc through TOG domain interactions. Evidence to the contrary has come from a different in

vitro study using single molecules of XMAP215 to measure microtubule dynamics using total internal reflective fluorescence (TIRF) microscopy (Brouhard et al., 2008). Examining single molecules, the study's authors observed processive movement of XMAP215 with the growing or shrinking microtubule end. In addition, the authors observed XMAP215 formed a 1:1 complex with tubulin by gel filtration, suggesting that this was the normal stoichiometry at the plus end. The authors proposed an alternate model where by XMAP215 family members processively move with the plus end, rapidly adding or subtracting single heterodimers to the plus end. One key question is how these observations correlate with the in vivo functions of XMAP215 family members. Exploration of this topic will be the subject of later chapters.

Kinesin 13, or Kin I Depolymerase Motor Proteins

In contrast to growth promoting factors such as EB1 and XMAP215, Kinesin 13 family members are plus end factors that strongly promote microtubule depolymerization (for review see Moores and Milligan, 2006). While several classes of cargo-carrying, conventional kinesin motors can influence depolymerization, such as Kinesin 8 (Varga et al., 2006; Du et al., 2010), Kinesin 13 motors are solely devoted to regulating microtubule disassembly. Kinesin 13 motors lack cargo binding domains like conventional kinesins and have an internal motor domain rather than a N-terminal motor domain, prompting their initial characterization as Kin I (as hereby referred) for "internal" motors (Vale and Fletterick, 1997). Kin I proteins are generally composed of a an N-terminal

localization domain, a Kin I-specific neck domain, a conserved core motor domain, and a C-terminal homodimerization domain.

The motor core domain of Kin I proteins has conserved ATP-binding features compared to other Kinesin motors, but also has unique features that are thought to aid its function of microtubule depolymerization. In particular, the α4 helix is the main energy transducer of the motor domain. This helix is thought to protrude from the arrow-like configuration of the motor domain into the intra-dimer cleft between α and β tubulin (Niederstrasser et al., 2002; Ogawa et al., 2004; Mulder et al., 2009). Based on this structural modeling, it is hypothesized that Kin I proteins use ATP-driven motor activity to induce a “bent” confirmation to the tubulin heterodimer that destabilizes lateral interactions and promotes the peeling “rams head” depolymerizing plus end structure. Kin I proteins are competent to form these microtubule end structures in vitro even in the presence of microtubule stabilizing reagents such as paclitaxel or the non-hydrolyzable GTP analog, GMPCPP (Desai et al., 1999; Hertzer et al., 2006). This suggests that Kin I proteins exert a measurable force to affect microtubules even in the presence of stabilizing agents that inhibit normal dynamic instability.

The N-terminal localization domain is competent to localize to most of the same structures as the full length molecule, but there is some indication that both the motor domain and C-terminus have roles in microtubule binding (Moore et al., 2005; Cooper et al., 2010). Expression of the motor core domain alone is sufficient to bind along the microtubule lattice, but this form is essentially inactive as a depolymerase (Moores et al., 2003). Another role the N-terminus is the

observed rapid diffusion of the molecule in vitro toward microtubule ends (Cooper and Wordeman, 2009). The discrimination of the Kin I motor for the microtubule ends versus the lattice seems to be a property of the N-terminus and neck domain, aided by dimerization through the C-terminus (Cooper et al., 2010).

The neck domain is a large stretch of highly charged residues. This appears to have multiple roles in the process of Kin I depolymerization. Kin I constructs missing the neck or with mutations that neutralize the neck's charged amino acids have lower microtubule association rates, suggesting that the neck is vital for the initial attachment to microtubules (Cooper et al., 2010). These same mutants also display lower rates of microtubule depolymerization, even at saturating concentrations when microtubule association and diffusion have negligible affects on depolymerization. This suggests that the neck has an additional role in Kin I removal of tubulin heterodimers at the plus end. The addition of the N- and C-terminus appear to offer specific advantages and disadvantages as a microtubule depolymerase. A construct encoding only the neck domain and motor core displays the most potent depolymerization activity in vitro (Cooper et al., 2010).

What purpose then do the other domains add to Kin I function? In the case of the N-terminal localization domain, it seems that this domain acts to specifically enrich Kin I motors at the growing end. In human MCAK and *Drosophila* KLP10A this is accomplished through EB1 SKIP motifs (Mennella et al., 2005; Honnappa et al., 2009). These depolymerases associate as comets on the plus end through an unknown mechanism, promoting catastrophe and

polymer shrinkage. It is not yet clear if this is a constitutively active process or if these proteins become active through some regulation such as phosphorylation (Jiang et al., 2009). At the C-terminus, the dimerization domain exerts the most negative effect on the total Kin I depolymerization activity in vitro (Cooper et al., 2010). From in vitro assays, monomeric constructs that retain the neck and N-terminus, associate and dissociate with microtubule lattice at elevated rates and seem to target to the plus end much faster than wildtype constructs. Surprisingly however, these constructs are ten fold less efficient at removing tubulin from the plus end in vitro. Dimerizing two full length motors may enhance the ability of Kin I motors to processively peel heterodimers off of the plus end as well as enhance their ability to dissociate from their heterodimer substrate to begin another cycle of depolymerization (Cooper et al., 2010).

The activities of Kin I motors have often been viewed as antagonistic to other +TIPs that contribute to microtubule growth and stability such as CLASPs (Laycock et al., 2006) and Dis1/XMAP215 (Hyman et al., 1999) family members. This simplistic model of polar antagonism toward either growth or shrinkage is largely based on the interpretation of opposing mitotic phenotypes in *Drosophila* syncytial embryos or using *Xenopus* mitotic extracts. In interphase cells, this antagonism may be species specific or more complex than direct antagonism. In mammalian cells, depletion or co-depletion of ch-TOG or MCAK does not seem to have any gross affects on microtubule organization or polymer level in interphase(Holmfeldt et al., 2004). Interestingly, treatment with nocodazole, a microtubule destabilizing drug, in ch-TOG depleted cells resulted in the same

degree of microtubule depolymerization as control treated cells. Overexpression of ch-TOG however, caused a surprising destabilization of microtubules that was entirely dependent on MCAK expression (Holmfeldt et al., 2004). This suggests that the role for mammalian ch-TOG and MCAK may be more specialized to regulate specific parameters of dynamic instability and not overall polymer and organization. This is in contrast to interphase *Xenopus* extracts, which have lower microtubule growth and shrinkage rates when depleted of XMAP215. In this experimental system, XKCM1 (the *Xenopus* MCAK) seems to specifically influence catastrophe frequency which can be elevated by depletion of XMAP215 (Hyman et al., 1999; Kinoshita, 2001), suggesting that the relationship between these proteins is much more complex than an antagonism between polymerase and depolymerase. This topic will be be further expanded upon in later chapters.

Novel +TIPs

The dynamic nature of microtubules allows for a rapid sampling of the cytosolic environment and delivery of key regulatory factors to specific locations. This requires an adaptable mechanism to couple the microtubule plus end to these sampling and delivery roles on non-microtubule proteins. Although there are specialized roles for the +TIPs discussed above to interact with non-MAPs such as endocytic vesicles with CLIPs (see above), this is primarily accomplished through the “SKIP” motif of EB1-dependent plus end localization signal. This allows proteins that either have no microtubule-binding domains or have other,

non-plus end microtubule interactions domains, to be coupled to the plus end to spatially regulate cellular behavior or microtubule organization.

One example of a non-microtubule protein that relies on an EB1 SKIP motif to localize to plus ends is the *Drosophila* Rho guanine nucleotide exchange factor, RhoGEF2. Immunofluorescence or GFP-tagged RhoGEF2 in *Drosophila* S2 cells revealed a localization identical to that of EB1, i.e. as a “comet” associated with the growing plus end (Rogers et al., 2004b). In *Drosophila* morphogenesis, RhoGEF2 works to activate Rho downstream of GPCR ligand binding to constrict the apical surface and internalize presumptive mesoderm cells (Parks and Wieschaus, 1991). EB1-mediated plus end tracking is thought to allow RhoGEF2 to probe the apical surface for Gα activation. Interestingly, this plus end association seems to be negatively regulated by G protein activation, as expression of a constitutively active Gα resulted in the mislocalization of RhoGEF2 from plus ends (Rogers et al., 2004b). Stromal interaction molecule 1 (STIM1) is another interesting example of a non-microtubule protein that localizes to the plus end through EB1 (Grigoriev et al., 2008). STIM1 is a transmembrane protein within the endoplasmic reticulum (ER) that regulates the influx of calcium ions into the ER (Dziadek and Johnstone, 2007). Using microtubule plus end association, STIM1 can translocate ER compartments toward the plasma membrane and thereby activate plasma membrane calcium channels. This provides a close proximity between the calcium channel and the ER to prevent the diffusion of large amounts of calcium into the free cytosol. This

also provides an additional mechanism for translocating and remodeling the endoplasmic reticulum.

One example of a MAP that uses EB1 plus end localization to affect microtubule behavior at the plus end is the ACF7 spectraplakin family of microtubule-actin crosslinkers (Kodama et al., 2003). These protein are enormous polypeptides with internal coil-coil plakin and spectrin-like repeats. At their N-terminus are a pair of actin binding calponin homology (CH) domains. At their C-terminus is GAS2 microtubule lattice binding domain. The *Drosophila* homolog of ACF7, named kakapo or shortstop, is essential in several processes that integrate cytoskeletal crosstalk between microtubules and actin, such as axon guidance and the formation of neuromuscular junctions (Subramanian et al., 2003). To effectively modulate these processes, shortstop and other spectraplakins must localize to the point of overlap between cytoskeletal systems. To accomplish this, mouse MACF7, Shortstop, and other spectraplakins contain a their extreme C-terminus an EB1-binding SKIP motif (Honnappa et al., 2009; Applewhite et al., 2010). Coupling microtubule and actin crosslinking to the plus end allows microtubules to track along actin bundles to facilitate the disassembly of integrin-based focal adhesions in motile cells (Wu et al., 2008). Crosslinking also allows microtubules to be anchored to the peripheral actin network to prevent their displacement by molecular motors. In the context of mammalian fibroblasts, spectraplakins act in a cortical complex with LL5β, ELKS, and CLASPs. Spectraplackins appear to be responsible for localizing CLASP within this complex (Lansbergen et al., 2006; Drabek et al., 2006).

Interfacing at the Plus End

Above, I have outlined the major +TIP families and how they contribute to regulate interphase microtubule dynamics. One of the enduring questions concerning +TIPs is how these proteins are integrated, regulated, and functionally balanced to produce the dynamics and behaviors at the microtubule plus end. This is an intriguing question, as the plus end is a somewhat nebulous cellular organelle, dynamic and below the diffraction limit of light microscopy. Added to that are the diverse set of molecules with contradictory functions that are all acting, seemingly simultaneously, on this same substrate, the plus end. Many studies have examined the individual contribution of proteins in vivo through depletion or overexpression techniques. Furthermore, structure-function studies at both the molecular and atomic level have yielded detailed domain maps of the major +TIP families. The next step will consist of taking these data and beginning to functionally test how these domains contribute to both microtubule behavior (dynamics and organization) as well as to the +TIP hierarchy among interacting partners, both known and unknown.

In addition to understanding how +TIPs function in regulating microtubule dynamics, another important area of research is understanding the contribution that those dynamics as well as extra +TIP domains have toward essential cellular and morphogenetic processes (Figure 3). This is a natural progression of study since it is clear that microtubules and their dynamic nature have many roles in cell processes such as mitosis, endocytosis, and membrane traffic. It will be

important to expand these roles for +TIPs to more complex processes such as cell polarity, cell migration, and collective cell movements. More than simply identifying the +TIPs involved, it will be essential to understand the mechanism by which +TIPs contribute to these processes; either indirectly through regulation of microtubule dynamics or directly through other non-microtubule-binding domains.

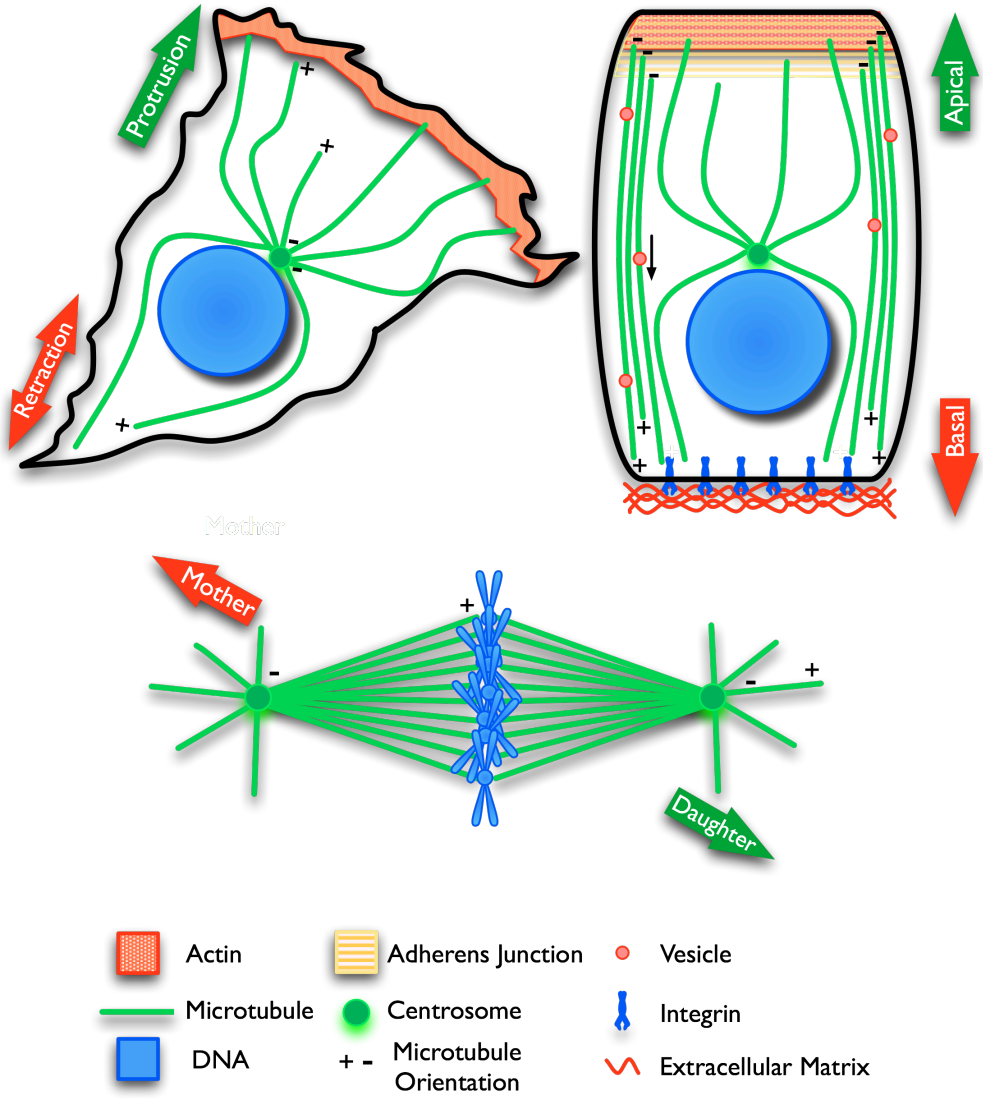
Protrusion
Retraction
Apical
Basal
Mother
Mother
Daughter
Actin
Adherens Junction
Vesicle
Microtubule
Centrosome
Integrin
DNA
+ - Microtubule Orientation
Extracellular Matrix

Figure 3. Microtubules are Essential for Key Cellular Processes.

Microtubules play an instructive role in epithelial polarity, chromosome segregation and spindle orientation, and cell migration. In polarized epithelial cells (right, top), microtubules help to establish and maintain the apical and basal cellular compartments. In addition, microtubules act as tracks for transcytosis, the directed traffic of nutrients from the intestinal lumen at the apical surface to tissue at the basal surface. During mitosis (bottom, middle), microtubules are not only essential for faithfully segregating chromosomes through each cell division cycle, but for orienting the spindle to define the cell division axis. During asymmetric cell division, the orientation axis determines mother stem cell fate and daughter progenitor fate. During cell migration (left, top), microtubules coordinate cell polarity, protrusion, cell adhesion, and retraction at the cell rear.

The Role of +TIPs in Cell Migration

Cell migration is a multi-step process that involves the coordination of distinct cellular pathways to produce net cell locomotion (for review see Ridley et al., 2003). Cell motility begins with an initial polarization of the cell that identifies a direction of migration via a chemotactic, haptotactic, or durotactic signal. This can happen before the cell undergoes any morphological changes, but once initiated, the unique morphological subdomains that are established give the cell an asymmetry that reinforces polarity through the positive feedback of master regulatory proteins.

Once polarity is established, the cell will send out a protrusion consisting of an Arp2/3-nucleated branched array of actin, termed the lamellipodia. The lamellipodia is thought to be the primary force generation machinery for motility and establishes the directional context for other motility-based structures. The lamellipodia acts to push the membrane forward and seed nascent adhesions that are essential for force production and focal adhesion formation. Behind the lamellipodia towards the cell center, the lamellipodia is broken down and either recycled back to the leading edge for reincorporation or is remodeled into linear, bundled stress-fibers that are linked to a subset of the matured product of the lamellipodia's nascent adhesions: the focal adhesion. Focal adhesions are clustered plaques of transmembrane integrins that connect the actin cytoskeleton to the extracellular matrix (ECM) substrate. Focal adhesions form the anchored structures that allow cells to produce the traction forces necessary for cell body

translocation and the final step of retraction of the cell rear. Cell retraction requires the de-adhesion of focal adhesions through endocytosis of integrin, disassembly of intracellular focal adhesion components, and myosin-II based constriction to pull up adhesions from the substrate. These multiple steps happen more or less sequentially in cycles and must be tightly coordinated between leading and lagging edge of the cell to couple protrusion and retraction to produce movement.

Microtubules are essential players within several parts of this process (for reviews see Rodriguez et al., 2003; Goode et al., 2000). During initial polarization, microtubules perform three key functions: 1) They must become stabilized in the new direction of migration to facilitate the transport of materials to and from the leading edge, such as the endocytic vesicles containing ligand-bound receptors; 2), in becoming stabilized toward the leading edge, microtubules reorient the centrosome and with it the Golgi apparatus and 3), microtubules deliver factors that both positively and negatively regulate Rho family small GTPases, which are needed to establish polarity and initiate protrusion. The stabilization of microtubules is thought to occur through two distinct mechanisms. In epithelial cells, microtubule stabilization is caused by the association of Adenamatous Polyposis Coli (APC) to the plus ends of microtubules downstream of Rho family GTPase, Cdc42 (Cau and Hall, 2005; Etienne-Manneville and Hall, 2003). In fibroblasts as discussed previously, cortical complexes of CLASP, LL5β, ELKS, and ACF7 stabilize leading edge microtubules downstream of PIP3 (Lansbergen et al., 2006). Delivery of GEFs

and GAPs to the leading edge via interactions with +TIPs, helps to regulate the balance between antagonistic Rho GTPases to create cycles of protrusive lamellipodia (Fukata et al., 2002; Pegtel et al., 2007).

Microtubules also have an important role in the maintenance of focal adhesions in migrating cells. Focal adhesions form through the initial binding of transmembrane integrins to extracellular matrix components such as fibronectins or laminins. Matrix binding causes a conformational change of the intracellular integrin tail and recruitment of a series of proteins to form a mature focal adhesion. Although the exact molecular events that lead to maturation and disassembly remain unclear, two molecular hallmarks that leads to focal adhesion disassembly are the phosphorylation and activation of focal adhesion kinase (FAK) as well as activated Rho-based contractility (Palazzo et al., 2004).

Microtubules are known to target mature focal adhesions and it is the targeted overlap between microtubules and focal adhesions that activates Rho and causes the breakdown of focal adhesions (Kaverina et al., 1998; Small and Kaverina, 2003). In turn, Rho activates its effector Diaphanous, or Dia, which stabilizes microtubules toward adhesions and the leading edge (Palazzo et al., 2004). In addition, the targeting of microtubules toward adhesions is promoted by the spectraplakin family of +TIPs. Using their bimodal actin and microtubule crosslinking domains, they guide growing microtubules along actin stress fibers that are anchored in adhesions (Wu et al., 2008). Embryonic fibroblasts isolated from knockout mice null for mACF7 have defects in migration that are due to long lived adhesions that are not efficiently targeted by microtubules and broken

down. In the same way that microtubules activate Rho at focal adhesions toward the direction of migration, microtubules similarly target the lagging edge of the cell to activate myosin II-based contractility downstream of Rho to facilitate retraction of the cell rear . This is also thought to be facilitated by endocytosis of the integrins at the cell rear to disassembly substrate attachments (Batchelder and Yarar, 2010).

+TIPs in *Drosophila* Cell Migration

Overall, the contribution of microtubules to cell migration is both permissive and instructive; coordinating and regulating the various events of polarization, protrusion, adhesion, and retraction in order to perfectly orchestrate cell locomotion. The key microtubule structure for coordinating these events seems appropriately to be the plus end, as it is often at the forefront of cytoskeletal interfaces. Due to their localization, +TIPs stand to be important regulators of cell migration. One of the problems thus far in investigating the role of +TIPs in cell migration and morphology has been the amount of gene redundancy in mammalian model systems. Several families of +TIPs such as spectraplakins, end binding proteins, and CLASPs exist in multiple isoforms in both mice and the human cell lines that are studied in cell migration. Although the advent of cell lines isolated from knockout mice have partially addressed this problem, this has prevented the systematic analysis of the major +TIP families in one cell migration model system.

Drosophila melanogaster represents an ideal model organism in which to study +TIP function. In terms of gene redundancy, *Drosophila* has only one isoform of most of the +TIP families, with the exception of EB proteins. In this regard, EB1 seems to be the major end binding protein and although similar proteins have been identified, they do not seem exhibit major overlap functionally with EB1. In addition to a more concise number of +TIPs, embryogenesis during the blastula stage of *Drosophila* development is dependent on the integrity of syncytial mitotic divisions, leading to the initial identification and characterization of many +TIPs through mutagenesis screens (Cullen et al., 1999; Lemos et al., 2000; Rogers et al., 2004a). In addition to being a developmental in vivo model organism, immortalized *Drosophila* cell lines such as Schneider's line 2 (S2) cells have provided an in vitro system to examine the molecular behavior of *Drosophila* +TIPs in cells (Rogers, 2002; Brittle and Ohkura, 2005; Sousa et al., 2007; Applewhite et al., 2010). S2 cells not only offer a concise genome and the ability to observe intracellular dynamics at high resolution, but they are also highly susceptible to RNA interference (RNAi) gene knockdown. Despite these advantages, S2 cell lines are limited in the number of cellular behaviors that can be analyzed ex vivo. S2 cells exist as single cells and do not form cell-cell contacts or exhibit any form of motility.

Using a recently characterized *Drosophila* motile cell line, named D17 (for protocol and characterization, see chapter 2), I conducted a small scale RNAi screen to identify the affect of +TIPs on D17 cell migration. To do this, I depleted D17 cells of +TIPs by RNAi and assayed their migration using a classical scratch

wound assay over 16 hours. To perform this assay, D17 cells were cultured to monolayer confluency and then wounded along a line of approximately 300-400μm with a sterile pipet tip. Cells on the wound margin sense the loss of cell contact and migrate in to fill the wound. Mammalian fibroblasts or epithelial cells often close the wound as a contiguous line of cells. In the case of D17 cells, the cells sometimes retain cell contacts as they move, but primarily populate the wound as single cells and then regain cell-cell contacts as their confluency increases. By manually tracking cells as they migrate into this scratch wound assay, I calculated parameters of migration such as velocity, distance traveled, and directionality for single cells as they migrated in to the wound.

From this initial screen, I was able to identify +TIPs that displayed specific loss and gain of function phenotypes upon RNAi depletion (Figure 4). RNAi of the *Drosophila* CLASP homologue, Orbit and CLIP190 resulted in an increase in migration velocity. In contrast, RNAi of EB1 or Mini spindles (Msps) the *Drosophila* XMAP215 homologue, caused a decrease in the overall velocity of D17 cell migration. As a positive control for RNAi-based affects on cell migration, I depleted the Arp2/3 activator, SCAR, to inactivate the protrusive actin machinery of D17 cells (Rogers et al., 2003). The overall trend between gain and loss of function phenotypes suggested that the overall "dynamicity" of microtubules might affect the rate of D17 migration. Loss of +TIPs such as Orbit and CLIP190, that are thought to stabilize microtubules, resulted in greater cell motility (Sousa et al., 2007; Komarova et al., 2002), while loss of EB1 and Msps, which enhance dynamic instability, resulted in lower rates of migration (Rogers,

2002; Brittle and Ohkura, 2005). This suggests that increasing the ability of microtubules to dynamically probe the cellular interior appears to have a positive effect on the rate of migration.

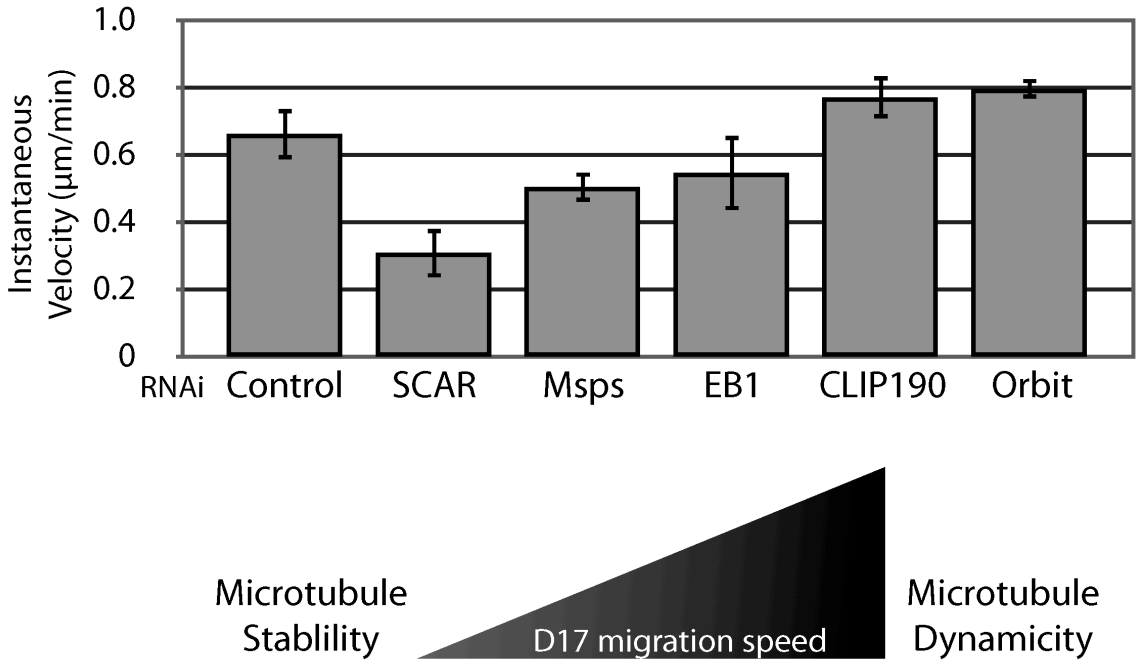

Figure 4. +TIPs involved in *Drosophila melanogaster* D17 cell migration.

Mean instantaneous velocity of single D17 cells migrating into a wound over 16 hours. D17 cells were treated with dsRNA against the indicated gene for 7 days before wounding a cell monolayer. RNAi depletion of SCAR disrupts Arp2/3-mediated actin assembly and inhibits D17 migration. Depletion of +TIPs that promote microtubule stability such as Orbit and CLIP190, result in a gain of migration. Depletion of +TIPs that enhance microtubule dynamics such as EB1 and Msps, give a loss in D17 migration velocity. This suggests that migration is positively regulated by dynamic microtubules and inhibit by static or stable microtubules.

Using these initial results, I decided to more carefully examine the interplay between +TIPs in S2 cells. My goal has been to understanding the complex hierarchy of protein interactions at the plus end. To this end, I have focused on the core plus end proteins: EB1 and XMAP215. EB1 is the primary plus end hub molecule (Akhmanova and Steinmetz, 2008) and acts as a primary localization signal for other +TIPs (Honnappa et al., 2009). XMAP215, in contrast, is one of the few +TIPs that has been shown to localize to plus ends independently of EB1 (Brouhard et al., 2008) and is thought of as a master regulator of microtubule growth (Kinoshita et al., 2002). It is both the interplay between EB1 and XMAP215 and other +TIPs, as well as the contribution of XMAP215's unique domain structure that sculpt in vivo dynamic instability (Chapter 3).

CHAPTER 2

D17-c3, A NOVEL *DROSOPHILA MELANOGASTER* CELL CULTURE SYSTEM FOR STUDYING CELL MOTILITY

This chapter is an initial characterization and protocol for using the D17 cell line that I developed in conjunction with my graduate advisor, Stephen Rogers. This manuscript is currently under secondary review for publication and the formatting of this chapter is based on the journal's protocol format.

Summary

Cultured *Drosophila melanogaster* cell lines such as S2 or S2R+, have become an important tool in uncovering fundamental aspects of cell biology as well in gene discovery. Despite their utility, these cells lines are non-motile and cannot build polarized structures or cell-cell contacts. Here we outline a previously isolated, but uncharacterized *Drosophila* cell line named Dm-D17-c3 (or D17). These cells spread and migrate in culture, form cell-cell junctions, and are susceptible to RNA interference (RNAi). Using this protocol, we will outline how investigators, upon receiving cells from the Bloomington stock center, can culture cells, and prepare the necessary reagents to plate and image migrating D17 cells to examine intracellular dynamics or observe loss of function

phenotypes through RNAi. From first thawing frozen ampules of D17 cells, investigators can expect to begin assaying RNAi phenotypes in D17 cells within roughly two to three weeks.

Introduction

Cultured *Drosophila melanogaster* cells have become a powerful genetic tool for the study of numerous cell biological processes. Established lines such as S2 and S2R+ offer high resolution cytology, simple culture conditions, a fairly homogeneous morphology when seeded on the lectin concanavalin A, and most importantly, a potent susceptibility to RNA interference (RNAi) that can be applied on a genomic level(Schneider, 1972; Yanagawa et al., 1998; Clemens et al., 2000; Rogers, 2002; Ramadan et al., 2007). These benefits are additionally advantageous due to the succinct nature of the fly genome(Adams et al., 2000) (roughly ~14,000 genes) and the potential to easily move cell culture observations into a model organism (Rogers et al., 2008). The end result has been a cell culture system that has been applied to disciplines as diverse as developmental biology (Wheeler et al., 2009; Johnston et al., 2009; Jiang et al., 2007), microbiology (Dorer et al., 2006), and high-throughput functional genomics (Wagner et al., 2007; D'Ambrosio and Vale, 2010).

Although lines like S2 and S2R+ have advanced our understanding of the basic mechanisms underlying cell morphology and cytoskeletal organization, their use is somewhat limited in this regard due to their lack of true cell locomotion. Moreover, these cell lines usually exist in culture as single, rounded

cells that lack characteristics such as cell-cell junctions, which are necessary structures for organismal development.

The Drosophila Genomics Resource Center (DGRC, https://dgrc.cgb.indiana.edu/) in Bloomington, IN is a repository for dozens of *Drosophila* cells lines derived from various fly tissues at different developmental stages. Many of these cell lines have remained uncharacterized with respect to their ability to respond to RNAi or their real-time dynamics in culture.

One such line, Dm-D17-c3 (hereafter referred to as D17), was isolated in addition to roughly two dozen other cell lines in the lab of the late Tadashi Miyake at the Mitsubishi-Kasei Institute of Life Sciences in Tokyo. Although only half of these lines were ever published(Ui et al., 1987), the entire collection of lines isolated from third instar larvae is currently available at the DGRC (https://dgrc.cgb.indiana.edu/cells/store/catalog.html?category=2). The D17 and their sibling lines were cultured from dissected imaginal discs, pools of multipotent cells in the developing Drosophila larvae responsible for creating the vast array of adult tissue needed during metamorphosis.

Characteristics of D17

When observing D17 cells in culture, the cells display a more heterogeneous set of morphologies than S2 cells, but usually spread and form islands of epithelial-like colonies or migrate non-directionally as single cells. In confluent culture, the cells often form a complete monolayer, but are not classically contact inhibited, resulting in foci of cells that build-up above the surface of the cell monolayer. Timelapse video microscopy of D17 cells revealed

a robust motility of roughly 25-30μm/hour (**Fig. 1, panel b**), similar to the initial speeds of *Drosophila* hemocytes in vivo as they migrate along the ventral midline(Wood et al., 2006) (~24μm/hour). Additionally, when migrating, these cells adopt a morphology reminiscent of mammalian cells migrating in culture; producing a polarized, triangular organization with a large fan-like lamella at the leading edge and trailing retraction fibers in the rear of the cell (**Fig. 2a**).

Although the D17 cells were originally believed to be epithelial cells due to the nature of the tissue they were derived from(Ui et al., 1987), the cells display properties reminiscent of *Drosophila* hemocytes which are migratory *Drosophila* immune cells. This is evident from their similar morphological properties during migration(Wood and Jacinto, 2007) as well as the D17's propensity for phagocytic clearance. Indeed, we often observe D17 cells in culture that exhibit a chemotactic attraction to the debris of their apoptosed neighbors and even undergo whole-cell engulfment (JDC and SLR, unpublished observations). D17 cells also mimic hemocytes in their ability to secrete extracellular matrix which they require for migration (see Box 1). In addition to this observational evidence for the D17's possible cell lineage, thanks to recent genomic information available from the modENCODE project (Celniker et al., 2009; http://www.modencode.org), we can make inferences about the differentiated state of the D17 cell line based on their transcriptional profile. Using these online tools we have found that similarly to S2 and S2R+ cells, D17 cells express elevated message levels of the hemocyte specific transcription factor Serpent(Rehorn et al., 1996)as well as other hemocyte specific genes,

suggesting that these two cell lines may have comparable expression profiles. Recent work from the modENCODE project has further characterized the transcriptional profile of 25 established *Drosophila* cell lines, including the D17 cell line(Cherbas et al., 2011). Expression profile clustering demonstrated that D17 cells share broad expression similarities to embryonic S2R+ cells. However, based on the expression of the homeotic transcription factor, Teashirt(Fasano et al., 1991), in D17 cells, the authors conclude that D17 cells are indeed imaginal haltere disc cells. This conclusion is somewhat confounded by the fact that embryonic S2 and S2R+ cells also express relatively high levels of Teashirt based on modENCODE expression data and it seems that this fact alone does not explicitly reveal the identity of the D17 cell line. Further work will be necessary to establish the identity of the D17 cell line based on gene expression, cell biological observations, and biochemical analysis between various *Drosophila* cell lines. Hopefully, continued use of the D17 cell line further open up intriguing questions about the mechanisms of cell identity, cell morphology, and cell motility.

Advantages and key applications of D17

The key component that makes *Drosophila* cells an advantageous system is their potent susceptibility to RNA interference and the relative simplicity in producing and treating cells with double stranded RNA (dsRNA). Generally, this procedure involves creating dsRNA that is transcribed from a target DNA template with flanking T7 RNA polymerase start sites. Addition of the produced dsRNA to cell growth medium is sufficient to induce cellular uptake and gene

depletion(Clemens et al., 2000) without the use of lipid-based transfections or virus infection. This methodology has been greatly enhanced by commercial and academic resources that provide online tools for designing dsRNA primers (Harvard Drosophila RNAi Screening Center, http://www.flyrnai.org), obtaining cDNA templates (Open Biosystems, http://www.openbiosystems.com), and procuring genome-wide as well as custom sub libraries (Harvard DRSC) of RNAi targets.

The utility of the D17 cell line should augment the studies of many in the cell biology and *Drosophila* communities that wish to study target genes and pathways in the context of biological processes such as cell migration and cell-cell interactions (**Fig. 3a**). In addition, many of the protocols already established for S2 cell culture(Rogers and Rogers, 2008) can easily be adapted for D17 cell culture. The D17 cell line represents an untapped resource to enhance existing questions in various fields as well as provide a model to ask new questions about the genetic basis of cell migration, chemotaxis, and cell differentiation.

Overview of the Procedure

We will outline in this protocol how to: thaw frozen ampules from the DGRC and establish cultures that can be passaged; prepare D17 growth medium and isolate a crude extracellular matrix preparation from conditioned media that allows users to plate D17 cells on glass surfaces. We will also outline how to experimentally assay D17 cells by transient transfection, dsRNA treatment, and examine migration through a classical wound healing assay that can be used to analyze RNAi phenotypes. Using the protocols outlined here we have been able

to previously demonstrate the negative regulation of D17 migration by the microtubule severing enzyme, Katanin(Zhang et al., 2011).

EXPERIMENTAL DESIGN

RNAi: D17 cells can be treated in much the same way as common S2 and S2R+ lines (Steps 9-13). For any RNAi experiment, it is important that users include important RNA interference controls to ensure that RNAi phenotypes are penetrant and effectively affect migration. We recommend using the small GTPase Rho as a positive control for penetrant RNAi phenotypes in S2 cells as well as D17 cells as it can be assayed by western blot (**Fig. 1e**) and produces a easily visible multinucleate phenotype (**Fig. 1d**)(Rogers and Rogers, 2008; Drechsel et al., 1997). As a positive control for RNAi migration phenotypes, we suggest using the *Drosophila* Arp2/3 activator SCAR. SCAR exists as a single isoform in *Drosophila* and significantly inhibits D17 migration (**Fig. 1c**). RNAi against the small GTPase Rac can also be used to inhibit D17 migration, but investigators should note the compensatory effects of the two *Drosophila* Rac isoforms and related GTPase Mtl(Paladi and Tepass, 2004; Stramer, 2005). Control treated cells can be treated with dsRNA made against the Bluescript plasmid(Rogers and Rogers, 2008).

The depletion of target proteins can vary between cell lines depending on the differential stability or expression level of the target polypeptide as well as the kinetics of protein dilution through sequential cell divisions, making a direct comparison of RNAi efficacy between S2 cells and D17 cells tenuous at best. Immunoblots of tubulin and Rho from equally loaded lysates reveal that S2 and

D17 cells express different levels of both proteins. Seven day treatment of dsRNA using the protocol outlined here results in a similar degree of knockdown between cell lines (**Fig. 1e)**., We suspect that the kinetics of protein depletion may be slightly slower in D17 cells due to their longer doubling time of 48-72 hours versus a 24 hour doubling time in S2 cells (JDC and SLR, unpublished observations). In our hands, potent depletion (greater than 80% knockdown) in D17 cells can usually be obtained within 7-9 days. We recommend that investigators empirically optimize the length of dsRNA treatment in D17 cells for each RNAi target to achieve the optimal knockdown.

Isolation of ECM: The methodology described in Box 1 is based on the early purification steps for isolating Drosophila ECM components outlined by John Fessler of UCLA(Fessler et al., 1994). So far, we have not yet identified the specific ECM components or factors that support D17 growth. Despite our attempts, commercial mammalian ECM components do not seem to replicate D17 ECM, and D17 ECM is not competent to convey cell spreading or motility to nonmotile S2 or S2R+ cells. D17 ECM is essential for culturing D17 cells on glass surfaces for wound healing assays, single cell motility, or fluorescent visualization. Although the above mentioned assays can be performed in tissue culture-treated plastic vessels, the use of glass surfaces allows greater resolution and decreased chromatic aberrations. One alternative is using a tissue culture-treated optical polystyrene that does not require ECM coating and can be used for oil immersion microscopy.

Because the concentration of ECM components can vary from batch to batch, it is important that investigators test newly made ECM to ensure consistency across many experiments. To do this investigators should plate and image D17 cells at a range of ECM concentrations (diluted in PBS, see step 14, generally ranging from 1:10 to 1:300). Analyzing the velocity and other parameters of migration (see step 21) for each concentration should allow investigators to find an ECM concentration that either replicates results from a previous ECM batch or displays the desired parameters of migration for a given experimental approach.

Transient transfection: D17 transfection will allow the user to image the dynamics and localization of exogenous transgenes through high resolution immunofluorescence or in real time using bioluminescent tags such as EGFP. D17 cells are amenable to most of the expression constructs currently used for S2 cells. One caveat is that D17 cells seem to be somewhat insensitive to the commonly used Metallothionein promoter constructs (referred to as pMT vectors). These reagents can be used, but require significantly higher doses of copper sulfate to induce gene expression (between 500μM-5mM concentrations). Based on our experience, constitutive promoters such as the actin promoter or the *OpIE2* promoter, give medium to high levels of expression and can be used when an endogenous protein promoter is unavailable. It is important that researchers use the proper controls to ensure both the expression of their desired transgene and to account for deleterious effects on D17 cell viability and cell migration. Expressing the empty vector backbone of a given transgene, that

only expresses an affinity or bioluminescent tag in D17 cells can both troubleshoot problems with the transfection protocol and control for the effects of toxic gene expression with a given assay. Users can also test transgenes by transfection in S2 cells or other non-motile *Drosophila* cell lines to determine the effects of their transgene on cell morphology. Using this protocol we normally achieve 10-40% transfection efficiency in D17 cells after 48 hours. The transfection protocol outlined here differs from protocols for transecting S2 cells by which we can commonly achieve 20-70% transfection efficiency, but both cell types seem to respond poorly to the transfection protocol of the other cell type.

Migration assays: The ability to assay cell migration is the key strength of designing experiments using the D17 cell line. We have outlined in this protocol a classical wound healing assay that has been previously used to measure the migratory capability of mammalian cells(Liang et al., 2007). One of the key advantages of this kind of assay is that it can easily be scaled from the examination of single conditions to high-throughput assays of many dsRNA treatments or conditions(Yarrow et al., 2004). We previous used this method to initially determine that depletion of the microtubule severing protein, Katanin, lead to an increase in the rate of wound closure. We then went on to examine the migration parameters of single cells migrating at subconfluent densities. This two-fold approach allowed us to determine an initial phenotype before further defining the exact mechanism of this migratory gain of function. In addition, investigators can often combine the two techniques (as described in step 21) to

measure both wound closure as well as the migratory properties of single cells moving into the wound.

When imaging D17 cells as single cells or within the context of a scratch wound assay, it is important that investigators consider: 1) the resolution of observation, 2) the temporal resolution of time series acquisition, and 3) maintaining consistency between conditions.

The magnification used for acquiring images of D17 migration should encompass the entire wound when using a scratch wound assay. When tracking single cells, the resolution for image acquisition should also be adequate to provide the necessary contrast and resolution to faithfully track cells as well as determine differences in morphology. We recommend using between 10 and 20x magnification for scratch wound assay, and increasing magnification to between 20-40x when imaging and tracking single D17 cells.

Users should be aware of the spatial resolution that are using to follow D17 migration. During a scratch wound assay, users should empirically determine, based on the size of their scratch, a time frame that would be feasible to detect both loss and gain of function migration phenotypes. This often means setting a final timepoint where control-treated cells migrate into the wound, but do not completely fill the wound area. When creating a timelapse series of wound healing or of subconfluent, single D17 cells, users should ensure that the rate of image acquisition is adequate to capture all cell movements. Lengthy intervals might lose small movements of cells and potentially skew measurements of directionality and velocity. This should be balanced by limiting

the cell's exposure to heat and evaporation caused by light illumination. Typically, intervals of 3-7 minutes should be an adequate rate of acquisition to alleviate these effects.

Finally, users should attempt to maintain consistent assay conditions across various experimental conditions. This includes the number of cells treated and plated for each condition, although this can difficult to avoid when treatments affect cell viability. Performing a wound healing assay with a pipette tip can also cause inconsistencies between conditions. Users should attempt to create the most uniform scratches possible between wells by maintaining a constant angle and pressure on the pipette tip while wounding cell monolayers. Custom and commercial apparatus can also be used to aid in wounding multiwell plates of D17 cells (Vitorino and Meyer, 2008; Yarrow et al., 2004).

Currently, one of the primary limitations of using the D17 cell line is the lack of directional migration assays toward chemotactic, haptotactic, or durotactic cues. Analysis of D17 migration using a scratch wound assay or imaging single cells migrating in culture is currently restricted to the non-directional migration of cells based on unknown cues. Because the migration of D17 cells is random, it also can lead to heterogeneity in the total number of cells in a population that are migrating as well as the persistence of migration in a single direction and the duration of migration. Investigators should be aware of this limitation and repeat experiments at least three times, sampling an adequate number of cells to truly determine the effect of dsRNA or other treatment on a population of cells. Understanding the cues that govern D17 motility will be an important advance in

order to harness these guidance cues to spatially and temporally direct D17 migration.

Figure 1

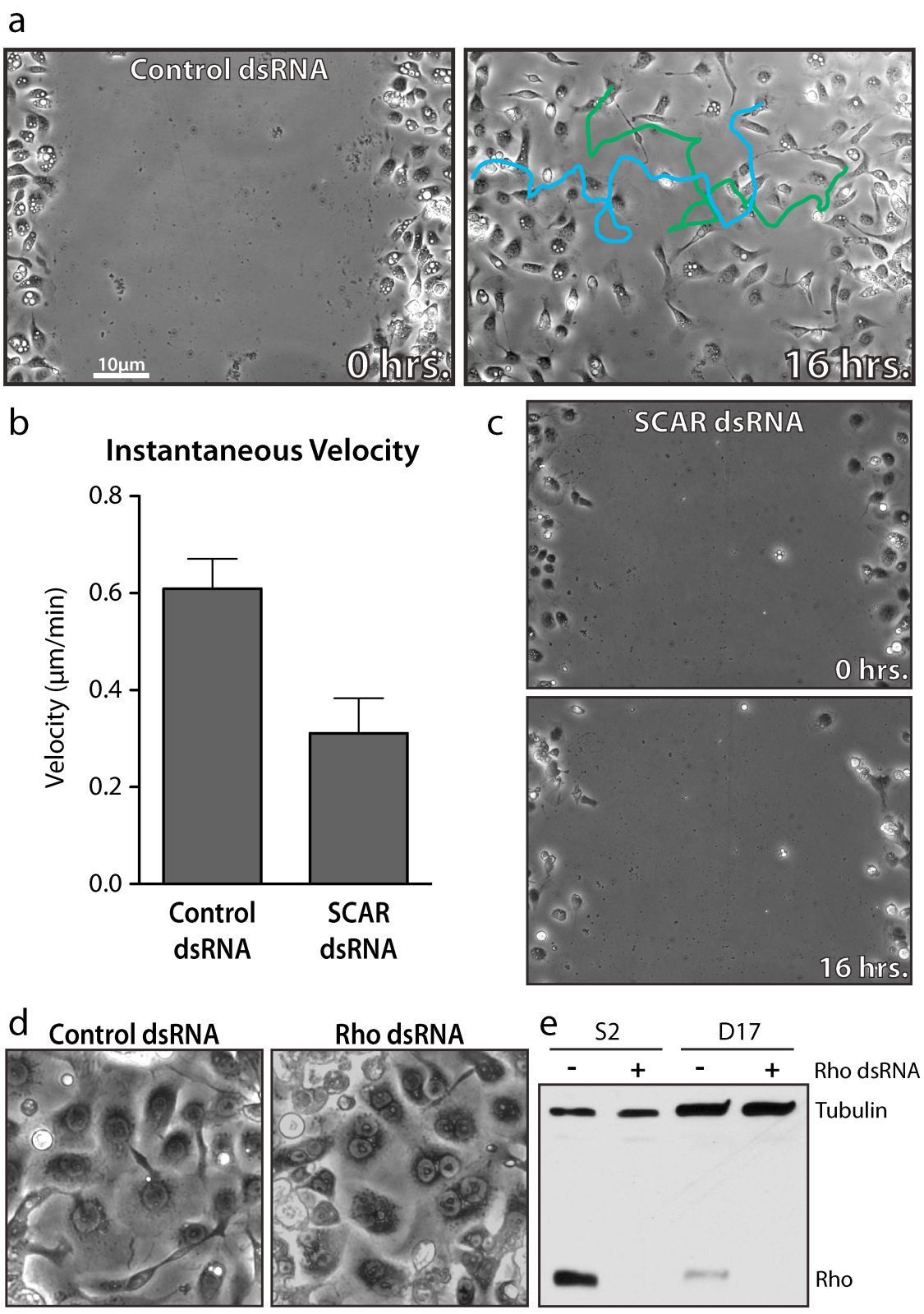

Figure 2-1. D17-c3 (D17) is a motile *Drosophila melanogaster* cell line.

(a) D17 cells plated to monolayer confluency and scratched with a 200µl pipet tip (left) and allowed to migrate into the the wounding area over 16 hours (right). Representative migration tracks from two cells are indicated on the right in blue and green. The full movie is can be found in Movie S1. (b) Measure instantaneous or step velocity of individual D17 cells from either a control or SCAR dsRNA treatment. N=3, 10 cells tracked for each experiment. Error bars indicate SEM. (c) D17 cells treated with SCAR dsRNA and wounded at 0 hours (top) and after 16 hours (bottom). (d) D17 cells after seven days of either control dsRNA (left) or Rho dsRNA (right). Depletion of Rho results in cytokinesis defects and multinucleate cells. (e) Immunoblots of S2 or D17 lysates for tubulin (DM1α, Sigma) or Rho1 (p1D9, Developmental Hybridoma Bank, University of Iowa). Lysates were taken from cells treated with control dsRNA or Rho1 dsRNA for seven days and represent equal protein load as determined by Bradford assay.

Figure 2

a

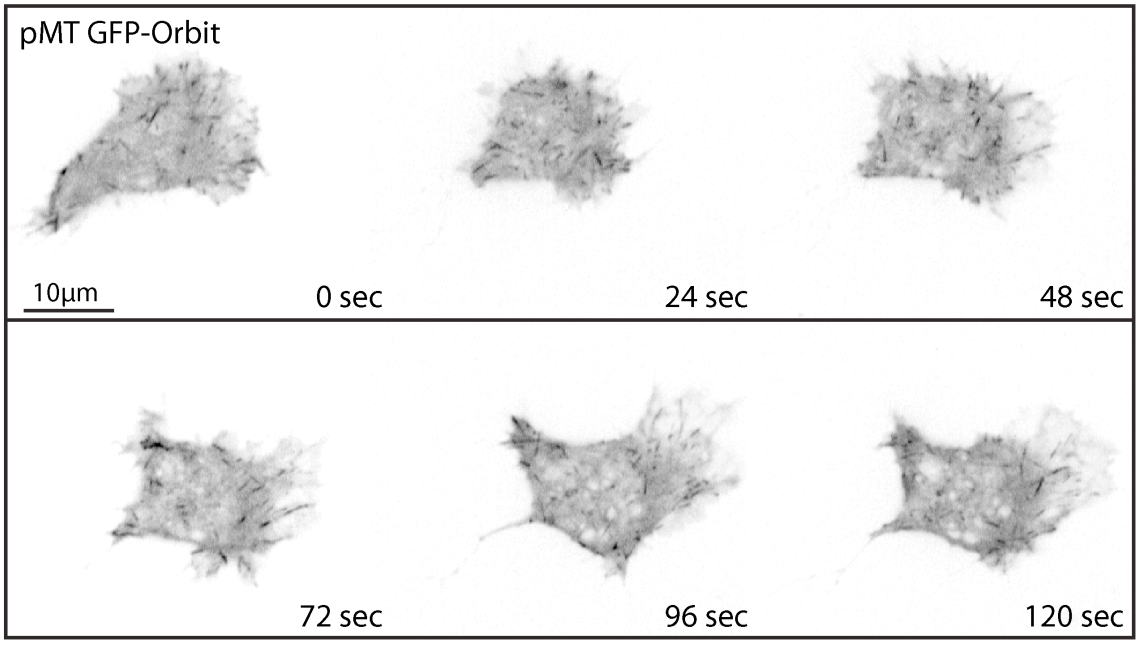

Figure 2-2. Dynamic protein localization within a migrating D17 cell.

(a) D17 cell expressing the *Drosophila* microtubule plus end protein Orbit/Mast tagged with GFP under the Metallothionein promoter (pMT GFP-Orbit) imaged by spinning disc confocal microscopy.

Figure 3

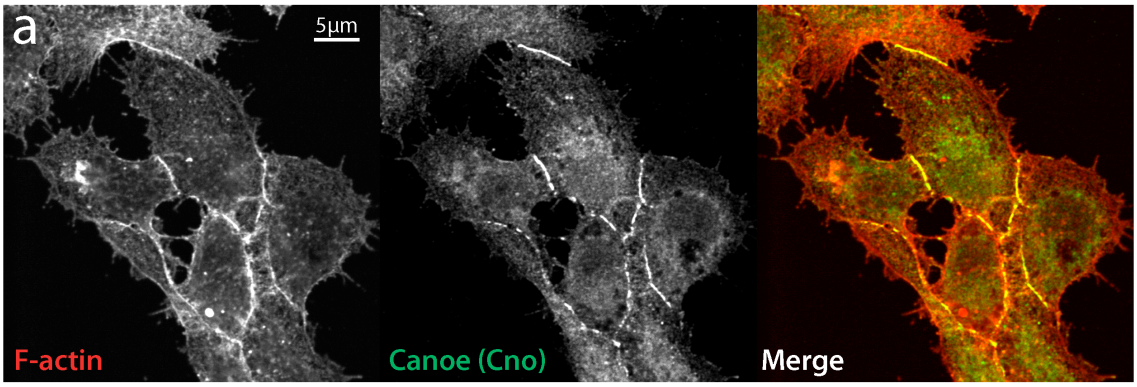

Figure 2-3. Immunofluorescence localization of cell-cell junction protein Canoe (Cno) in D17 cells.

(a) D17 cell stained for F-actin (left) using Alexa 488 phalloidin (Molecular Probes) and the junctional protein Canoe (Cno) (middle). Canoe localizes specifically to locations of cell-cell contact.

MATERIALS

Reagents:

- ML-DmD17-c3 cell stocks are available from the Drosophila Genomics Resource Center (https://dgrc.cgb.indiana.edu/)
- Schneider's Insect medium (Invitrogen, cat. no. 11720-034)
- Antibiotic/Antimycotic (Invitrogen, cat. no. 15240-096)
- Fetal Bovine Serum (FBS) (Invitrogen, cat. no. 10099-141)
- Human Insulin (Invitrogen, cat. no. 12585-014)

CRITICAL Many vendors sell FBS that is already heat-inactivated, usually at temperatures exceeding 65°C. This heat-inactivated serum is not suitable for D17 cell culture as it does not support long term cell passage, presumably because of the inactivation of important trophic factors. Non-heat-inactivated serum can be purchased and heat-inactivated by submerging the thawed serum in a 55°C water bath for one hour with occasional inversions to mix the serum.

- Cell Dissociation Buffer, PBS based (Invitrogen, cat. no. 13151-014)
- D17 growth medium (see REAGENT SETUP)

CRITICAL D17 growth medium should be made in advance of receiving frozen ampules from the Bloomington stock center.

- Sulfuric Acid (Fisher Scientific, cat. no. SA212-1)*CAUTION* Caustic reagent.

- Hydrogen Peroxide (Fisher Scientific, cat. no. H325-100)*CAUTION* Irritant.
- Sterile Phosphate buffered solution (PBS) (Invitrogen, cat. no. 10010-023)
- Saturated Ammonium Sulfate solution (Sigma-Aldrich, cat. no. A6387) (see REAGENT SETUP) *CAUTION* Irritant. Users should wear gloves when handling ammonium sulfate.
- Conditioned D17 growth medium (see Box 1)
- Fugene HD Transfection reagent (Roche, cat. no. 04709705001)
- sterile water
- Suitable transfection vectors e.g. Metallothionein promoter pMT vectors (Invitrogen, cat. no. V4120-20), *OpIE2* promoter pIZ vectors (Invitrogen, cat. no. V800001) or Actin promoter pAc5.1 vectors (Invitrogen, cat. no. V4110-20). Vector backbones can be modified or purchased to accommodate bioluminescent probes and other user-specific transgenes.
- D17 freezing medium (see Reagent Setup)
- dsRNA. These are user-defined and created based on standard methods(Rogers and Rogers, 2008)

Equipment

- UV transilluminator (such as Fisher Scientific, cat. no. PBDLT88AQ) or other power source such as a plasma treater that can bombard treated coverslips with at least 8000μw/cm^2. *CAUTION* Always use appropriate eye and skin apparatus and necessary shielding when using UV light.

- Polystyrene petri dishes, 35 x 10 mm^2 (Becton-Dickinson, cat. no. 351008)
- Glass bottom multi-well plate (Greiner, cat. no. 662892)
- Optical grade polystyrene/Polymer base multiwell plate (Nunc, cat. no. 165305)
- Glass coverslips, no. 1.5, 22mm^2 (Corning, cat. no. 2940-225)
- Coverslip rack, porcelain (Coors, via Thomas Scientific cat. no. 8542E40)
- swinging -bucket tabletop centrifuge
- tissue culture flask vessels, 25cm^2 (T25) (Becton-Dickinson, cat. no. 353082)
- tissue culture flask vessels, 75cm^2 (T75) (Becton-Dickinson, cat. no. 353135)
- Sterile, laminar flow hood
- 500ml sterile bottle-top filter flask (Corning, cat. no. 431117)
- 25cm cell scraper (Becton-Dickinson, cat. no. 353086)
- Dialysis tubing (Pierce cat. no. 68035)
- Dialysis clips (Pierce cat. no. 68011)
- Inverted microscope with CCD camera
- Microscope image acquisition software e.g. MetaMorph (Molecular Devices) or NIS Elements (Nikon)
- ImageJ software (http://rsbweb.nih.gov/ij/)

Equipment Setup

Coverslip preparation (Timing - 1.5 hours) Before ECM-treating glass coverslips, coverslips should be cleaned by immersion in a strong acid for at least one hour. Before treatment, load untreated coverslips into porcelain racks. To prepare the acid solution, add two parts sulfuric acid to one part hydrogen peroxide. Typically this volume is 200ml of sulfuric acid added to 100ml of hydrogen peroxide within a one liter glass beaker. Carefully lower the porcelain rack(s) into the acid solution and ensure that the coverslips are fully immersed. After one hour acid treatment, coverslips should be rinsed continuously with sterile running water for 15 minutes and dried. Once dry, place in 35mm dishes either individually or together to prevent dust accumulation on their surface.

Reagent Setup

D17 growth medium (Timing - 15 minutes) Prepare growth medium (cell culture medium) within a sterile, laminar flow hood by combining 5 mls antibiotic/anitmycotic (100x stock concentration), 50 mls heat-inactivated FBS (10% total medium volume), 1.25ml of human insulin (4mg/ml stock concentration to final 10µg/ml final concentration), and 445 mls Schneider's medium to a final volume of 500 mls. This solution should then be sterile filtered using a 2µm filter filter flask to exclude any precipitated serum or contaminates. Store at 4°C and warm to room temperature (approximately 25°C) before use. D17 growth medium is stable for 1-3 months, although serum crystals will form over time. These crystals should remain on the bottle bottom and do not seem to affect D17 culture.

D17 freezing medium: (Timing - 10 minutes) D17 freezing medium can be made by mixing 4ml of conditioned D17 growth medium, 4ml of fresh D17 growth medium, and 1ml of sterile DMSO.

Saturated Ammonium Sulfate solution (Timing - 30 minutes) Prepare a saturated ammonium sulfate solution by adding approximately 750g of ammonium sulfate to 1L of distilled and deionized water. Heat the solution until the ammonium sulfate is totally dissolved and then cool to room temperature (25 ^{o}C). Upon cooling, crystals should form, indicating the solution is indeed saturated. The saturated ammonium sulfate can be stored and used at room temperature and has an indefinite shelf life.

PROCEDURE

Thawing D17 cells *Timing - 1.5-2.5 hours*

1. In a sterile laminar flow hood, add 7 mls of D17 growth medium to a T25 tissue culture flask; this should be carried out prior to thawing the cells.

CRITICAL STEP Because the delivery conditions of dry ice are suboptimal for the storage of frozen cells, it is important that the ampule of cells be plated as soon as it arrives from Bloomington.

2. Remove the vial of cells from the dry ice delivery container and immerse the bottom of the ampule in a 37°C water bath, shaking often to thaw the ampule as quickly as possibly to room temperature.

CRITICAL STEP All attempts should be made to keep the cryo vial lid from coming into contact with the water bath water. This will prevent contamination of the D17 cells.

3. Once the ampule contents are liquid, remove from the water bath and sterilize the ampule by wiping the outside with a 70% ethanol solution.

4. In the laminar flow hood, add the contents of the ampule to the 7 mls of D17 growth medium in the T25 culture flask prepared in step 1.

5. Leave the cells for 1-2 hours at room temperature (25 ^{o}C) to attach and spread on the bottom of the culture flask. Then, remove the medium and replace it with a fresh 7 mls of growth medium to remove any DMSO that was present in the frozen cell solution. D17 cultures can be grown in a sterile incubator or on a shelf at 25°C. Flasks do not require gas exchange vents or special atmospheric considerations.

Passaging D17 cultures *Timing - 20-60 minutes*

6. Remove the D17 growth medium from the culture flask and store this conditioned medium at 4°C for extracellular matrix production (See Box 1).

7. Split D17 cells using either Cell Dissociation Buffer (option A) or using a cell scraper (option B).

(A) **Passaging using Dissociation Buffer**

(i) Wash the cells in the culture vessel by gently pipetting 2 mls of Cell Dissociation buffer onto the cells, briefly tilting the vessel to allow the buffer to wash over the cells, and removing the buffer with a pipette from the tilted culture vessel.

(ii) Add another 2 mls of Cell Dissociation buffer, or enough volume to cover the bottom of the flask. Incubate the cells for 25-30 minutes at room temperature outside the laminar flow hood. Under

magnification, the cells should be seen to round up and lose cell-cell adhesion.

Troubleshooting

(iii) Gently remove the Cell Dissociation Buffer with a pipette and add 5 mls of fresh D17 growth medium. Vigorously pipette the medium up and down several times to detach the cells from the bottom of the culture flask.

(B) **Passaging using a cell scraper**

(i) Add 6mls of fresh D17 growth medium to the flask. Insert the cell scraper into the flask and move the blade across the flask bottom, trying to remove a maximum amount of cells with the least blade strokes.

8. Seed the cell suspension into new culture vessels at concentrations of 1 to $2x10^6$/ml or roughly 40-60% confluency in either a T25 or T75 flask. The D17 cells should reach 100% confluency after 3 to 7 days depending on the concentration of cells seeded. Within the culture flask, the cells should reach a monolayer with small foci of additional cell growth above the monolayer. In cases where the cells are grown from sparse conditions, the user may find large colonies of cells that form islands of monolayers with exaggerated foci of cells on top. This is also adequate to passage to new

vessels as the cells contained within the foci should be competent to repopulate a new vessel. Aliquots of D17 cells can be frozen in D17 freezing medium using previously published protocols for S2 cells (Rogers and Rogers, 2008).

CRITICAL STEP The growth rate and survival of D17 cells is very sensitive to plating density. The most common error when culturing D17 is to plate them at low densities which can result in extremely slow growth or cell death. An optimal density of 40-60% is essential for healthy cells and confluent passaging between 3-6 days.

CRITICAL STEP: The user should keep track of passage iterations as D17 cells will reach a terminal state after 25-30 passages where they may respond poorly to RNAi or transfection and may have slow growth or abnormal morphology.

Troubleshooting

RNA interference treatment *Timing*: 7-9 days

9. Plate cells in tissue culture-treated multiwell culture vessel at subconfluent density (40-60% or 4,000-5,000 cells/mm). We recommend performing RNAi in tissue culture-treated vessels and then transferring cells to coverslips or glass vessels, when possible.

10. Allow the cells to adhere to the vessel bottom for one hour at room temperature (25°C). Cells can be transfected (see Box 2) within 30 minutes after plating and at anytime during RNAi treatment.

11. Remove media and replace with culture medium containing approximately 10μg/ml dsRNA. Treated cells should be incubated as normally passaged cells at room temperature (25°C).

12. Repeat dsRNA treatment (step 11) every two days for 7-9 days of treatment.

13. At 6-9 days of dsRNA treatment, harvest cell lysates for western blot analysis or transfer to ECM-coated vessels to assay for loss of function phenotypes e.g. migration phenotypes can be assayed as described in steps 18-21 below. The user should empirically determine the optimal length of treatment for each dsRNA construct and gene product. *Troubleshooting*

Plating D17 cells on ECM-coated surfaces *Timing- 1 hour*

14. Using a stock solution of D17 cell ECM (see Box 1), dilute the ECM solution in sterile PBS to the desired concentration. The exact concentration of ECM will need to be determined empirically by the user

based on the optimal assay conditions and the yield of ECM purified per batch (see Experimental Design). As a general starting point, dilutions of ECM to PBS ranging from 1:50 - 1:200 seem to support robust attachment and migration in our hands.

Troubleshooting

15. Apply enough of the ECM/PBS solution to cover the surface of the coverslip or glass-bottom plate intended for culture.

16. Crosslink the ECM solution to the glass surface by plasma treatment for several minutes or high energy UV treatment for 45 minutes. For many users, placing the dish or coverslip onto the surface of a UV transilluminatior used to visualize Ethidium bromide-stained agarose gels is sufficient, provided it can produce enough energy (approximately 8000 $\mu w/cm^2$) to crosslink the ECM to the glass surface.

CRITICAL STEP D17 cells should be plated within several hours of ECM crosslinking. Plasma or UV treatment is a temporary crosslinking procedure which can affect the efficiency of D17 adherence and motility for some applications. *Troubleshooting*

17. After crosslinking, remove the ECM/PBS solution. Plate the cells at the desired density to produce an adherent monolayer or single cells. D17 cells should adhere and spread on the crosslinked glass surface within 1

hour. Cells are viable on these crosslinked surfaces for several days and can proliferate to form confluent monolayers if plated in sub-confluent number. Generally, for sub-confluent plating, cell densities of 4,000-5,000 cells/mm surface are sufficient while densities of 7,000-8,000 cells/mm when cell monolayers are desired.

Wound Migration Assay *Timing - 18-24 hours*

18. Seed cells at monolayer densities on either tissue-culture treated vessels or ECM-coated glass surfaces at room temperature (25°C). Cells can be allowed to settle anywhere from 2-24 hours before wounding cell monolayers. Additionally, if too few cells are initially seeded, users can apply additional cells to increase the confluency of D17 cells to monolayer density.

19. Once monolayers are obtained, use a 200µl pipette tip or other pointed implement to scratch though the monolayer, creating a wound. Wounds should be at least 200µm in size without visible obstructions of cell debris or substrate etching.

20. Once wounded, pipette off the growth medium and wash the wells with fresh medium to remove debris.

21. Mount the vessel on an inverted light microscope with phase contrast or DIC filters and begin imaging. D17 wounded monolayers can be imaged over the course of 18-24 hours using either discrete timepoints (option A) or a timelapse series (option B).

(A) Imaging D17 wounded monolayers using discrete timepoints

(i) Keeping the vessel stationary on the inverted microscope throughout the migration assay, acquire images of the wound at regular intervals or a acquire a set of images representing the beginning and end of the migration assay.

(ii) After acquiring all timepoint images, ImageJ software can be used to outline the scratch area and measure the area of the wound at each timepoint. By comparison of the total area between the initial timepoint and later timepoints, investigators can obtain the percentage of wound closure over a given time.

(B) Imaging D17 wounded monolayers using a timelapse series

(i) Keeping the vessel stationary on the inverted microscope throughout the course of the assay, acquire

images at regular intervals of between 3-7 minutes (see Experimental Design).

(ii) Using ImageJ software, timelapse intervals can be assembled into a multi-image tiff file.

(iii) Apply the Manual Tracking plugin (Fabrice Cordelières, http://rsbweb.nih.gov/ij/plugins/track/track.html) to the multi-image tiff files to track individual cells as they migrate into the wounded area. Parameters such as instantaneous and mean velocity, distance, and directionality can be obtained using this plugin. Analysis of D17 single cell motility at subconfluent densities can also be performed using steps i-iii.

TROUBLESHOOTING

Troubleshooting advice can be found in Table 1

TIMING

Equipment Setup: coverslip preparation ~ 1.5 hours

Reagent Setup: D17 growth medium ~ 15 minutes once all ingredients are thawed

Reagent Setup: Saturated ammonium sulfate ~ 30 minutes

Steps 1-5: Thawing D17 cells, 1.5-2.5 hours

Steps 6-8: Passaging cells via:

Step 7(A) Cell Dissociation buffer: 25-60 minutes

Step 7(B) cell scraper: 20 minutes

Steps 9-11: RNAi plating and initial treatment, 1.5 hours

Step 12: Subsequent dsRNA treatment, 30 minutes

Step 13: Full dsRNA treatment, 7-9 days

Steps 14-17: Plating D17 cells on ECM surfaces, 1 hour

Steps 18-21: Wound healing assay, 18-24 hours and can be performed concurrently with the end of dsRNA treatment

Box 1: Preparing D17 ECM, 18-24 hours

Box 2: D17 transient transfection, 30 minutes and can be performed concurrently with dsRNA treatment, wound healing treatment, or both.

Box 1 Preparing D17 Extracellular Matrix *Timing - 18-24 hours*

1. Collect conditioned medium from confluent flasks of adherent D17 cells and store at 4°C. This can be collected every 3 days from 100% confluent flasks or every 6 days from subconfluent flasks. The most straightforward approach is to save the medium that cells have been cultured in when passaging cells to new culture vessels.

2. Once a sufficient amount has been collected (at least 100 mls), spin the media at 200xg for 10minutes to remove any cells or large precipitants. *CRITICAL STEP* Because there is some variability between lots of prepared ECM, in an effort to maintain consistency it is important that a large enough batch of conditioned media is processed to accommodate the user's aims. To this end we would recommend processing between 200-400ml of conditioned medium at any one time which will produce enough ECM to last the user over one hundred experiments depending on the final concentration it is used at.

3. Pour the cell-free medium into a glass beaker and stir slowly on a stir plate.

4. Add approximately 40% volume of saturated ammonium sulfate dropwise to the slowly stirring medium (i.e. 40 mls ammonium sulfate added to 100 mls conditioned medium). The key to success at this step is to continue adding ammonium sulfate until the medium is cloudy and opaque (which indicates the precipitation of large proteins out of solution) rather than adding a precise volume.

5. Pour the precipitated medium solution into 50ml conical tubes and spin at speeds in excess of 3000xg for 30 minutes to 1 hour at 4°C. After

centrifugation, the precipitated proteins should be pelleted and the supernatant should again be clear.

6. Discard the supernatant and resuspend the pellet in 1/100th of the original medium volume (i.e. for 100 mls conditioned medium, resuspend the pellet in 1ml) in cold, sterile PBS.

7. Pipette the resuspend pellet into a dialysis bag and dialyze in 1L of PBS at 4°C, changing the PBS out 2 to 3 times over the course of 16 to 24 hours to remove the ammonium sulfate from the ECM solution.
Pause Point The resuspended ECM pellet can be left to dialyze in fresh PBS overnight at 4°C.

8. Aliquot the dialyzed ECM into 1.7ml microcentrifuge tubes and spin in a tabletop centrifuge at 4°C at speeds in excess of 16,000xg for 10 minutes and transferring the supernatant to another microcentrifuge tube to remove any remaining precipitate.

9. The ECM is now ready for use (see Steps 14-17 of the main Procedure). Test each new batch for efficacy to match the ideal assay conditions (see Experimental Design).

PAUSE POINT: ECM can be stored short-term (1-2 months) at 4 ^{o}C or long-term by flash freezing in liquid nitrogen and storing at -80 ^{o}C.

Box 2 Transient Transfection of D17 cells *Timing - 30 minutes*

1. Plate D17 cells in either an ECM-coated glass vessel or a tissue culture-treated polystyrene multi-well dish to a confluency of 50-80% and leave them to adhere at room temperature (25°C) for 30 minutes to 24 hours.

2. After the cells have adhered to the culture vessel surface, replace the medium to remove cell debris.

3. Make up the Fugene HD transfection mixture and treat cells according to the manufacturer's protocol at a ratio of 3µl Fugene HD to 2µg total DNA (3:2) diluted in sterile water, although we recommend that each user empirically determine their optimal transfection conditions for each transgene. The transfection reagent can remain on the plated D17 cells indefinitely.

4. Assess gene expression; this can be carried out within 24 hours depending on the type of promoter used to induce transgene expression.

    Troubleshooting

ANTICIPATED RESULTS

Using either a wound healing assay (**Fig. 1a**) or by imaging single cells (**Fig. 2a**) over various time periods, the investigator can acquire timelapse data sets from which they may derive various parameters of cell migration including distance, velocity (**Fig. 1b**), and directional persistence.. In a wound healing assay, an investigator can expect control-treated cells to migrate from both sides, not necessarily as a single cell sheet, to fill in approximately 150-250μm of the wound area over 18-24 hours.

By optimizing the length of dsRNA treatment to obtain greater than 85% knockdown by western blot analysis, the user should expect a highly penetrant RNAi migration phenotype. Combining transfection of D17 cells with a wound healing assay

or single cell migration assay will also allow the user to determine the affects of overexpression on cell migration. Investigators can also take advantage of dsRNA against the 5‘ or 3‘ untranslated region (UTR) of an endogenous gene, allowing them to express exogenous cDNA transgenes to examine the sufficiency of a particular gene to rescue RNAi migration phenotypes. In these cases, the lower transfection efficiency of 10-40% expressing cells can be advantageous, as the user can use untransfected cells within the same condition as controls.

Acknowledgments

The authors would like to thank members of the Rogers lab for helpful discussions regarding the application of this protocol. We would also like to acknowledge M. Peifer for the generous gift of Canoe antibody and the *Drosophila* Genomics Resource Center for cell lines and helpful protocols.

Author Contribution

JDC performed the protocol under the supervision of SLR. JDC and SLR wrote the protocol manuscript.

Competing financial interests

The authors declare that they have no competing financial interests.

Table 2.1: Troubleshooting

Step	Problem	Possible reason	Possible Solution(s)
7(A)i	D17 cells fail to de-adhere after treatment with Cell Dissociation Buffer	D17 growth medium may remain after washing with Dissociation buffer or D17 cells are present in high density and are more resistant to Dissociation Buffer.	Incubate D17 cells for longer periods with Cell Dissociation Buffer. Use a more powerful electronic pipet to mechanically remove cells.
8	D17 cultures die after a short number of initial passages	Lack of growth factors in the medium can lead to a death of D17 cells over the course of several passages. This can be caused by an improper inactivation of fetal bovine serum (FBS).	Be sure that FBS is heat inactivated at a temperature of 55˚C (see Materials).
8	D17 cells never reach 100% confluency, but instead form large foci and single cells adopt a spindly morphology.	D17 were possibly plated at too low a density.	Consider dissociating and passaging the foci with vigorous pipetting or Dissociation Buffer into a smaller culture flask. Consider replacing 1/2 the culture medium with fresh D17 growth medium to provide fresh growth factors.
13, Box 2, Step 4	D17 cells stop responding to dsRNA treatment or transient transfection. D17 cultures begin to die after more than 20 passages.	Although D17 cells are an immortalized line, they begin to lose their susceptibility to RNAi and reach a terminal growth sometime after 20 passages.	Consider ordering new cells or thawing fresh aliquots of D17 cells.

14, 16	D17 cells do not adhere and migrate on ECM-crosslinked glass surfaces	This could be due to an inefficient crosslinking process or inefficacious ECM.	If using a UV crosslinking treatment, determine the power output of the UV source or use a plasma treatment system. D17 migration can be impaired by too low or too high concentrations of ECM. The user should empirically test a range of ECM concentrations to determine the optimal concentration per ECM batch (see Experimental Design).

Chapter 3

THE MICROTUBULE LATTICE AND PLUS-END ASSOCIATION OF *DROSOPHILA* MINI SPINDLES IS SPATIALLY REGULATED TO FINE-TUNE MICROTUBULE DYNAMICS

This chapter represents a manuscript currently in resubmission. I performed all of the experimentation under the support and advice of my graduate advisor, Stephen Rogers. I also depended on my committee member Kevin Slep for critical advice and specific key reagents. An undergraduate under my mentorship, Gregory Schimizzi, assisted me with some of the molecular biology necessary for this project. Shannon Stewman, a postdoctoral fellow under the advisement of Ao Ma, at Albert Einstein Medical College, performed automated tracking and analysis of microtubule dynamics for this project.

Summary

Microtubules exhibit a signature behavior, termed dynamic instability, in which individual microtubules cycle between phases of growth and shrinkage while the total microtubule polymer remains constant. These dynamics are promoted by the conserved XMAP215/Dis1 family of microtubule-associated proteins (MAPs). We have conducted an *in vivo* structure-function analysis of the *Drosophila* homologue, Mini spindles (Msps). Msps exhibits EB1-dependent and spatially regulated localization to microtubules, localizing to microtubule plus ends in the cell interior and decorating the lattice of growing and shrinking microtubules in the cell periphery. RNAi rescue experiments revealed that Msps'

NH_2-terminal four TOG domains were sufficient to promote microtubule dynamics and EB1 comet formation and that the TOG domains function as paired units. We also identified TOG5 and novel inter-TOG linker motifs that are sufficient for binding to the microtubule lattice. These novel microtubule contact sites are necessary for Msps peripheral lattice association and to allow Msps to regulate dynamic instability.

Introduction

Microtubules are non-covalent polymers of the protein tubulin that perform essential transport and structural roles within eukaryotic cells (Lansbergen and Akhmanova, 2006; Rodriguez et al., 2003; Howard and Hyman, 2003). Microtubules exhibit a steady state behavior, termed dynamic instability, in which individual microtubules randomly switch between phases of growth and shrinkage while the total level of microtubule polymer within the cell remains constant (Mitchison and Kirschner, 1984). Dynamic instability is crucial to microtubule function and allows cells to rapidly remodel the microtubule network in response to cell cycle cues or extracellular signals and to perform "search-and-capture" functions producing stable interactions between microtubules and organelles, kinetochores, or cortical binding sites. In many cell types, the slow growing minus ends are attached to a microtubule-organizing center, while growth and shrinkage is caused by addition or loss of α- and β-tubulin heterodimers at the fast growing plus ends. Microtubules prepared from purified tubulin do not exhibit the same parameters of dynamic instability as microtubules observed in extracts or in cells, underscoring the role of microtubule-associated

proteins (MAPs) as key regulators of microtubule behavior (Kinoshita, 2001; Gardner et al., 2008; van der Vaart et al., 2009). MAPs may be categorized into two types: conventional MAPs, that bind along the microtubule lattice and stabilize, and microtubule tip-interacting proteins (+TIPs), which preferentially associate with plus ends to regulate growth, shrinkage, and attachment to other structures within the cell. Although many MAPs and +TIPs have been individually studied through genetic, biochemical, and cell biological approaches, it has become widely accepted that these molecules function in a complex hierarchy of interactions (Akhmanova and Steinmetz, 2008). For example, the +TIP EB1 has emerged as a key molecule necessary for recruitment of other +TIPs to growing plus ends (Vaughan, 2005). Currently, we lack a mechanistic understanding about how these interactions work in concert to regulate microtubule dynamics.

XMAP215 was the first protein identified that affected microtubule dynamics at their plus ends; since that time members of the XMAP215/Dis1 protein family have emerged as key regulators of dynamic instability (Kinoshita et al., 2002). XMAP215 was originally identified in *Xenopus* egg extracts as a factor that stimulated the polymerization rate of purified tubulin almost ten-fold *in vitro* (Gard and Kirschner, 1987). Conserved homologues have been found across all eukaryotic taxa and, where tested functionally, they have all been implicated as promoters of microtubule dynamics and are required for proper assembly and function of meiotic and mitotic spindles (Cullen et al., 1999; Cullen and Ohkura, 2001; Gergely et al., 2003; Srayko et al., 2003; Gard et al., 2004). All XMAP215/Dis1 proteins exhibit a conserved domain structure characterized

by the presence of NH_2-terminal TOG domains. Tandem pairs of TOG domains bind to tubulin and can trigger robust microtubule nucleation *in vitro* when present as multiple pairs (Slep and Vale, 2007). In almost all multicellular eukaryotes, XMAP215 homologues possess an array of five TOG domains that can be classified into three types based on sequence similarity: TOG domains 1 and 3 are type A, TOG domains 2 and 4 are type B, while TOG domain 5 is classified as type C (Gard et al., 2004; Slep, 2009). This pattern suggests that animal XMAP215 homologues evolved by sequential duplications of their TOG domains, generating a pair of TOG domains that reduplicated to produce the modern day tandem arrangement of five copies. Crystal structures of isolated TOG domains from several species (Al-Bassam et al., 2007; Slep and Vale, 2007) revealed that they are flat, "paddle"-shaped domains composed of six tandem HEAT-repeats. HEAT repeats have a helix-loop-helix motif with the highly conserved intra-helical loop regions serving as the proposed tubulin contact sites (Slep, 2009).

Although a role for XMAP215/Dis1 proteins as promoters of microtubule plus end dynamics is well established in several systems, there is no unifying framework for how the domain structure of these proteins contributes to their localization and unique effects on microtubules in living cells. Two recent studies using high-resolution *in vitro* assays both demonstrated that XMAP215 acts as a microtubule polymerase,, although they arrived at different conclusions as to the exact molecular mechanism of XMAP215's "enzymatic" action (Kerssemakers et al., 2006; Brouhard et al., 2008). In addition to the large body of work indicating

that XMAP215/Dis1 family members affect microtubule growth, there is evidence that this family of proteins have a more complex role that also involves regulating microtubule shrinkage. Several *in vitro* studies have found potent effects on microtubule depolymerization in the presence of XMAP215 and other family members (van Breugel et al., 2003; Shirasu-Hiza, 2003; Brouhard et al., 2008). Perhaps most telling, depletion of *Drosophila* Mini spindles (Msps) in S2 cells resulted in non-dynamic, paused microtubules (Brittle and Ohkura, 2005). Based on these data, the authors of this study suggested that XMAP215/Dis1 family members might act as "anti-pause" factors that exist to rapidly catalyze the transition from pause to either growth or shrinkage, thereby enhancing the dynamics of microtubules in addition to their ability to add monomers to the growing end.

In this study, we have conducted an *in vivo* characterization of *Drosophila* Mini spindles (Msps) in cultured *Drosophila* S2 cells. We found that Msps exhibits EB1-dependent and spatially regulated localization to microtubules, localizing to microtubule plus ends in the cell interior and decorating the lattice of growing and shrinking microtubules in the cell periphery. RNAi rescue experiments revealed that the NH_2-terminal four TOG domains of Msps were sufficient to promote microtubule dynamics and EB1 comet formation and that the TOG domains function as paired units. We also identified TOG5 and novel inter-TOG linker motifs that are sufficient for binding to the microtubule lattice. These novel microtubule contact sites were necessary for Msps peripheral lattice association and allowed Msps to regulate dynamic instability. Thus, Msps regulates

microtubule dynamics through several mechanisms that involve its unique, multi-domain structure.

Results

Msps exhibits a differential localization to microtubule plus ends in the cell interior and to the microtubule lattice in the periphery of interphase S2 cells.

Brittle et al. (2005) previously described the localization of Msps in S2 cells plated on concanavalin A (con A) and found it to be present on spindle microtubules and centrosomes in mitotic cells, and as punctae along individual microtubules with prominent foci present at microtubule plus ends. We reexamined Msps localization using novel antibodies (Supplemental Figure S1A) raised against the second TOG domain (TOG2). Msps distribution in S2 cells was roughly similar in our hands; however, we observed more discrete patterns of localization along microtubules during interphase. Endogenous Msps accumulated at microtubule plus ends in the interior of the cell, labeling "comet"-like structures with a similar mean length to that of EB1 (Figure 1E). Triple labeling for Msps, microtubules and EB1-GFP (Figure 1A) revealed that Msps colocalized extensively with EB1 at these interior microtubule plus ends and confirmed prior observations that Msps behaves as a microtubule plus end-interacting protein (+TIP) (Lee et al., 2001). In the cellular periphery, however, Msps exhibited a strikingly different interaction with microtubules; in addition to plus end localization, we found that endogenous Msps decorated the microtubule lattice in a discontinuous pattern over several microns in length (Figure 1E). We

also observed that some of the peripheral microtubule segments that exhibited Msps lattice association lacked EB1 (Figure 1C), suggesting that these microtubules had stopped growing just prior to fixation.

The periphery of S2 cells plated on con A is made up of concentric actin-based sub-compartments - the peripheral lamellipodium, the lamella, and the convergence zone - that are defined by local actin dynamics and are established by intracellular signaling

Figure 1

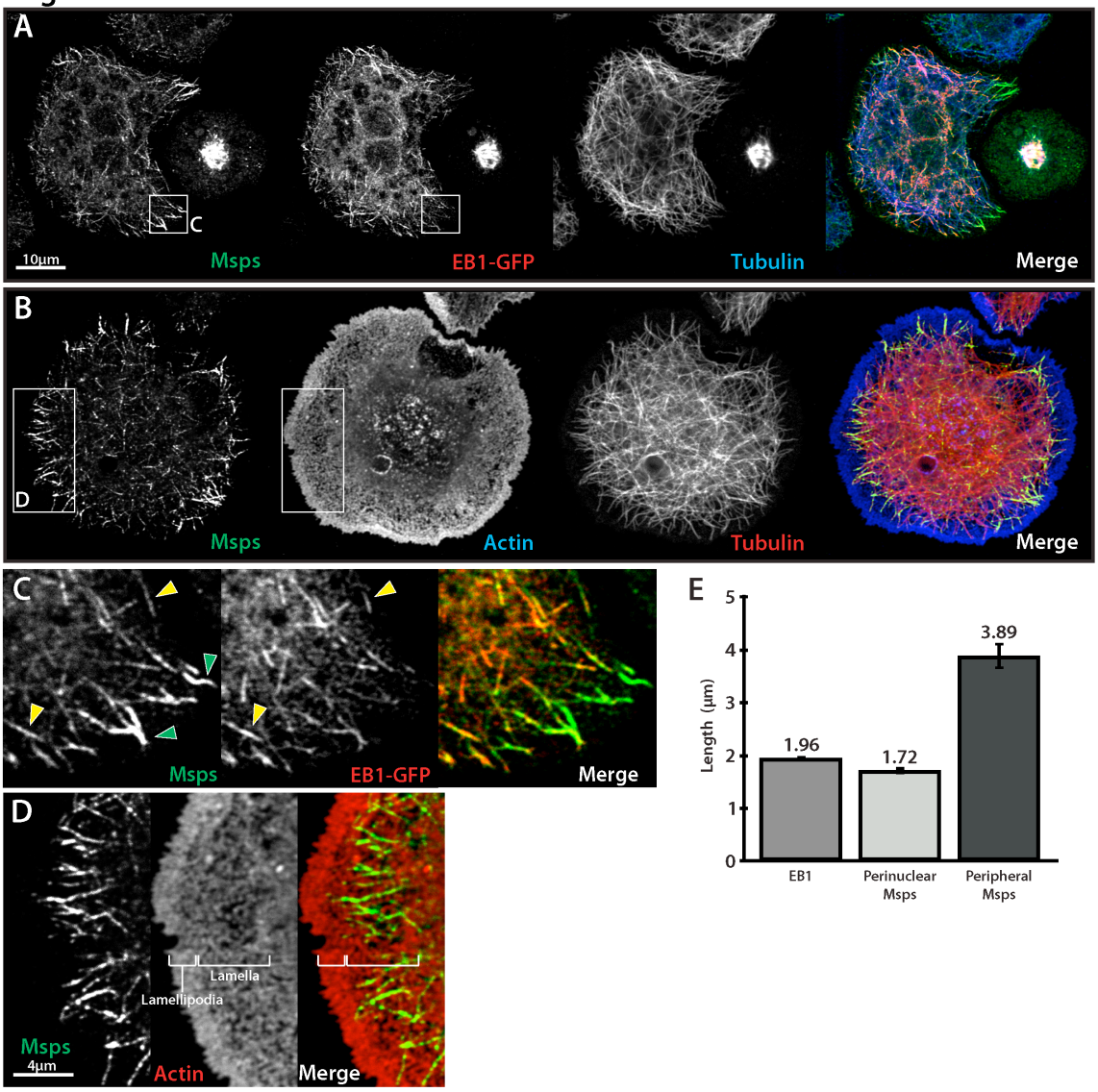

Figure 3-1. Msps localizes to both microtubule plus ends and to the lattice of peripheral microtubules.

(A) Interphase *Drosophila* S2 cell transfected with EB1::EB1-GFP (middle) and immunostained for Msps (left) and α-tubulin (right). (B) S2 cell immunostained for Msps (left), actin (middle), and α-tubulin (right). (C) Inset from (A), Msps

colocalizes with EB1 and peripheral microtubules that are EB1 negative. (D) Inset from (B), Msps lattice accumulations (left) are coincident with actin-rich lamella (right). (G) Graph of microtubule decoration length for immunostained EB1, and interior-localized and peripheral Msps. Error bars are 95% CI.

cascades downstream of Rho family GTPases (Iwasa and Mullins, 2007). Wittmann and Waterman-Storer (2005) previously demonstrated that the +TIP CLASP exhibited regional differences in dynamics of certain mammalian cells; CLASP tracks with microtubule plus ends in the central cell body, but associates with the microtubule lattice in the lamella and lamellipodium. In order to test the hypothesis that Msps' compartment-based behavior resembled mammalian CLASP, we plated S2 cells on con A and stained them to visualize Msps, microtubules, and actin (Figure 1B). While Msps staining rarely extended to the very peripheral lamellipodia in S2 cells, the pool of microtubule lattice-associated Msps coincided predominantly with the peripheral lamella (Figure 1D). This association did not depend on the actin cytoskeleton, as latrunculin treatment did not alter Msps localization to the microtubule lattice (data not shown). These data indicate that Msps is able to interact with microtubules through at least two different modes - via an association with growing microtubule plus ends in a manner analogous to EB1, and to segments of the microtubule lattice similar to mammalian CLASP, and suggests that these two modes are spatially regulated in response to the localized cytoplasmic environment within the cell.

In order to characterize Msps dynamics relative to microtubules, we used confocal microscopy to perform 2-color time-lapse imaging of Msps-GFP and mCherry-tubulin in S2 cells. The localization of Msps-GFP in living cells was identical to that of the endogenous protein observed by immunofluorescence (Figure 2A, Movie 1). In the interior of the cell, Msps-GFP localized to growing microtubule plus ends. As microtubules grew into the periphery of the cell, Msps-

GFP at the plus ends of individual microtubules frequently converted to a lattice-bound population that extended along the microtubule lattice in a discontinuous, punctate pattern (Figure 2A, arrows, Figure 2B). Remarkably, these lattice-associated GFP punctae in the cell periphery were very dynamic and seemed to exhibit frequent, short, bidirectional movements along microtubules (Figure 2B, Movie 2), often coalescing onto the end of a depolymerizing microtubule. In addition, foci of Msps-GFP often remained associated with the plus ends of microtubules after catastrophe and could track with the tips as they depolymerized (Figure 2C, Movie 3), consistent with a recent *in vitro* report of family member, XMAP215 (Brouhard et al., 2008). In addition to microtubule localization, we also observed Msps-GFP associating with non-motile cytoplasmic punctae (Figure 2A, arrowhead); double labeling with antibodies to PLP revealed these structures to be centrioles (data not shown). From these observations we conclude that Msps is able to track microtubule plus ends during phases of growth or shrinkage in living cells and that it also interacts with the microtubule lattice in peripheral regions of the cell.

S2 cells exhibit two distinct populations of microtubule plus ends based on their origin and location between the cell interior and periphery

We next wanted to examine how Msps effects microtubule dynamics in living cells. We began by characterizing the behavior of microtubule plus ends in interphase S2 cells using either EB1-GFP or GFP α-Tubulin. EB1-GFP allowed us to specifically characterize the growth of microtubules in the cell interior which is challenging due to absence of an interphase microtubule organizing center in

Drosophila cells (Rogers et al., 2008), making the cell interior a complex meshwork of overlapping microtubules with indistinguishable plus and minus ends. The cell periphery, however, was amenable to analysis by GFP-Tubulin, which allowed us to employ an automated microtubule tracking algorithm (see Materials and Methods and Figure S4)(Zhang et al., 2011) to analyze the various parameters of microtubule dynamic instability.

Observation of EB1-GFP dynamics in S2 cells revealed that the majority of plus end EB1 comets originated in the cell interior and translocated persistently through the cell with a velocity of 11.91 μm/min (±0.57, 95%CI) toward the cell periphery, so that the majority of plus ends were oriented radially at the cell periphery (Figure S1B, green tracks). When these interior EB1-GFP comets reached the cell cortex, they would disappear or stall momentarily before disappearing. We also observed a second population of EB1-GFP comets that specifically arose in the cell periphery, a region we defined coincidental with the cell lamella or roughly 3μm from the cell edge(Iwasa and Mullins, 2007). These peripheral EB1-GFP comets likely represented rescue events, growth of paused microtubules, or *de novo* nucleation of new microtubules originating in the cell periphery. Most surprisingly, these peripheral EB1-GFP comets polymerized at a slower velocity of 6.11 μm/min (±0.6, 95%CI)(Figure S1B, red tracks), suggesting that they perhaps experience different physical forces, such as actin retrograde flow, that influence their polymerization, or they have a different molecular complement at their plus ends than those in the cell interior.

In a series of complimentary experiments, we observed peripheral microtubule dynamics by imaging GFP-tubulin. Microtubules formed a fairly stable polymer mass in the cell interior (Figure S4A), while the peripheral microtubule ends were highly dynamic, best characterized by single growth and shrinkage events that spanned several microns with intermittent pauses and transitions to other dynamic states (Figure S4C). The growth rate of these peripheral GFP-Tubulin microtubules (6.134 μm/min, Table 1) also correlated to the slower population of peripheral EB1-GFP we had previously observed (Figure S1B). Thus, interphase S2 cells possess two populations of microtubule plus ends that exhibit different dynamics: 1) fast-growing interior plus ends that grow persistently with little pause or catastrophe, and 2), slower peripheral microtubules that are extremely dynamic, undergoing large growth and shrinkage events interspersed with pause.

Msps and EB1 are mutually dependent for their normal dynamics at microtubule plus ends.

We next wanted to test the hypothesis that Msps interacts with other +TIPs for its localization and ability to regulate dynamic instability. We focused specifically on EB1, since Msps and EB1 exhibit two interesting parallels with respect to their dynamics and functions in S2 cells: 1) both proteins localize to microtubule plus ends throughout the cell cycle; and 2) depletion of either molecule results in reduced dynamic instability and

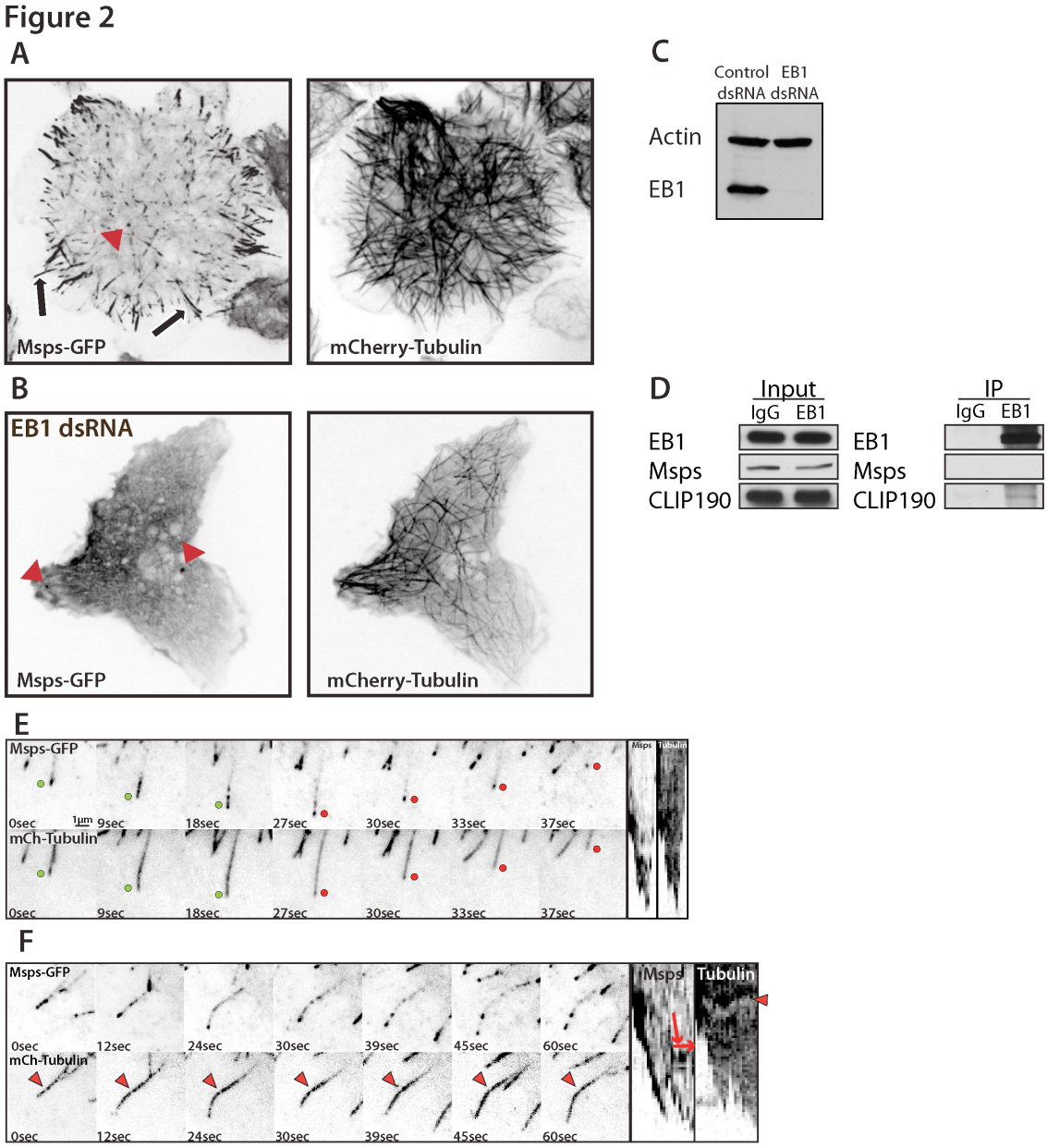

Figure 3-2. Msps-GFP dynamics in S2 cells is EB1 dependent.

(A, Movie 1) Interphase S2 cell expressing mCherry α-tubulin (right) and Msps-GFP (left) on microtubule plus ends in the interior, peripheral lattice accumulations (arrows) and centrioles (red arrowhead). (B) EB1-depleted S2 cell

expressing Msps-GFP (left) and mCherry α-tubulin (right). (C) Western blot demonstrating EB1 knockdown from (B) over 6 days RNAi. (D) Immunoprecipitation of EB1 and western blot for EB1 (right, top), Msps (right, middle), and EB1-binding protein CLIP190 (right, bottom). (E, Movie 3) Times series and kymograph of S2 cells expressing Msps-GFP (above) and mCherry α-tubulin (below). Growing ends are indicated by green dots and shrinking ends by red. (F, Movie 2) Msps-GFP dynamically moving along peripheral microtubules, represented as a kymograph (right). Yellow arrows on the kymograph (far right) indicate the direction of movement and red arrowheads represent a fiduciary fluorescent mark along the microtubule that indicates microtubule translocation (kymograph, right).

an increased microtubule “pause” state (Rogers, 2002; Brittle and Ohkura, 2005). Given these similarities, we wanted to explore how Msps influenced the dynamics of EB1 and vice versa by depleting one protein using RNAi and observing the other. Depletion of EB1 after 7 days RNAi treatment (Figure 2E) completely abolished the accumulation of Msps-GFP at the plus end and lattice of microtubules (Figure 2B), and this loss of Msps-GFP from microtubules seemed to enhance its localization to centrioles during interphase (Figure 2D, arrowheads, Movie 4). In control experiments, immunofluorescence of the endogenous Msps in EB1 RNAi conditions and exactly matched the localization of the exogenous transgene (Supplemental Figure S2A, B). In the reciprocal experiment, depletion of endogenous Msps dramatically reduced the accumulation and pattern of endogenous EB1 (Supplemental Figure S2C) or EB1-GFP at microtubule plus ends in most cells (Figure 3D-E) and completely eliminated it in a minority of the population (~10% of cells, data not shown). Under these conditions, EB1-GFP did not resemble typical EB1 “comets” observed in control cells (Figure 3A-B), but instead formed spot-like punctae on microtubule ends in the cell interior that exhibited short back-and-forth displacements (Figure 3F) moving at a velocity of 3.72 μm/min (±0.21, 95%CI) as opposed to the persistent, track-like vectors seen in controls (Figure 3C) that moved at a rate of 11.91 μm/min (±0.57, 95%CI). Similar observations were recently reported in *Drosophila* sensory neurons (Stone et al., 2008), as well as with temperature sensitive alleles of the *Arabidopsis* XMAP215 homolog, MOR1 (Kawamura and Wasteneys, 2008). To see if these proteins interact, we

performed co-immunoprecipitation using antibodies against EB1. Although we were able to pull down endogenous EB1 and a known EB1-binding protein, CLIP190, we were unable to co-precipitate endogenous Msps (Figure 2F), consistent with previous attempts to demonstrate binding in interphase extracts (Niethammer et al., 2007). This suggests that the mutual dependency for normal dynamics between EB1 and Msps may be due to synergistic effects on microtubule dynamics or may be mediated indirectly through another protein. Together, these data demonstrate that EB1 relies on Msps-dependent microtubule polymerization for normal dynamics, while proper localization of Msps is entirely dependent on EB1, although the two proteins may not interact directly.

Msps TOG domains are sufficient to promote microtubule polymerization and EB1 dynamics.

If Msps functions as a microtubule polymerase in living cells as it does *in vitro*, we hypothesized that the non-dynamic microtubules produced by Msps-depletion could not accommodate normal EB1 comet motility. Since TOG domains are sufficient to potently stimulate microtubule polymerization *in vitro* (Slep and Vale, 2007), we asked whether expression of the NH_2-terminal domains of Msps was sufficient to rescue microtubule growth, and concomitantly, EB1 behavior. We depleted endogenous Msps using RNAi targeting either the 5' untranslated region (5' UTR) or the non-TOG domain-containing COOH-terminus (Figure S1A), then expressed versions of the gene tagged at its COOH-terminus with TagRFP and observed EB1-GFP dynamics specifically in the cell interior

where we could observe persistent and fast plus end tracks in wildtype cells. Cells treated with Msps dsRNA and transfected with TagRFP alone exactly recapitulated the aberrant EB1 tip localization pattern described above (data not shown). Cells depleted of endogenous Msps and transfected with full-length Msps-TagRFP, however, exhibited EB1 comets of normal size that moved with an average velocity of 12.24μm/min (±0.72, 95%CI), a rate that was not statistically different from EB1 movements in cells treated with control dsRNA (11.91μm/min) (Figure 3S). We next prepared an expression construct embodying all five TOG domains (TOG1-5: residues 1 to 1428), transfected together with EB1-GFP, into cells depleted of endogenous Msps. Consistent with our hypothesis, TOG1-5 was able to rescue persistent EB1 plus end tracking (Figure 3G-I, Movie 5) to velocities of 8.12 μm/min (±0.74, 95%CI)(Figure 3S). To exclude the possibility that rescue of microtubule dynamics was due to overexpression of EB1-GFP, we performed the rescue without EB1-GFP and examined the localization of endogenous EB1 by immunofluorescence. We found that expression of TOG1-5 was sufficient to partially restore the localization pattern and length of endogenous EB1 on microtubule tips (Figure 3T), which has been shown to correlate to the measured velocity of EB1 comets in cells (Bieling et al., 2008). These data demonstrate that the TOG domains of Msps are sufficient to promote microtubule growth and indirectly support EB1 plus end tracking in living cells.

TOG domains function in paired functional units during microtubule growth *in vivo*.

We previously demonstrated that a tandem construct of Msps TOG1-2 formed a complex with tubulin by gel filtration chromatography, but did not promote microtubule polymerization *in vitro* unless artificially homodimerized or expressed as an arrayed construct (TOG1212)(Slep and Vale, 2007). These data suggested that the TOG domains of Msps functionally interact with tubulin as alternating paired arrays of A-type and B-type TOG domains. To test this hypothesis *in vivo* using the Msps RNAi/EB1-GFP rescue as an assay, we prepared an expression construct encoding the first four TOG domains (TOG1-4: residues 1 to 1080) fused to TagRFP and used this to replace endogenous Msps. As predicted by the model, TOG1-4 was also sufficient to partially rescue persistent EB1-GFP tip tracking to 9.42 μm/min (±0.66, 95%CI) (Figure 3J-L). This rescue of EB1 velocities was approximately equivalent to that of TOG1-5, suggesting that the first four TOG domains of Msps comprise the functional microtubule polymerase portion of the protein.

We next addressed whether individual pairs of TOG domains could functionally substitute for endogenous Msps using constructs encoding TOG1-2 (residues 1 to 498) or TOG3-4 (residues 583 to 1080). Strikingly, TOG1-2 exhibited a small rescue of EB1-GFP velocities within Msps-depleted cells (Figure 3M-O, Movie 6). EB1-GFP comets in TOG1-2-expressing cells were smaller than in control RNAi or TOG1-4-expressing cells and exhibited slower velocities of 6.0 μm/min (±0.7, 95%CI). Although comet movement was less processive as compared to control or TOG1-4-rescued cells, EB1-GFP movement usually persisted in a single direction, albeit slower with short phases

of pause, unlike the saltatory, back and forth movement in untransfected Msps RNAi cells (Figure 3O and Supplemental Figure S3). This EB1 movement produced by TOG1-2 was never observed under any other condition. Expression of TOG3-4, however, failed to produce any qualitative rescue of EB1 velocity (Figure 3P-R), although the measured velocity of 4.6 μm/min (±0.5, 95%CI) was statistically different than that of Msps depleted cells. These data suggest that Msps requires two paired arrays of TOG domains to act cooperatively *in vivo* to promote microtubule polymerization. Our results also suggest that Msps' TOG domains are not functionally equivalent and may have differential affinities for tubulin. To further test this, we used a previously described construct (Slep and Vale, 2007) that has the first two TOG domains arrayed twice in a single polypeptide with the normal linkers preserved (linker1 and linker2) between the TOG domains (TOG1212 tRFP). Surprisingly, this construct was not able to significantly rescue EB1 velocities (5.2 μm/min ±0.4, 95%CI, Figure 3S) compared with TOG1-4, suggesting that the unique combination of TOG domains 1-4 are required to effectively act as microtubule polymerase.

In addition to measuring EB1-GFP velocities, we also wanted to determine if the same TOG domain constructs could rescue other aspects of microtubule dynamics, specifically the highly dynamic peripheral microtubules we previously observed (Figure S4C). Using our automated microtubule tracking algorithm, we measured the dynamics of visible microtubule ends in the cell periphery after seven days of either control or Msps dsRNA. After Msps depletion, microtubules in the periphery no longer exhibited the large growth and shrinkage events that

characterized the wildtype peripheral microtubules. Although the average velocity of growth was unchanged between Control and Msps dsRNA treatment (Table 1), as previously observed (Brittle and Ohkura, 2005), the amplitude of these growth and shrinkage events was severely diminished, with small spurts of growth and shrinkage interrupted by pause or a small rescue/catastrophe transition (Figure 4C). Additionally, the primary characteristic of this treatment was the significant increase in the frequencies of pause (Table 1), in agreement with a previous study (Brittle and Ohkura, 2005). These data are consistent with a role for Msps as an important enhancer of microtubule dynamicity. Expression of either TOG1-4 or TOG1-5 was able to partially restore most of the parameters of dynamic instability, although these conditions maintained higher frequencies of transitions from growth to pause, suggesting that they could suppress catastrophe but were not able to fully restore the large persistent growth events seen in control cells. Interestingly, when these constructs were expressed in control or Msps dsRNA conditions, both TOG1-4 and TOG1-5 showed an increase in the microtubule shortening velocity over control cells, and in the case of TOG1-5/control dsRNA (7.55μm/min), significantly greater than that of untransfected Msps depleted cells (6.894μm/min). This suggested to us that in addition to promoting microtubule polymerization, these constructs also influence microtubule disassembly. The measured parameters of dynamic instability are summarized in Table 1. Overall these data reinforce the conclusion that the NH_2-terminus of Msps is capable of partially rescuing both EB1 velocities and dynamic instability.

Msps has a novel microtubule lattice-binding site that spans the linker region between TOGs 4 and 5 and TOG5 itself.

Having identified a function for the NH_2-terminal TOG domains in regulating microtubule behavior, we wondered how other uncharacterized domains might also contribute to Msps' function in cells. Since full-length Msps exhibited dual modes of microtubule interaction, we wanted to identify the domain(s) that allowed the protein to interact with either the lattice or to the plus end. When transfected into S2 cells, TOG1-5 exhibited a very robust localization along the lengths of microtubules during interphase and mitosis (Figure 4B and C), as well as spindle poles and condensed chromosomes in mitosis (Figure 6C). This pattern differed from the localization of full-length Msps, which was recruited, to plus ends and to peripheral microtubule segments, as described above. Transfected cells exhibited relatively low cytoplasmic pools of TOG1-5-TagRFP, suggesting that this construct interacted with microtubules with a relatively high affinity. In contrast, TOG1-4, was predominantly soluble in transfected cells (Figure 4D). TOG1-4 did not localize to mitotic spindle microtubules or poles, but did accumulate at condensed

Figure 3

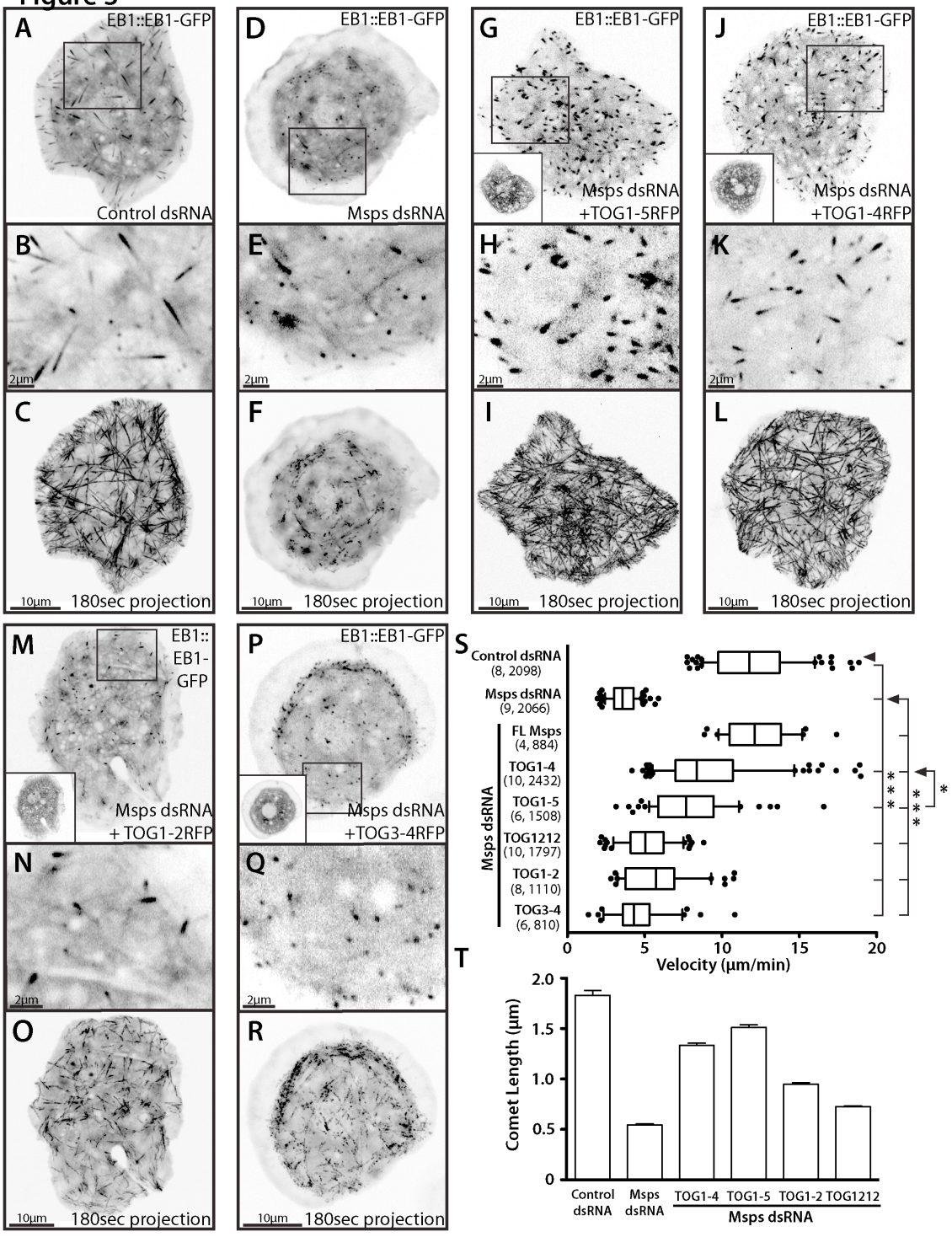
A
EB1::EB1-GFP
Control dsRNA
B
2µm
C
10µm
180sec projection
D
EB1::EB1-GFP
Msps dsRNA
E
2µm
F
10µm
180sec projection
G
EB1::EB1-GFP
Msps dsRNA
+TOG1-5RFP
H
2µm
I
10µm
180sec projection
J
EB1::EB1-GFP
Msps dsRNA
+TOG1-4RFP
K
2µm
L
10µm
180sec projection
M
EB1::
EB1-
GFP
Msps dsRNA
+ TOG1-2RFP
N
2µm
O
10µm
180sec projection
P
EB1::EB1-GFP
Msps dsRNA
+TOG3-4RFP
Q
2µm
R
10µm
180sec projection
S
Control dsRNA
(8, 2098)
Msps dsRNA
(9, 2066)
Msps dsRNA
FL Msps
(4, 884)
TOG1-4
(10, 2432)
TOG1-5
(6, 1508)
TOG1212
(10, 1797)
TOG1-2
(8, 1110)
TOG3-4
(6, 810)
***
***
***
*
0
5
10
15
20
Velocity (µm/min)
T
Comet Length (µm)
2.0
1.5
1.0
0.5
0
Control dsRNA
Msps dsRNA
TOG1-4
TOG1-5
TOG1-2
TOG1212
Msps dsRNA

Figure 3-3. Expression of Msps TOG domains are sufficient to partially rescue Msps microtubule polymerization and EB1 dynamics.

(A, Movie 4) Interphase S2 cell expressing EB1::EB1-GFP with wildtype localization (inset, B) and velocity visualized using a 180-second maximum projection (C). Localization and velocity is altered when cells are Msps dsRNA-treated (D-F), but can be partially rescued by addition of TOG1-5 TagRFP (G-I), TOG1-4 TagRFP (J-L), TOG1-2 (M-O, Movie 5) and by a very small amount by TOG3-4 (P-R). Insets in G, J, M, and P show TagRFP expression. (S) Distribution of EB1 velocities, dots indicate velocities outside the 10 and 90th percentile. Numbers in parentheses indicate cells analyzed and number of velocities, respectively. (T) Endogenous EB1 immunofluorescent comet length in cells treated with control or Msps dsRNA. Error bars are 95% CI. Asterisks indicate p value calculated using an unpaired t-test between two conditions (*, $p < 0.05$; ***, $p<0.0005$).

chromosomes in a fashion similar to TOG1-5 (Figure 4E). These data led us to hypothesize that Msps possesses a microtubule lattice-binding site in the region of the TOG5 domain. To test this possibility, we generated a series of additional Msps truncations fused to TagRFP, cotransfected them into S2 cells together with GFP-tubulin, and scored them for their ability to localize to the interphase microtubule lattice and to the mitotic spindle and spindle poles (Figure 4A).

Using the portion that comprised the difference between TOG1-4 and TOG1-5-TagRFP, we designed an expression construct starting from the linker region between TOG4 and TOG5 extending to TOG5 (linker4-TOG5: residues 1079 to 1428). When transfected into cells, linker4-TOG5-TagRFP associated strongly with microtubules, spindles, and poles (Figure 4F) indicating the presence of a microtubule binding activity in this region of Msps.

Multiple TOG domains are thought to have evolved through duplication events, such that linker2-TOG3 and linker4-TOG5 are similar class TOG domains and linkers of similar size with an overall positive charge. Therefore, we postulated that linker2-TOG3 might be a second microtubule lattice-binding domain similar to that of linker4-TOG5. To assess this, we generated an equivalent construct that included the linker between TOG2 and TOG3 extending to the end of TOG3 (linker2-TOG3-TagRFP: residues 498-821). We found that linker2-TOG3 did exhibit microtubule- and spindle-binding activities as well as the localization to condensed chromosomes as seen with TOG1-4 and TOG1-5 constructs (Figure 4G). The fact that this microtubule-binding activity is only apparent when the individual domain is expressed, as opposed to a larger region

such as TOG1-4, suggests that it is either regulated or somehow masked in the context of full-length Msps or TOG1-4.

Finally, we examined the localization of the COOH-terminal domain (residues 1407 to 2050) of Msps fused to TagRFP. This construct did not associate with the lattice of interphase microtubules, but was recruited to mitotic spindle poles (data not shown) consistent with published observations that the COOH-terminus of XMAP215 targets it to the centrosome in *Xenopus* (Popov et al., 2001).

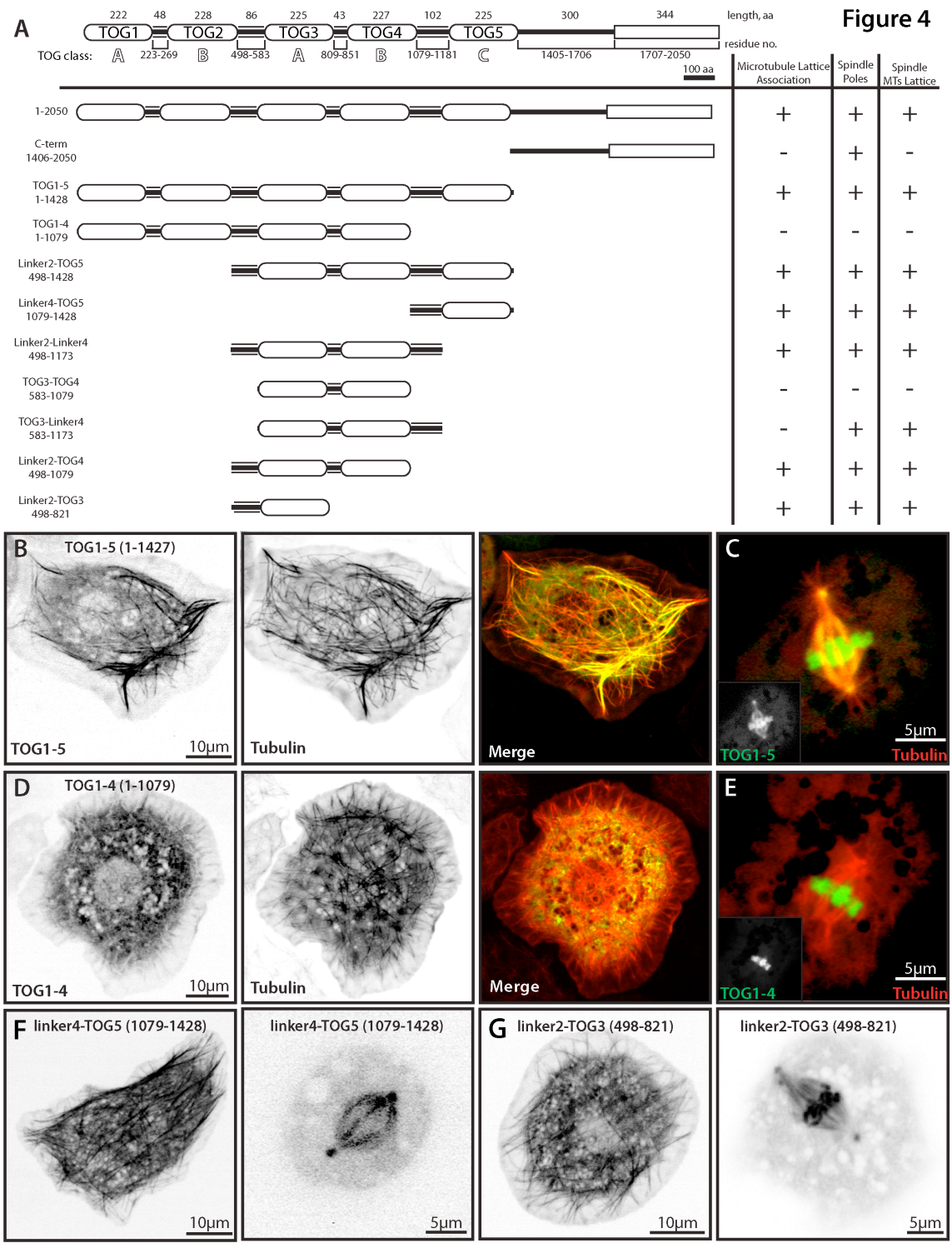

Figure 3-4. Structure/function analysis of Mini spindles reveals two microtubule lattice-binding sites.

(A) Domain structure of *Drosophila* Dis1/XMAP215 homolog, Mini spindles. COOH-terminal TACC interaction domain is indicated as a rectangle. All Msps constructs were COOH-terminally tagged with TagRFP and transfected with GFP-α-tubulin to observe localization to distinct microtubule structures. (B) Msps TOG1-5 TagRFP (left) colocalizes with GFP-α-tubulin (middle) in interphase and spindle poles, spindle microtubules, and condensed chromosomes in mitosis (C). (D) Msps TOG1-4 TagRFP (left) does not colocalize with GFP-α-tubulin (middle) in interphase or mitosis, but does localize to condensed chromosomes in mitosis (E). Insets represent single TagRFP channel from merge. (F) Linker4-TOG5 TagRFP in interphase (left) or mitotic (right) S2 cells. (G) Linker2-TOG3 in interphase (left) and mitotic (right) S2 cells.

Msps possesses conserved microtubule-binding motifs within the inter-TOG linker regions.

Our next objective was to define the minimal structural components in Msps linker4-TOG5 that were required for association with the microtubule lattice. Given the well-documented interactions between other TOG domains and tubulin, we hypothesized that TOG5 would be sufficient to mediate this interaction. We subdivided the construct into only the linker4 (residues 1079-1173) or TOG5 (residues 1173-1427), fused these fragments to TagRFP, and expressed them in S2 cells (Figure 5A). We were surprised to observe that neither fragment associated with microtubules *in vivo* alone, but rather exhibited a diffuse localization throughout the cytoplasm (data not shown), demonstrating that elements in both the linker4 and TOG5 domains were required together for microtubule lattice association. The orientation of the TOG domain and linker was also important, as TOG4-linker4 was not sufficient to bind microtubules in S2 cells (data not shown).

We hypothesized that TOG5 interacts with the microtubule lattice in a similar fashion to other TOG domains *in vitro*, via its intra-HEAT repeat loops (Slep and Vale, 2007). We previously found that a conserved non-polar residue on the first HEAT repeat loop is absolutely required for tubulin binding *in vitro* (Slep and Vale, 2007). In TOG5 this residue is a phenylalanine at position 1204. Mutagenesis of F1204 to glutamic acid in linker4-TOG5 prevented its localization to microtubules in interphase cells (Figure 5B). This result suggests that TOG5 is able to bind microtubules using the same surface used by other

TOG domains to bind to tubulin. Surprisingly however, this point mutation did not prevent linker4-TOG5 from localizing to the spindle or spindle poles in mitotic cells, indicating that there is either an enhanced affinity or an indirect association with the spindle during mitosis (Figure 5B, bottom).

To identify the residues in linker4 that are necessary for microtubule association, we made a series of NH_2-terminal truncations of the linker4-TOG5 fragment. Using this strategy, we found that a construct composed of residues 1099-1427 associated with microtubules, but a construct spanning residues 1111-1427 did not (Figure 5A). This observation suggested that the 12 residues (EEPKLKTVRGGG) spanning amino acids 1099-1111 were important for microtubule lattice binding. Because microtubule binding is often mediated through electrostatic interactions between positively charged residues on MAPs and the overall negatively charged surface of tubulin, we hypothesized that reversing the amino acid charge of residues within this necessary region of linker4 would eliminate microtubule association. Mutation of lysines and an arginine in this region of linker4-TOG5-TagRFP to either glutamic acid or alanine was sufficient to eliminate microtubule association in interphase (Figure 5B). To our surprise, this construct exhibited a weak, albeit very distinct, localization to the spindle and spindle poles as cells entered mitosis, similarly to linker4-TOG5 F1204E. These data indicate that this positively charged patch of residues in the linker4-TOG5 sequence is required for its association with microtubules during interphase.

We also tested if TOG5 was unique in its ability to cooperatively bind microtubules with linker4 or if other TOG domains would be sufficient for recruitment to microtubules by preparing a chimeric protein consisting of linker4 fused to TOG1, a type A TOG domain. Linker4-TOG1 did not associate with microtubules in interphase; however, it did localize to the spindle and spindle poles during mitosis (Figure 5D), which suggests that some region of the linker may act as a second mechanism to recruit Msps to the mitotic spindle. Indeed, GFP fusions of either linker2 (data not shown) or linker4 localized to the cytoplasm during interphase and to the spindle and spindle poles in dividing cells (Figure 5E). Taken together, these data identify a region in linker4 required for binding of linker4-TOG5 to interphase microtubules and further suggest that there is some specificity for TOG5 for this association. They also suggest that a second mechanism exists for recruiting Msps to the mitotic spindle via the inter-TOG linkers.

We next examined the sequences of linker2 or linker4 to determine if there were additional microtubule-binding motifs present in these regions of the protein. Although many Dis1/XMAP215 family members retain a high degree of sequence similarity within TOG domains, the linker regions connecting them share less sequence similarity.

Figure 5

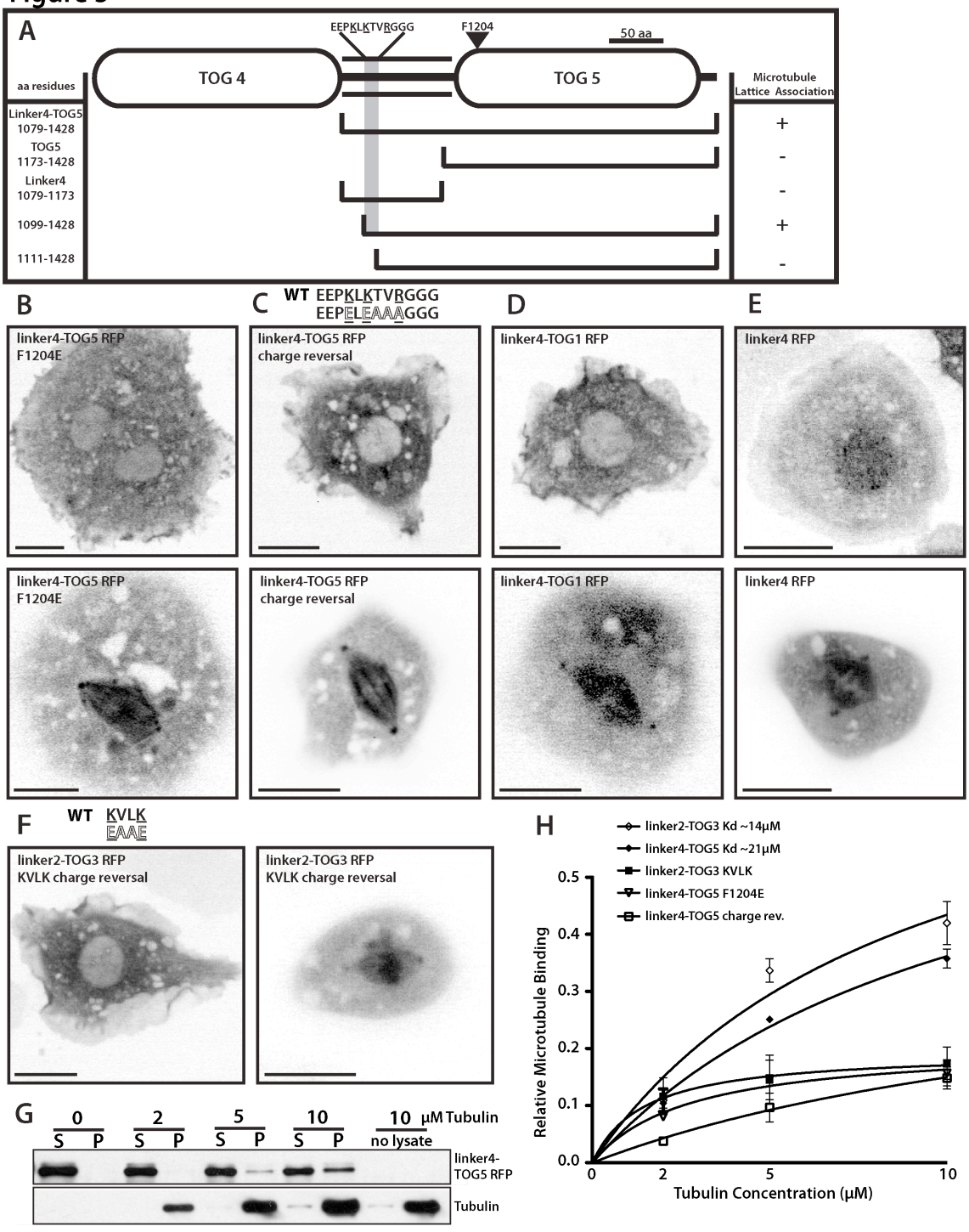

Figure 3-5. Msps has a novel microtubule lattice binding site that spans the linker region between TOGs 4 and 5 and TOG5 itself.

(A) Detailed domain structure of TOG4 through TOG5 (821-1428). Interphase (above) and mitotic (below) localization of linker4-TOG5 F1204E TagRFP (B), linker4-TOG5 charge reversal TagRFP (residues 1102-1107) TagRFP (C), chimeric linker4-TOG1 TagRFP (D), linker4 TagRFP (residues 1079-1173) (E). (F) linker2-TOG3 TagRFP with KVLK charge-reversal mutation in interphase (left) and mitosis (right). Scale bars represent 10μm. (G) Representative western blot of *in vitro* microtubule cosedimentation assay. (H) Binding curves summarizing *in vitro* cosedimentation assays for various Msps constructs. Dissociation constants are indicated where applicable. Error bars are 95% CI.

Generally, the linker2 and linker4 among higher animal and plant XMAP215 family members share similar lengths (approximately 100 amino acids) and an overall higher percentage of positively charged residues relative to linkers 1 and 3. By using the previously described region within either linker2 (residues 498-583) or linker4 (1099-1111) we were able to distinguish three unique motifs that occurred from NH_2-terminal to COOH-terminal within the linker2 or 4 region of Dis1/XMAP215 family members (Figure S5). The most conserved feature of these motifs was a sequence exactly matching or similar to “KVLK” within the third linker motif. Although the exact EEPKLKTVRGGG sequence was absent from Msps linker2, this domain does possess a stretch of residues rich in basic and non-polar amino acids that also contains this KVLK motif. To test if this region of homology could represent another cryptic microtubule binding site, we mutated the KVLK motif to EAAE within linker2-TOG3 and found that this completely abrogated the interphase microtubule-binding activity, but not mitotic spindle localization of linker2-TOG3 (Figure 5F). These data suggest the presence of a second microtubule interaction site in the second inter-TOG linker that contains at least one highly conserved binding motifs.

To verify that the microtubule interactions that we observed in S2 cells were mediated directly by the expressed fragments of Msps, we tested their ability to cosediment with microtubules *in vitro*. We expressed various pieces of Msps tagged at their COOH-terminus with TagRFP using a reticulocyte transcription/translation system, incubated the lysate proteins with taxol-stabilized microtubules, and centrifuged them through a glycerol cushion. The

supernatant and microtubule pellet were then collected and immunoblotted for the presence of TagRFP (Figure 5G). Both linker4-TOG5 and linker2-TOG3 cosedimented with microtubules, and by varying the concentration of tubulin we were able to extrapolate an apparent Kd, which is the concentration of tubulin at which half the translated construct would be expected to pellet (Figure 5H). Linker2-TOG3 and linker4-TOG5 had similar apparent Kd's of 14μM and 21μM, respectively. Linker-TOG constructs containing mutations that abrogated microtubule association *in vivo* only minimally cosedimented with tubulin at levels approaching background detection. These domains bind tubulin at lower affinities than what has previously been observed for other full length XMAP/Dis1 family members (Spittle et al., 2000; Al-Bassam et al., 2010). We postulate that this may be due to cooperative interactions within the full-length protein between both microtubule binding sites and the added interactions of TOGs 1, 2, and 4 with tubulin.

The linker regions are necessary for Msps peripheral lattice association and influence microtubule dynamics in the cell periphery

To determine how Msps microtubule lattice association via linker2-TOG3 and linker4-TOG5 influence its dynamics and function in cells, we created full-length constructs that contained either the linker2 KVLK charge reversal mutation, the linker4 charge reversal mutation, or both mutations (Figure 6A). When tagged COOH-terminally with GFP and expressed in cells depleted of endogenous Msps using 5'UTR dsRNA, either of single mutants appeared qualitatively similar (data not shown) to wild type Msps (Figure 6B). This

suggests that in context of the full-length molecule, the inter-TOG linker microtubule binding sites act redundantly or can compensate for loss of the other. The double mutant Msps (Double Mut Msps), on the other hand, displayed significantly altered localization and dynamics compared to wild type Msps when expressed in Msps depleted cells (Figure 6C). Firstly, in the peripheral lamella, the microtubule lattice association was greatly reduced (Figure 6E, Movie 7) compared to wild type (Figure 6D). Double Mut Msps-GFP displayed no discernible association along the length of microtubules, and no longer decorated the lattice as a discontinuous patch of GFP fluorescence (Figure 6D). Instead the Double Mut Msps localized primarily to small comet-like structures on the plus end of lamella microtubules (Figure 6E). Using fluorescent intensity line-scans, this reduction in the peripheral lattice binding was readily apparent compared to both wild type Msps-GFP and EB1-GFP (Figure 6F). In addition to the alteration of Msps dynamics, expression of Double Mut Msps also affected the morphology and dynamics of microtubules in the cell periphery. In control cells, microtubules that enter the cell lamella are often highly dynamic, growing straight until they encounter the cell cortex at a perpendicular angle before undergoing a catastrophe that depolymerizes the microtubule out of the peripheral region (Figure 6B, D). In cells only expressing Double Mut Msps, however, long microtubules were often observed to curl away from the periphery (Figure 6C, E, Movie 7); we postulated this was caused by continued microtubule growth after contact with the cell cortex. Our hypothesis was confirmed by time-lapse images in which microtubule plus ends in the cell periphery grew and stalled at the cell

edge or would begin to curve and grow parallel to the cell lamellipodia. These peripheral microtubules were decorated with small comet/dots of Double Mut Msps and seemed to exhibit shorter durations of depolymerization before recovering and growing again (Figure 6H, Movie 8) compared with wild type Msps (Figure 6G, Movie 8).

In order to examine the dynamics of these peripheral microtubules we first wanted to set a baseline of microtubule dynamics within cells expressing exogenous full length (FL) Msps-GFP. Expression of FL Msps-GFP in addition to endogenous Msps (Control treated cells) closely replicated untransfected control cells with the exception of increased growth and shrinkage rates (Table 2). Rescue of Msps 5' UTR dsRNA-treated cells with FL Msps-GFP caused an increase in microtubule growth and shrinkage, suppressed catastrophe, and increased microtubule transitions out of pause. Expression of a single linker2-mutated full length Msps-GFP elevated growth and shrinkage rates, but had no affect on the dynamic transitions of control-treated cells and was fully competent to rescue Msps 5'UTR depletion.

We next examined the effect of Double Mut Msps on peripheral microtubule dynamics. In control treated cells, Double Mut Msps had little effect on microtubule dynamics, although it did result in elevated growth and shrinkage rates. However, when S2 cells were depleted of endogenous Msps by 5'UTR dsRNA, Double Mut Msps had a notable effect on both the rates of growth and shrinkage and the dynamic transitions of microtubules. Double Mut Msps did not elevate growth rates as other full length

Figure 6

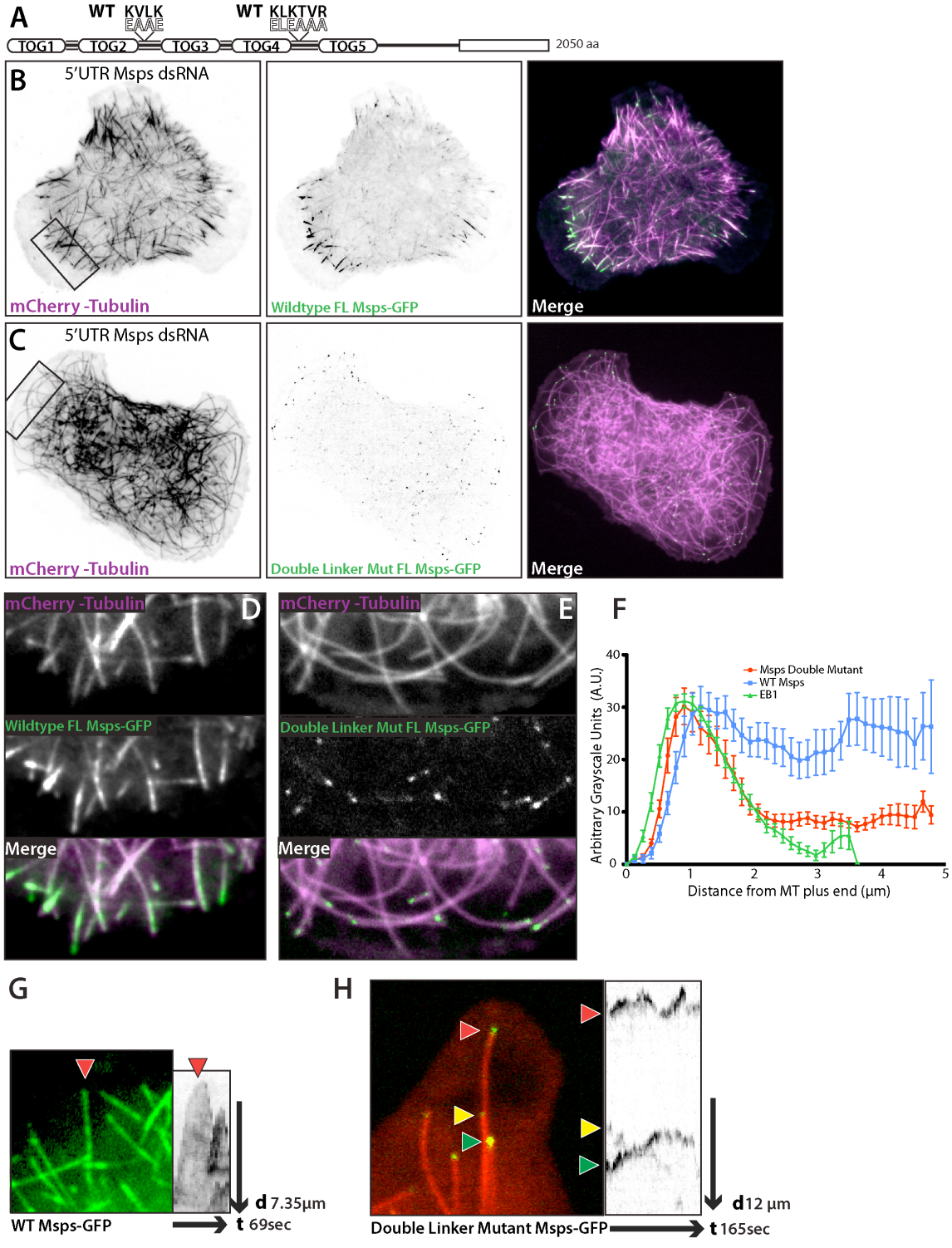

Figure 3-6. Mutation to the linker regions of Msps abrogates interaction with the lattice of peripheral microtubules.

(A) Cartoon schematic of full-length double mutant Msps (Double Mut Msps) that contains the linker2 “KVLK” charge reversal and linker4 charge reversal. (B) Interphase S2 cell depleted of endogenous Msps using 5‘UTR dsRNA, expressing wild type Msps-GFP (B, Movie 6) or Double Mut Msps-GFP (C). (D) Inset of B, with Msps Double Mut-GFP (top), mCherry-Tubulin (middle), and the merge (bottom). Linescans across plus ends of S2 cells expressing either EB1::EB1-GFP, full length wild type Msps-GFP, or full-length double mutant Msps-GFP (Double Mut Msps). Linescans for Msps are of peripheral microtubules at equal exposures and time frames, error bars are standard deviation. (E, Movie 7) Peripheral microtubule decorated with wild type Msps-GFP and the associated kymograph. (F, Movie 8) Peripheral microtubule end with Double Mut Msps-GFP and kymograph.

constructs could and had a slightly negative effect on growth rates, unlike any other construct we had previously analyzed. More surprising, was the affect on dynamic transitions. Rescue by Double Mut Msps-GFP resulted in a decrease in transitions from either growth or shrinkage into pause (G/S ➔ P) as well as the inverse of paused microtubules transitioning into growing or shrinking microtubules (P ➔ G/S) (Table 2). If we broadly classify paused microtubules as non-dynamic and growing or shrinking microtubules as dynamic, these data suggest that Double Mut Msps-GFP microtubules were more likely to stay locked in either dynamic or non-dynamic states and were unable to transition normally between these states. This suggests that Msps' interactions with the lattice of peripheral microtubules plays a key role in balancing dynamic instability in this population of plus ends.

Discussion

Growing evidence from several model systems indicates that members of the XMAP215/Dis1 protein family enhance microtubule dynamic instability and mitotic spindle assembly (Kinoshita et al., 2002). These multi-domain proteins are highly conserved across taxa and there is particular interest in the human homologue, ch-TOG, as its overexpression has been documented in several cancer cell types (Charrasse et al., 1995; 1998). Despite the importance of these proteins, we know relatively little about their dynamics in living cells or about how their domain structure relates to their function *in vivo*. In this study, we have used the *Drosophila* XMAP215 homologue, Mini spindles (Msps), as a model to

address these questions in living S2 cells. We found that Msps exhibits a complex and dynamic behavior *in vivo*. It localizes both to growing and shrinking microtubule plus ends. In the actin-rich cell periphery, Msps-GFP punctae exhibit a discontinuous and dynamic association with the microtubule lattice. Consistent with roles for both Msps and EB1 as key regulators of dynamic instability, we observed that depletion of either of these proteins lead to alteration of the other's dynamics at microtubule plus ends. Remarkably, microtubule dynamics and EB1 velocity could be partially restored by replacing endogenous Msps with the NH_2-terminal four TOG domains TOG1-4. Our structure/function analysis also revealed the presence of novel microtubule lattice-binding domains, which include sequences in two of the inter-TOG linker domains. These linkers contain novel motifs responsible for this interaction and are important for the normal dynamics of Msps as mutation of these motifs causes a loss of Msps from the lattice of peripheral microtubules and an alteration to the morphology and dynamics of the microtubule cytoskeleton. Thus, our data demonstrate that Msps is able to interact with microtubules through at least two mechanisms and that this bimodal interaction is required for normal dynamic instability.

Our study, the first detailed examination of a Msps/Dis1 family member in a living animal cell, revealed that Msps exhibits a complex pattern of dynamics. Throughout the cell, Msps localizes to the plus ends of growing microtubules, consistent with other published descriptions of Msps behavior in early *Drosophila* embryos (Lee et al., 2001) and *in vivo* dynamics of homologues Stu2 (*S. cereviscae*, (He et al., 2001; Kosco et al., 2001; van Breugel et al., 2003; Tanaka

et al., 2005; Wolyniak et al., 2006), Alp14 (*S. pombe*, (Sato et al., 2004; Garcia, 2001; Nakaseko et al., 2001), and AlpA (*A. nidulans*, (Enke et al., 2007). Our observations in S2 cells are in line with family members acting as microtubule polymerases that promote the incorporation of free tubulin at the plus end. Msps also exhibits dynamics similar to the *in vitro* behavior of XMAP215 (Brouhard et al., 2008) as both proteins remain associated with microtubules during phases of growth and shrinkage. At present, the biological significance of Msps association with shrinking microtubules is not understood, however, Stu2 and XMAP215 do destabilize microtubules under specific *in vitro* experimental conditions (van Breugel et al., 2003; Shirasu-Hiza, 2003; Brouhard et al., 2008). Persistent interaction with shrinking microtubules may reflect a physiologically important role for Msps during depolymerization *in vivo*. We favor a model based on this interaction with both growing and shrinking microtubules, first articulated by Shirasu-Hiza *et al.* (2003) and further elaborated by Brittle and Ohkura (2005), in which Msps acts, not only as a polymerase, but as an anti-pause factor that is capable of “catalyzing” the transition to either polymerization or depolymerization (Figure 7). Although it has primarily been shown to enhance the growth of microtubules, Msps is also necessary for their transition to disassembly *in vitro* and *in vivo*. These two seemingly opposing roles are mediated by 1) the TOG domains and plus end localization which enhance microtubule growth; and 2) microtubule lattice binding sites within linker2-TOG3 and linker4-TOG5 which enhance the transition between dynamic and non-dynamic states and also influence microtubule disassembly rates. Regulation and balance of these two

domains maintain normal microtubule dynamics. In the future, it will be interesting to learn if these *in vivo* dynamics also apply to XMAP215 or human chTOG, which remain largely uncharacterized in cells.

One of the central observations from this work was that the NH_2-terminal TOG domains of Msps are the key determinants of the protein's activity *in vivo*. Several previous studies have indicated a role for TOG domains as primary binding sites for tubulin in XMAP215/Dis1 proteins (Spittle et al., 2000; Popov et al., 2001; Gard et al., 2004; Al-Bassam et al., 2007; Slep and Vale, 2007). Biochemical analysis of the TOG domains from Msps revealed that TOG1-2 was the minimal construct that was able to bind tubulin (Slep and Vale, 2007). Moreover, a construct consisting of a tandem array of TOG1212 functioned as a potent microtubule nucleator *in vitro*, suggesting that multiple pairs of TOG domains act in concert to promote polymerization. We found that a fragment of Msps containing TOG1-4 was sufficient to rescue many aspects of microtubule dynamic instability in living S2 cells depleted of endogenous Msps, both in terms of interior EB1-GFP growth velocities and persistence as well as the frequencies of catastrophe and rescue. Consistent with the *in vitro* data, constructs embodying TOG1-2 imparted only a slight rescue of microtubule growth in S2 cells, while TOG3-4 did not. These data imply that individual pairs of TOG domains may contribute unequally to the activity of the protein, but do function cooperatively to promote persistent microtubule growth. The lack of rescue by TOG1212 also indicates that each pair of TOG domains is uniquely suited to fulfill the cooperative function of tubulin addition. Although TOG1-4 exerted a

strong effect on tubulin incorporation and loss from the plus end as measured by GFP-Tubulin and EB1-GFP growth rates, the TOG1-4 protein exhibited a predominantly cytoplasmic localization and did not accumulate at microtubule tips. These data suggest a mechanism in which TOG1-4 is able to associate with one or more tubulin heterodimers to transiently promote their addition or loss from the plus end (Figure 7, number 2) without interacting in a processive manner (Figure 7, number 1) or associating with the microtubule lattice (Figure 7 number 3).

Another key observation is the identification of novel microtubule interaction sites spanning the TOG3 and TOG5 and their preceding inter-TOG linkers. These sites are necessary for association with the microtubule lattice and for the lattice-associated diffusive movements exhibited by full-length Msps. Our analyses identified the presence of conserved motifs in the inter-TOG regions that were enriched in basic amino acid residues, which we predict form an electrostatic interaction with the negative COOH-terminus of tubulin. The linkers between Msps' TOG domains are predicted to be disordered stretches without secondary structure that that we found to cooperate with the highly structured TOG3 or TOG5 to mediate microtubule binding. The cooperation between ordered and disordered domains to mediate microtubule binding has become a common trend as more of the structural determinants of MAP-microtubule association have recently been elucidated (Subramanian et al., 2010; Guimaraes et al., 2008). These disordered regions seem to allow a diffusion-capable attachment to microtubules in addition to the ability to "titer" the interaction

strength by charged residue addition or modification (i.e., phosphorylation) (Kumar et al., 2009).

Whatever the structural basis for microtubule lattice-association, we observed that Msps employs this mechanism in a spatially restricted manner in the actin-rich lamella of S2 cells. In other cell types, microtubules that enter this subcellular compartment exhibit decreased catastrophe rates, due to the small GTPase Rac1 regulating MAPs that influence microtubule dynamics (Wittmann et al., 2003; 2004). In this regard, the spatial transition from plus end binding to MAP lattice association has also been observed in mammalian epithelial cells for the +TIP CLASP (Wittmann and Waterman-Storer, 2005). In our hands, the *Drosophila* CLASP homolog, Orbit/MAST, when tagged with GFP displayed plus end dynamics similar to that of EB1 and did not differentially localize in the periphery of the cell (unpublished observations, J.C and S.R.). One possibility is that Msps functions in an orthologous manner to mammalian CLASP, which could be due to their shared structure as TOG domain-containing proteins. In any case, we speculate that this transition from tip-tracking to lattice-binding reflects a regulated change in the conformation of Msps. Given the observation that TOG1-5 decorates the microtubule lattice constitutively, we also hypothesize that the COOH-terminus of the protein is involved in this regulation and acts to "gate" the microtubule binding activity of linker4-TOG5 in the full length protein. Future studies will address the basis of this regulation.

Ablating these microtubule lattice association sites in the full-length molecule had a dramatic effect on the dynamics and morphology of the

microtubule cytoskeleton. Although lattice association is commonly a stabilizing property of most MAPs, we were surprised to find that without its normal lattice association, Msps Double Mutant produced very stable microtubules that exhibited fewer transitions and continuous growth after microtubules encountered the cell cortex. In contrast, although Msps dsRNA also produces very stable microtubules, these microtubules are seldom able to persistently grow against the actin retrograde flow in the peripheral lamella. These data, in conjunction with the increased shrinkage rates we observed when cells expressed TOGs1-4 or TOG1-5, lead us to propose that these lattice association sites may influence the catalysis between dynamic states and the shrinkage rates of peripheral microtubules. Microtubules in peripheral regions of S2 cells exhibit increased dynamic instability as compared to the interior of the cell and our data suggest a mechanism through which Msps may regulate these peripheral behaviors through its lattice association.

We hypothesize that this influence on dynamics could be caused by three non-mutually exclusive mechanisms. Firstly, Msps lattice association could act to "strip" Msps from the plus end, potentially taking heterodimers with it and lowering the concentration of this polymerase from the microtubule tip. Secondly, Msps' lattice binding domains could act to slightly perturb lateral interactions between heterodimers along the decorated protofilament. This cascade of small perturbations could act to prime the microtubule lattice for depolymerization several microns distal to the plus end. Finally, lattice-bound Msps could be acting

in concert with other +TIPs, such as kinesin-13 depolymerases, to influence catastrophe and shrinkage.

Msps' dependence on EB1 for its plus end localization in interphase is novel in light of our current knowledge of XMAP215/Dis1family members, but is a property of most +TIPs characterized to date. Unlike most other EB1 interactions, however, there is a mutual reliance on each protein for normal plus end dynamics. For Msps, EB1 seems to be absolutely required for plus end localization as well as for its association with microtubule lattice structures. Although we have no data for how this might happen, it suggests that the ability of full-length Msps to recognize the microtubule lattice is in some way tied to its plus end association. One possibility could be a whole-molecule conformational change that occurs when Msps interacts with EB1 at the growing end, which might be required to license Msps for association along the microtubule lattice. This most likely is concurrent with some other spatially regulated control that gives Msps a bimodal function between the cell interior and the periphery. EB1's plus end localization does not require Msps, as a population of EB1 remains on microtubule tips following Msps depletion, however, its dynamics are drastically altered. Rescue of EB1 velocities using the TOG domain region of Msps suggests that EB1 relies on the polymerase activity of Msps for its normal dynamics. This also seems true since Msps fragments that rescue EB1-GFP comet formation do not seem to localize to the microtubule plus end, although we cannot rule out the possibility that there may be transient pools of TOG domain-fragments at the plus end. Instead, we favor a model where these TOG domain

fragments act en masse to chaperone tubulin onto the plus end, subtly influencing the on and off rates of heterodimer addition. This creates a plus end structure with sufficient binding sites to support more normal EB1 comets.

Based on our data, Msps exhibits at least two modes of interaction with microtubules, both of which are essential to promote normal parameters of dynamic instability. We envision a cycle of interactions that begins upon association between soluble Msps and one or more tubulin heterodimers. The Msps-tubulin complex then recognizes the microtubule plus end and associates transiently. The molecular basis of this recognition is unknown, but may reflect a conformation of tubulin at the plus end (e.g. a growing sheet), a chemical signature (e.g. a cap of GTP tubulin), the presence of another +TIP such as EB1, or some combination of these. Upon binding, Msps delivers its tubulin 'cargo' to promote polymerization. In the cell interior, Msps then dissociates, thus behaving as a typical +TIP. In the cell periphery, however, following tubulin delivery, Msps receives a signal that causes it to engage its lattice-binding activity and to diffuse along the microtubule surface. Msps also associates with microtubule plus ends upon transition to catastrophe, perhaps working cooperatively with destabilizing factors such as kinesin-13 proteins and stathmin/OP18.

Acknowledgements

We thank Mark Peifer and members of the Rogers, Peifer, and Slep labs for helpful advice and H.O. Lee for critically reading the manuscript. We also thank

Hiro Ohkura, Jordan Raff, and Roger Tsien for sharing reagents. S.S. and A.M. are supported by the NIH grant R01GM086536 to A.M. This work was supported by grants from the NIH (RO1GM081645) and Beckman Foundation to S.L.R.

Methods

Cell culture and RNA interference

Culture and RNAi of *Drosophila* S2 cells was performed as previously described (Rogers and Rogers, 2008). For RNAi, the T7 promoter sequence was appended to gene-specific primer sequences to generate dsRNA using T7 RiboMAX *in vitro* transcription (Promega). Primer sequences used for approximately 1.5Kb of the Msps 5'UTR are fwd 5' CGCAACGACGCTGTTGG-3' and rev 5'-TCGTGTTTCGTACGCTAC-3'. Msps COOH-terminal dsRNA was made against amino acids 1752-1927, fwd 5'-GCCGAAGTTTACAGACCTGC-3' and rev 5'-TGTACTTGTGAAATGGGGCA-3'. EB1 dsRNA primers fwd 5'-GAGAATGGCTGTAAACGTCTACTCCACAAATGTG-3' and rev 5'-GAG ATGCCCGTGCTGTTGGCACAGGCGTTTA-3'.

Immunofluorescence microscopy

Methodology for the fixation of S2 cells was adapted from previously described protocols (Rogers and Rogers, 2008). S2 cells were seeded on coverslips coated with concanavalin A (con A) for 1 hour, washed briefly in BRB80 buffer

(80mM PIPES, pH 6.9; 1mM magnesium sulfate; 1mM EGTA), and fixed for 10 minutes in methanol pre-chilled to -80°C. Antibodies used in this study for immunofluorescence were: Msps (described below) 1:1,000, actin (Millipore MAB1501) 1:500, α-tubulin (Sigma DM1α) 1:1,000, and anti-EB1 (Rogers et al., 2002). Secondary antibodies Cy2, Rhodamine red, and Cy5 (Jackson ImmunoResearch Laboratories) were used at a final concentration of 1:300. Cells were imaged using either a Nikon Eclipse Ti-E or a Leica TCS SP5 X laser-scanning confocal.

Immnunoblotting

Samples for immunoblots were prepared as described (Rogers et al., 2009) and resolved on 7-12% SDS-PAGE gels. RNAi efficacy was assayed by immunoblot and the protein loads were normalized using α-actin antibody (Millipore MAB1501). Percent depletion was determined by densitometry using scanned film images with ImageJ (NIH).

Immunoprecipitation

S2 cells grown under normal culture conditions (see above) were pelleted at 8,000 rpm for 2min and resuspended in lysis buffer (150 mM NaCl, 1 mM DTT, 50 mM Tris, 0.5% Triton X-100, 2.5 mM PMSF, 0.5 mM EDTA, and Complete EDTA-free protease inhibitor cocktail (Roche). Lysates were precleared by centrifugation and then diluted two fold with lysis buffer. Samples were removed for input controls before being incubated with either mouse IgG (Sigma), or anti-EB1 (Rogers, 2002) at 4°C for 2 hours followed by incubation with Sepharose

Protein A beads for another 2 hours. Sepharose Protein A bead immuno-complexes were washed three times with lysis buffer and then resuspended in Lamelli sample buffer. Samples were run on SDS-PAGE and immunoblotted using either anti-EB1 (Rogers, 2002), anti-Msps (this manuscript), or anti-CLIP190(Dzhindzhev et al., 2005).

Antibody production

Antibodies were raised in rabbits (Proteintech Group) against *Drosophila* Mini spindles TOG2 domain (residues 267-500) (Slep and Vale, 2007). Antibodies were further affinity-purified using either recombinant TOG2 or TOG1-TOG2 (residues 1-505) (Slep and Vale, 2007).

Microtubule Cosedimentation Assay

Microtubule cosedimentation was performed using a variation of previously published work (Spittle et al., 2000); Campbell and Slep, 2010). Briefly, fragments of Msps were subcloned using Topo-D pEntry vectors (Invitrogen) with a COOH-terminal TagRFP and then recombined into the pDEST17 bacterial expression vector with 5' T7 promoter sites. These plasmids were then used as templates for *in vitro* transcription/translation reactions (TNT, Promega). After a 90 minute incubation, the lysates were diluted threefold in BRB80 buffer and clarified for 30 minutes at 100,000xg. 60µl of the clarified lysate (representing 100-200ng translated protein according to the manufacturers estimates) were then added to varying concentrations of taxol-stabilized microtubules for 20 minutes. These reactions were then spun through a glycerol cushion for 30

minutes at 100,000xg and samples were taken from the supernatant (60µl supernatant added to 60µl 2x Lamelli buffer) and washed pellet (60µl fresh BRB80 with 60µl Lamelli buffer). Equal volumes were loaded onto a SDS-PAGE gel from all reactions and were immunoblotted for TagRFP at 1:1000 (Evrogen) and then 1:750 anti-rabbit HRP. The resulting film was scanned and densitometry was performed to determine the relative amount of translated protein in the supernatant and microtubule pellet. Relative binding affinity was plotted as the percent of total protein pelleted, i.e., the pellet's intensity divided by the added intensity of both supernatant and pellet. These were plotted against the concentration of microtubules and a curve was fit to the points using non-linear regression of one-site binding (Graphpad Prism). Based on the curve formula, an apparent Kd was calculated where exactly half of the translated protein would be expected to pellet with microtubules.

Molecular biology and Transfection

EB1::EB1-GFP was constructed subcloning ~1.5Kb genomic DNA sequence 5' of the EB1 gene in front of the 5' start of EB1-GFP (Rogers et al. 2002). All fragments of Mini spindles were sub-cloned into a metallothionein promoter, pMT A vector backbone (Invitrogen) that contained a COOH-terminal fusion of TagRFP (Roger Tsien; Shaner et al., 2008). A previously described Msps construct (Lee et al., 2001) was used as a cDNA template and all constructs were amplified by either Pfu or KOD polymerase (Novagen). Full-length Msps-GFP was sub-cloned using the Gateway TopoD pEntr system (Invitrogen) into a final zeocin-selectable pIZ backbone (Invitrogen) that had both the

metallothionein promoter as well as the Gateway (Invitrogen) LR recombination sites inserted into the multi-cloning site. Transfections were performed using the Amaxa Nucleofector II transfection system (Lonza) according to manufacturers' protocols. Constructs were induced 24 hours after transfection with 40μM copper sulfate for approximately 12-18 hours before imaging.

Live Cell Microscopy

S2 cells were seeded onto ConA-coated glass-bottom dishes (MatTek) in Schneiders growth medium at room temperature (~25°C) one hour prior to imaging. Time-lapse images were acquired with a 100x NA 1.45 Plan Apochromat objective using a Yokogawa (Perkin-Elmer) or VT-Hawk(Visitech) confocal systems, captured with Hamamatsu Orca-ER and Orca-R2 cameras, respectively. MetaMorph and VisiTech Vox software were used to control the respective confocal systems and acquire images. Images were acquired at three second intervals over periods of 3-10 minutes.

EB1-GFP Comet Tracking

EB1-GFP velocities were acquired from timelapse movies (described above, Yokogawa spinning disc) using the ImageJ (NIH) Manual Tracking plugin (Fabrice Cordelieres, Institut Curie). Single comets were manually tracked for their full life time and the mean comet velocity was calculated using the instantaneous frame-to-frame velocity. The collection of mean comet velocities

were then plotted by a box and whisker plot and statistical comparisons were made between two conditions using an unpaired t-test (Graphpad Prism).

Automated Microtubule Tracking

Definition of the tracking region. For each cell, we tracked microtubules in a hand-selected region-of-interest (ROI). It consists of an outer (the cortex; Figure S4) and an inner (to avoid tracking the crowded interior) boundary. In all calculations, the data from cells of the same treatment (Control dsRNA, Msps dsRNA + TOG1-4, etc.) were pooled.

Definition of growth and shrinkage.

To define growth and shortening behavior, we calculated the angle α between the direction of the displacement of the microtubule tip and the direction of the microtubule itself. A value of $\cos(\alpha)>0.2$ ($\alpha<\sim78°$) indicated probable growth, and $\cos(\alpha)<-0.2$ ($\alpha>\sim101°$) indicated probable shortening. For a microtubule to be counted as growing or shortening, we required that it display the same behavior (either growing or shortening) for at least two consecutive frames, and that the overall displacement in a run of growth or shrinkage be at least 3 pixels.

Calculating state populations.

State populations were calculated as the total amount of time observed for a state (growing, shortening, or paused) divided by the total amount of time observed in the trajectories. Confidence intervals were estimated by a BCa-

corrected bootstrap procedure that resampled the trajectories included in this statistic 1000 times.

Calculating transition rates.

To calculate transition rates, each frame of a microtubule trajectory was marked as either grow, shorten, or pause. Grow and shorten states were defined as previously described. Pause was defined as neither growing nor shortening. The lifetimes of states that began and ended in the middle of a trajectory (not on a boundary), as well as the state they transitioned to, were collected. The rate of transition between an initial state k (k=grow, shrink, or pause) and a final state l (l≠k) is

$$\left[\frac{\#\text{ Transitions from } k \text{ to } l}{\#\text{ Transitions out of } k}\right] \times \left[\frac{1}{\#\text{ Transitions out of } k}\right] \sum_i \left(\frac{1}{\left[\begin{array}{l}\text{length in state } k \\ \text{before transition } i\end{array}\right]} \right)$$

We used a bootstrap approximation to construct 95% confidence intervals of each transition, with 1000 resamples of all lifetimes. Statistical significance was established using a two-sided permutation test with 10000 resamples of the statistic $r_{control,i} - r_{treatment,i}$, where $r_{control,i}$ and $r_{treatment,i}$ correspond to the rates calculated in resample *i* of the control vector and the treatment vector (e.g., Msps dsRNA, Msps dsRNA + TOG1-4, etc.).

Table I. Microtubule dynamics parameters rescued with NH^2-terminal TOG domain constructs

	Events / minute (min^{-1})						μm / minute	
	G → S	G → P	S → G	S → P	P → G	P → S	Growth velocity	Shortening velocity
Control dsRNA (5, 2230)†	1.057	6.137	1.114	6.223	3.037	2.813	6.134	6.076
Msps dsRNA (3,1008)	1.161	6.871 *P* = 0.004**‡	0.740 *P* = 0.039*	6.728 *P* = 0.035*	1.930 *P* = 0.007*	4.057 *P* = 0.001**	6.406	6.727 *P* = 0.017*
Control dsRNA +TOG1-4 (3, 990)	0.974	6.284	0.985	6.547	3.208	3.206	6.087	6.813 *P* = 0.0071*
Msps dsRNA +TOG1-4 (4, 440)	0.945	7.0362 *P* = 0.0076*	1.116	6.460	2.786	3.602	6.062	6.229
Control dsRNA +TOG1-5 (6, 2011)	1.08	6.757 *P* = 0.0018**	1.127	6.800 *P* = 0.0037**	3.114	3.116	6.192	7.551 ****
Msps dsRNA +TOG1-5 (5, 2753)	1.08	6.383	1.051	6.413	3.298	3.240	6.183	6.534 *P* = 0.043*

Table 3.1. Microtubule dynamics parameters rescued with NH2-terminal TOG domain constructs

†Numbers in parentheses indicate the number of cells analyzed and the analyzed events for each condition, respectively. ‡ Indicates values statistically different from Control dsRNA where $P < 0.05$. * indicates $P < 0.05$, ** $P < 0.005$, *** $P < 0.0005$, and **** $P < 0.00005$. Statistical significance for transition rates was determined using a two-tailed permutation test with 10,000 resamples. For growth and shrinkage rates, a two-sample t-test was used to determine statistical significance.

Table II. Microtubule dynamics parameters with full-length Msps transgenes

	Events / minute (min^{-1})						μm / minute	
	G → S	G → P	S → G	S → P	P → G	P → S	Growth velocity	Shortening velocity
Control dsRNA (5, 2230)†	1.057	6.137	1.114	6.223	3.037	2.813	6.134	6.077
Control dsRNA + FL-Msps (3, 545)	1.286	6.415	1.149	6.107	2.446	3.219	6.568 *P* = 0.0029**§	7.283 **** §
Msps dsRNA (3, 1008)	1.161	6.871 *P* = 0.004** §	0.740 *P* = 0.039* §	6.728 *P* = 0.007* §	1.930 *P* = 0.035* §	4.057 *P* = 0.001** §	6.406	6.727 *P* = 0.017* §
Control dsRNA + FL-Msps (3, 545)	1.286	6.415	1.149	6.107	2.446	3.219	6.568	7.283 **** §
Msps dsRNA + FL-Msps (3, 1219)	1.313	5.842 *P* = 0.011*‡	1.633 *P* = 0.0096*	5.577 *P* = 0.018*	3.275 *P* = 0.0023**	2.971	7.021 *P* = 0.011*	8.415 ****
Control dsRNA + Linker2 Mut (3, 473)	1.633	6.257	1.573	5.930	2.886	2.594	7.591 ****	9.092 ****
Msps dsRNA + Linker2 Mut (3, 509)	1.202	6.050	1.534	5.635	2.813	3.949	7.585 ****	9.063 ****
Control dsRNA + Linker2&4 Mut (3, 665)	1.266	6.233	1.238	5.976	2.306	2.373 *P* = 0.0076*	7.334 *P* = 0.0007**	9.795 ****
Msps dsRNA + Linker2&4 Mut (3, 421)	1.019	5.658 *P* = 0.0089*	1.2010	5.513 *P* = 0.0315*	1.751 *P* = 0.0159*	2.113 *P* = 0.0016**	5.516 ****	7.329

Table 3.2. Microtubule dynamics parameters with full-length Msps transgenes

†Numbers in parentheses indicate the number of cells analyzed and the analyzed events for each condition, respectively. § Indicates values statistically different from Control dsRNA were $P < 0.05$. ‡ Indicates values statistically different from Control dsRNA + FL-Msps where $P < 0.05$. * indicates $P < 0.05$, ** $P < 0.005$, *** $P < 0.0005$, and **** $P < 0.00005$. Statistical significance for transition rates was determined using a two-tailed permutation test with 10,000 resamples. For growth and shrinkage rates, a two-sample t-test was used to determine statistical significance.

Supplemental Figure S1

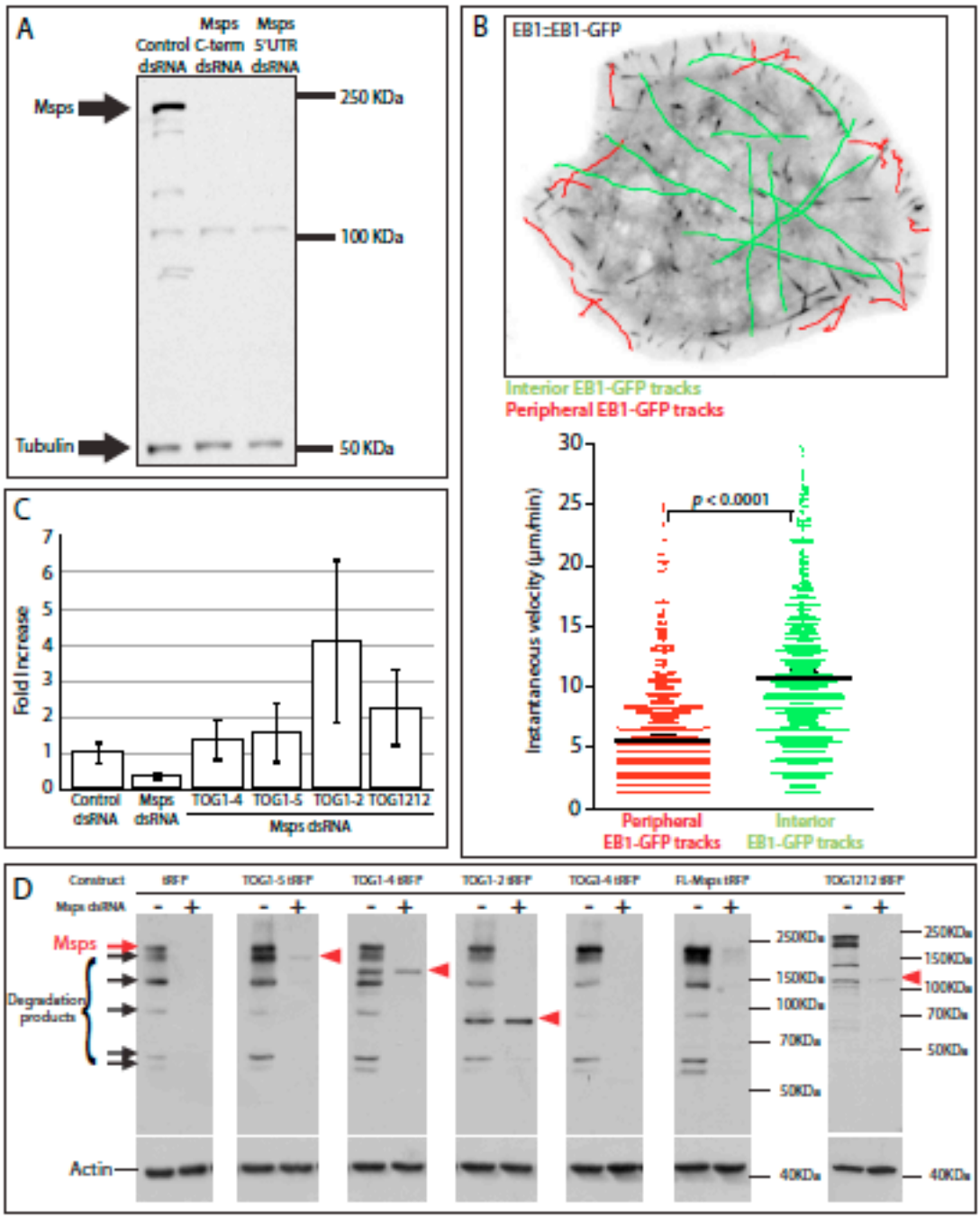

Figure 3-S1. Expression levels of endogenous and exogenous *Drosophila* Msps using a novel antibody raised against TOG domain 2.

(A) Rabbit polyclonal antibody raised against *Drosophila* Msps recognizes a 220KDa band in control treated S2 cells as well as a non-specific band at approximately 125KDa. Msps is depleted upon treatment with either C-terminally targeted dsRNA or dsRNA against the 5‘UTR of Msps. Anti-α-tubulin is also present at 55KDa to represent equal protein load. (B) Representative EB1-GFP cell tracks from the cell interior (green) and EB1-GFP comets originating in the cell periphery (red), denoted as a 3μm region from the cell cortex that encompasses the actin-rich lamella (Iwasa and Mullins, 2007). Scatter plot of instantaneous velocities of EB1-GFP comets from the cell interior (green, right) or the cell periphery (red, left). Error bars represent 95% confidence intervals and center bar represents mean. N = 5 cells, approximately 7 EB1-GFP comets per cell, approximately 1000 velocity points per condition. (C) Relative fold increase in fluorescence of transiently transfected S2 cells expressing various Msps transgenes in the presence of either control dsRNA (left) or Msps dsRNA (right) stained with Msps antibody. Error bars indicate standard deviation. (D) Western blots of cells from (C). Several degradation products are denoted (left) in control lysates and the Msps transgene where detectable is denote by red arrowhead. A separate blot from the same lysates is below to show equivalent protein load.

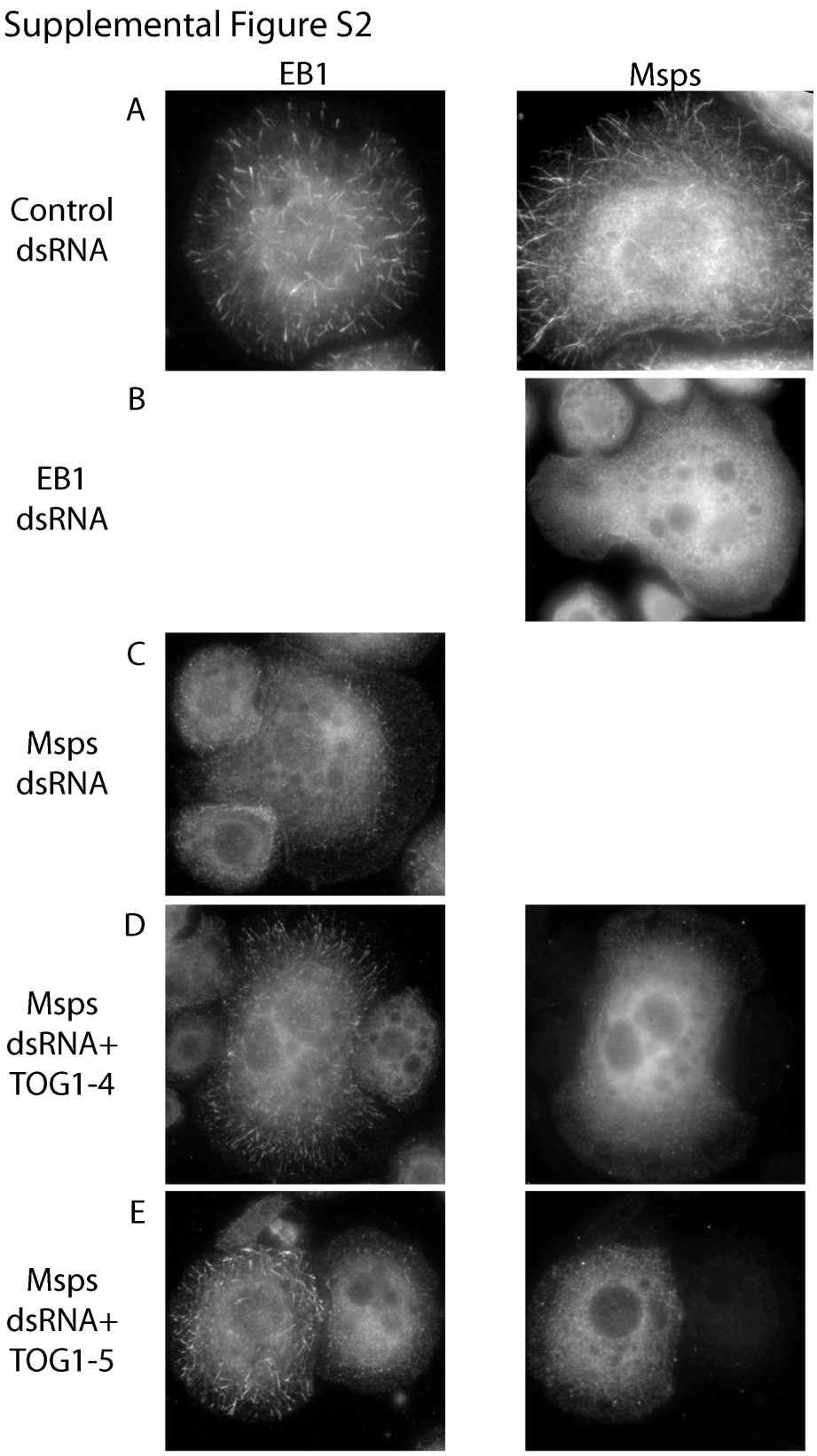

Figure 3-S2. Expression of Msps fragments TOG1-4 and TOG1-5 restore

normal plus end localization to endogenous EB1.

S2 cells stained for endogenous EB1 (left) or Msps (right) treated with (A) control dsRNA, (B) EB1 dsRNA, (C) Msps dsRNA, (D) Msps dsRNA with TOG1-4, and (E) Msps dsRNA with TOG1-5.

Supplemental Figure S3

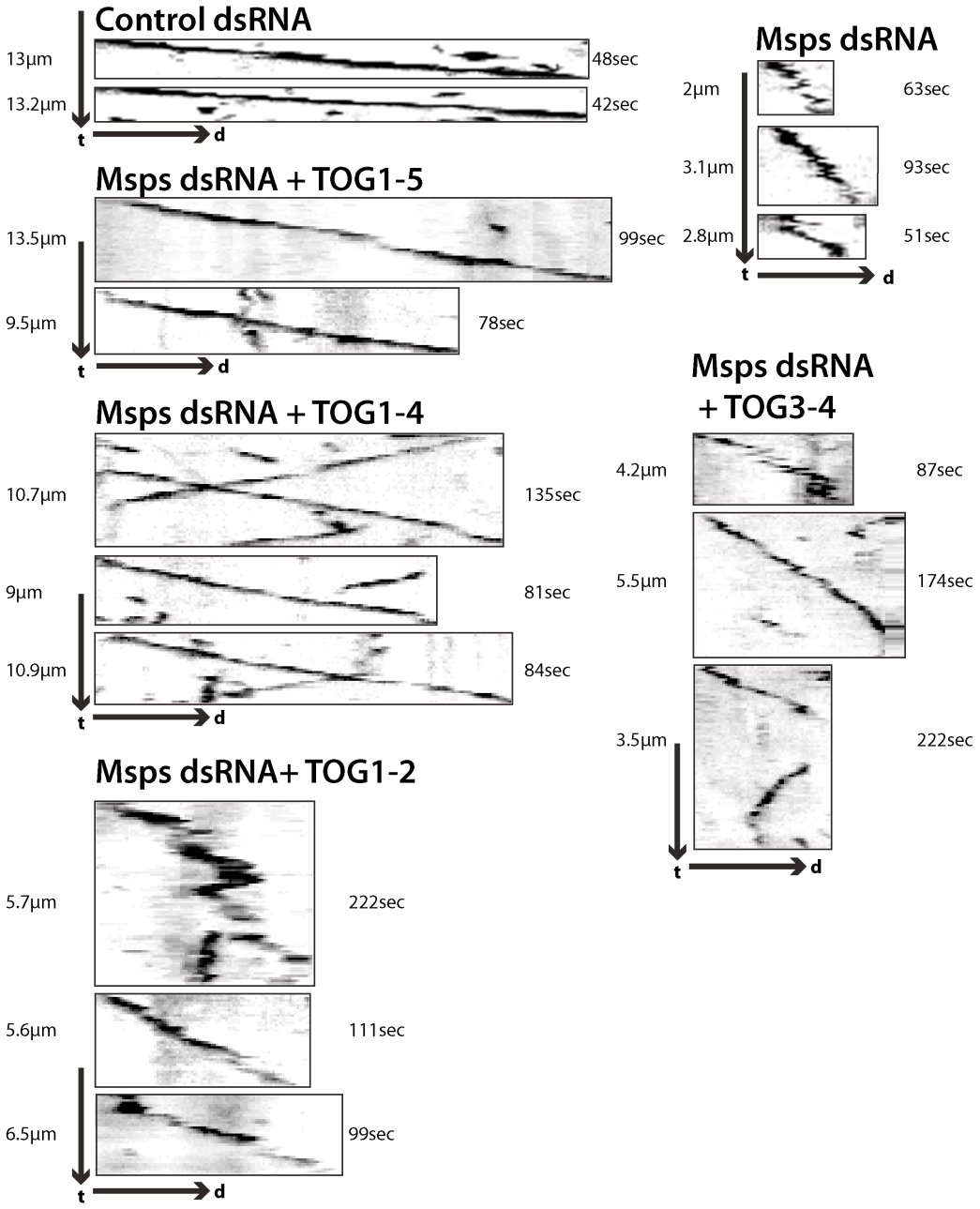

Figure 3-S3. Representative EB1::EB1-GFP kymographs of S2 cells treated with control or Msps dsRNA and transfected with Msps fragments.

Distance in micrometers is indicated to the left of each kymograph and the y axis of time is indicated to the right. Each kymograph represents the full life span of one EB1 comet for each condition.

Supplemental Figure S4

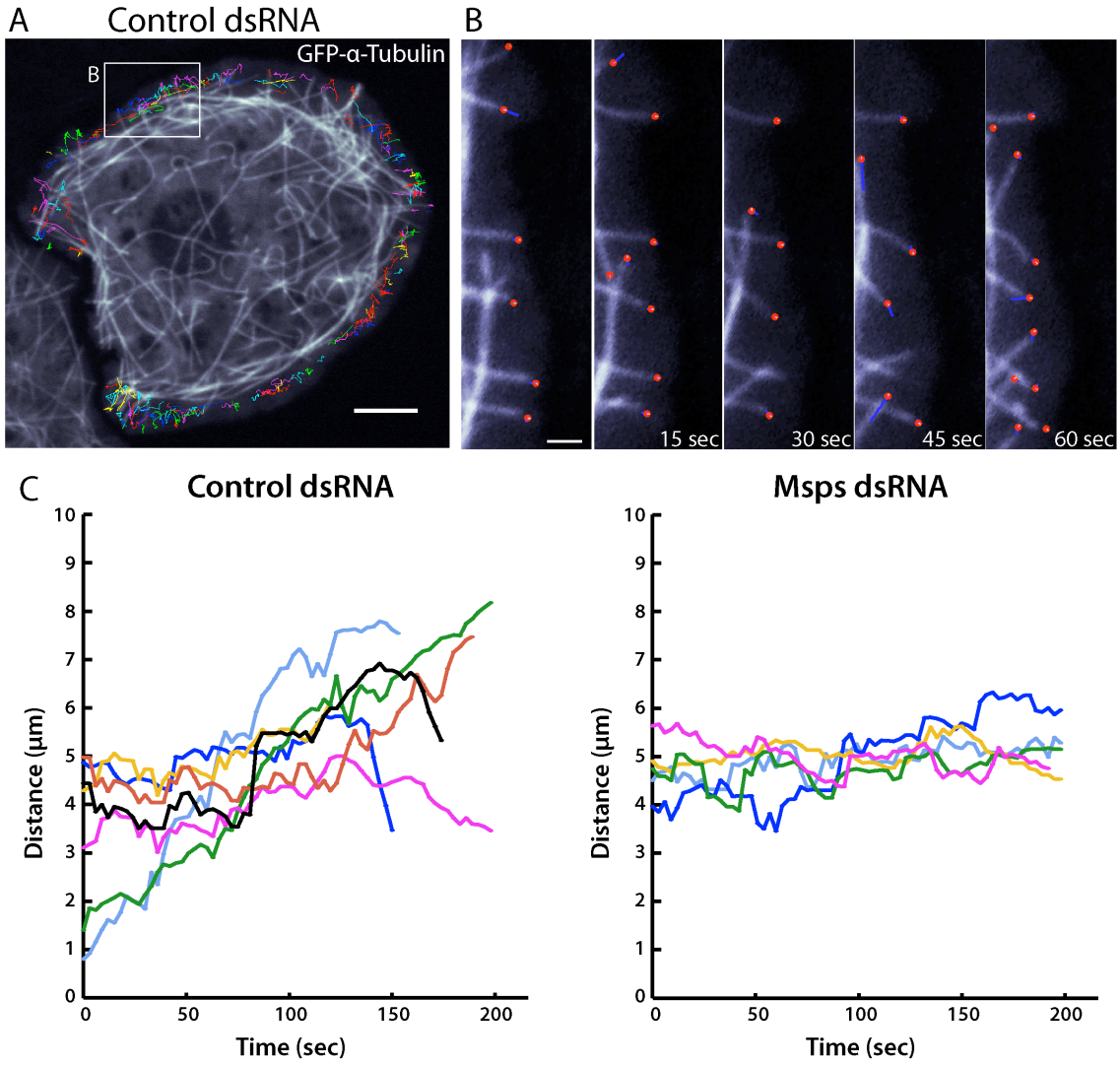

Figure 3-S4. Automated microtubule tracking algorithm.

(A) Representative control cell with trajectories of at least ten frames overlaid. Scale bar is 5 microns. (B) Zoom of inset from (A) showing 15 second intervals over 1 minute. Scale bar is 1.5 microns. (C) Microtubule lifetime plots of representative microtubules shown for Control dsRNA and Msps dsRNA treatments. Plots are arranged on the distance axis to indicate a mean distance

of 5 microns.

Supplemental Figure S5

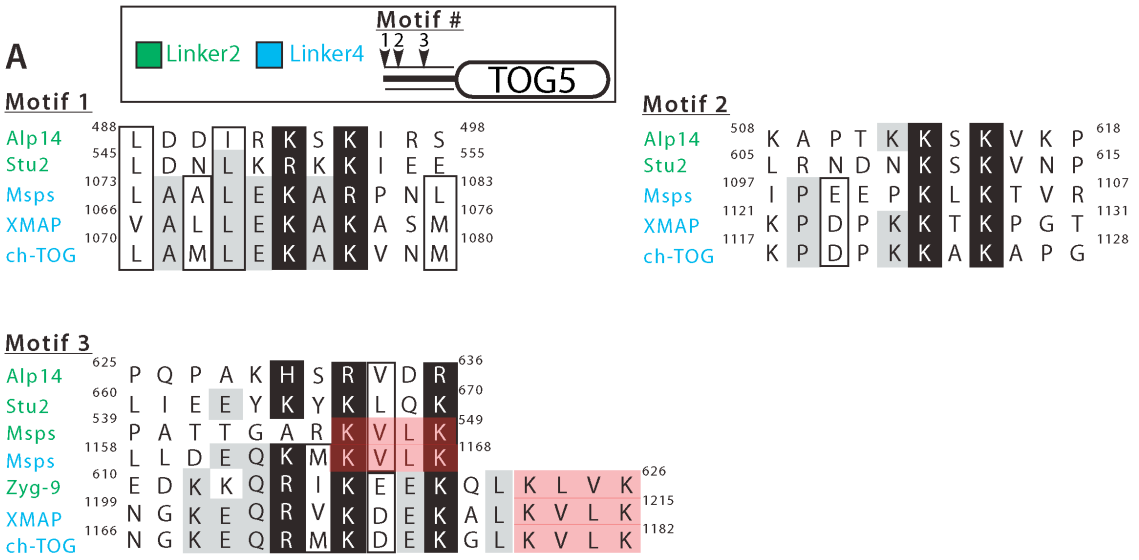

Figure 3-S5 Conserved motifs within the linker2 and linker4 of *Drosophila* Msps and other Dis1/XMAP215 members.

(A) Partially conserved motifs found in linkers of XMAP215/Dis1 members are labeled 1-3 based on their occurrence from NH_2-terminal to COOH-terminal within the linker. Green titled sequences indicate a position within the linker2 and blue within the linker4 where applicable. Outlined boxes are partial amino acid conservation, gray boxes absolute conservation in at least three members, black boxes indicate key positively-charged residues, and red boxes indicate the "KVLK" motif.

CHAPTER 4

SENTIN REGULATES THE PLUS END ASSOCIATION OF THE *DROSOPHILA* XMAP215 HOMOLOGUE MINI SPINDLES

This chapter represents a manuscript in preparation based on two related works in press from other labs. I have done all the experimentation, with the exception of identifying the minimal Msps plus end association domain, which was done by an undergraduate, Greg Schimizzi, under my supervision. This work was facilitated by the support and advice of my graduate advisor, Stephen Rogers.

Summary

Microtubule dynamics allow the cell to quickly remodel its cytoskeleton to perform a wide range of essential tasks. Plus end proteins or +TIPs are vital to regulating this rapid assembly or disassembly of microtubules. Recent evidence points to a key adaptor protein, SLAIN/Sentin, which link two of the core microtubule +TIPs, EB1 and ch-TOG/Msps. We demonstrate that in *Drosophila* S2 cells, Sentin interacts with Msps on plus ends and also influences its interaction on the microtubule lattice. EB1 and EB1-GFP are largely unaffected by Sentin RNAi, but do exhibit a loss of growth velocity and comet lifetime in Sentin RNAi cells. Sentin also plays a key role in maintain the balance of Msps between the mitotic spindle and the centrosome.

Introduction

Microtubules are dynamic polymers that can be quickly remodeled to transport materials between organelle compartments, asymmetrically polarize intracellular signaling, or build the mitotic spindle. The properties of the tubulin heterodimer's GTPase activity bestow both the rapid kinetics of polymer addition and subtraction as well as the unequal dynamics of monomer addition or subtraction to one end of the microtubule, termed the plus end (Howard and Hyman, 2009). At a critical concentration in vitro, purified tubulin will polymerize into microtubules and display a stochastic switching behavior between growth and shrinkage termed dynamic instability (Mitchison and Kirschner, 1984). This same behavior is observed in living cells, although the rates of growth and shrinkage and the frequency of transitions between growth, shrinkage, and pause are much higher in vivo (Kinoshita, 2001).

The ability to enhance and regulate microtubule dynamics selectively at the plus end is a property of a diverse class of proteins referred to as plus end proteins or +TIPs (Akhmanova and Steinmetz, 2008). Despite their diverse domains and in some cases antagonistic effect on microtubules, +TIPs exist as a complex hierarchy of interactions at the plus end. End binding proteins such as EB1, are the core +TIP molecules that act as a localization hub to recruit most other plus end proteins (Vaughan, 2005). One method in which +TIPs associate with EB1 is via one or multiple "SKIP" motifs that link proteins to the dimerization domain of EB1 (Honnappa et al., 2009). SKIP motifs are necessary and sufficient to link both microtubule associated proteins (MAPs) such as CLASPs (Mimori-

Kiyosue et al., 2005) and non-MAP proteins such as RhoGEF2 (Rogers et al., 2004b) to the plus end.

Dis1/XMAP215 family members represent another class of essential microtubule regulators (Popov and Karsenti, 2003; Kinoshita et al., 2002; Slep, 2009). With the exception of fission yeast, which have two related proteins (Garcia, 2001; Nabeshima et al., 1995), other eukaryotic taxa each have one conserved member (Gard et al., 2004). Dis1/XMAP215 members share a series of N-terminal TOG domains. In vitro, a pair of TOG domains can bind a single tubulin heterodimer, giving rise to the hypothesis that TOG proteins use arrays of TOG domains to successively add heterodimers to the plus end and increase the rate of polymerization (Slep and Vale, 2007). Yeast TOG proteins display two TOG domains followed by a microtubule lattice binding domain and a coiled-coil for homodimerization (Wang and Huffaker, 1997), bringing the functional number of TOG domains to four. In higher eukaryotes: amoeba (Gräf et al., 2003), plants (Kawamura and Wasteneys, 2008), and animals (Vasquez et al., 1994), TOG proteins are monomeric, but display an array of five TOG domains.

Previously, we found that the *Drosophila* TOG protein, Mini spindles (Msps), contains two microtubule lattice binding domains. Both consisted of an inter-TOG linker and its C-terminal TOG domain. Linker2-TOG3 was functional to bind microtubules in vitro and in cells, but this activity was masked when expressed within TOGs 1-4. Linker4-TOG5 in contrast, acted as a general microtubule lattice binding domain when expressed individually or within TOGs 1-5. This suggests that *Drosophila* Msps uses TOGs 1-4 for tubulin addition in a

similar fashion to their homo-dimerized yeast counterparts, while linker4-TOG5 functions in microtubule binding with the contribution of linker2-TOG3 under certain situations where this domain is unmasked.

C-terminal to the fifth TOG domain is a helical domain without any predicted domain structure. The function of this region, encoding roughly one-third of an animal TOG protein's sequence, has remained largely uncharacterized. It is mainly thought to mediate an interaction at the very C-terminus with TACC proteins that recruit TOG proteins to the centrosome (Lee et al., 2001; Srayko et al., 2003). From our previous structure-function analysis of Msps we could make two inferences as to the function of this C-terminal domain. Firstly, the C-terminus of Msps must be involved in the plus end localization of the molecule, as N-terminal TOG fragments never displayed plus end association. Secondly, the C-terminus must act to regulate the microtubule lattice association of the full length molecule. Previously, we found that Msps displayed a bimodal localization, associating with plus ends in the cell interior and along the microtubule lattice in the cell periphery. Msps TOG1-5, lacking the C-terminus, lost this regulated change in localization and instead bound constitutively to the microtubule lattice.

Recently, several studies have identified novel EB1-binding proteins that influence the localization of TOG domain proteins to the plus end. In vertebrates, SLAIN links the Msps homolog, chTOG, to EB1 as well as to CLIP and CLASP. SLAIN is necessary to localize chTOG to plus ends. In *Drosophila*, a novel EB1-interacter named Sentin was recently shown to be responsible for the plus end

accumulation of Msps, but this study failed to examine the functional consequence of this association.

In this study we examine the role for Msps' association with EB1 through the linker molecule, Sentin. We find that depletion of Sentin causes a mislocalization of endogenous Msps from microtubules. In cells depleted of Sentin, Msps-GFP is reduced at microtubule plus ends, but still associates with the plus end and constitutively with the microtubule lattice at higher expression levels. In mitosis, depletion of Sentin causes a reduction of Msps from the mitotic spindle, but not the centrosome. I have mapped the plus end association domain within Msps to a 150 amino acid region within the C-terminus of Msps. The N-terminus of Sentin is essential for association with Msps and expression of an N-terminal fragment is sufficient to compete Msps from endogenous Sentin and exert a dominant negative affect on the localization of Msps at microtubule plus ends. Finally, we find that this EB1 and Sentin-dependent localization of Msps to plus ends is essential for enhancing the lifetime and velocity of wildtype plus end growth.

Results

Sentin affects the localization of endogenous Msps to microtubules

To begin to examine the relationship between Sentin and Msps, I first depleted S2 cells of Sentin by RNAi and examined endogenous Msps and EB1 by immunofluorescence. In control cells, Msps localized to microtubule plus ends

in the cell interior and to the microtubule lattice in the cell periphery as we have

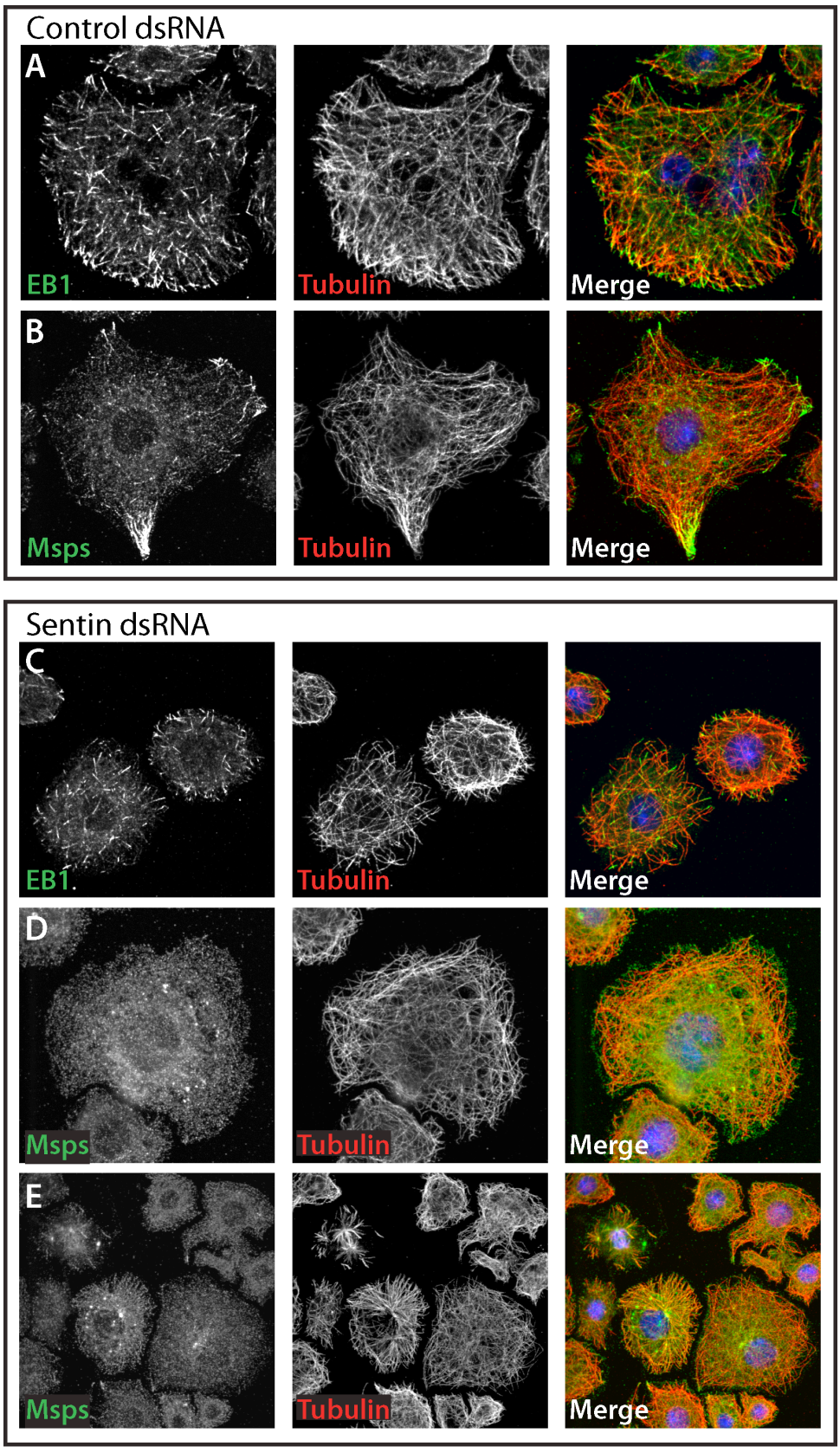

Figure 4-1. Sentin RNAi affects the localization to microtubules of

endogenous Msps, but not EB1.

(A-B) S2 cells treated with control dsRNA and stained with anti-tubulin, DAPI, and either anti-Msps or anti-EB1. (C-E) Cells treated with Sentin dsRNA and stained with anti-tubulin, DAPI, and either anti-Msps or anti-EB1.

previously shown (Figure 1B). Surprisingly, upon Sentin depletion, although there was some coincidence of Msps along microtubules, Msps no longer strongly labeled either the microtubule plus end or the microtubule lattice (Figure 1D-E). In some cells, Msps could be seen accumulated in larger dots which may represent centriole localization or alternatively, protein aggregation (Figure 1E). In contrast, EB1 showed little if any change in localization upon Sentin RNAi (Figure 1C). EB1 still labeled microtubule plus ends as a comet-like accumulation in control and Sentin RNAi cells (Figure 1A, C).

EB1-GFP velocity and lifetime are effected in Sentin RNAi

To examine the realtime behavior of EB1 and Msps in the absence of Sentin, I first expressed EB1::EB1-GFP in control and Sentin dsRNA treated cells. In both conditions, EB1-GFP labeled growing plus ends that tracked throughout the cell (Figure 2A). In Sentin RNAi cells, EB1-GFP comets exhibited shorter lifetimes of growth as seen from projections of EB1-GFP over one minute (Figure 2, bottom). In addition, EB1-GFP comets were slightly small than those in control treated cells and moved at a statistically slower average velocity than control cells (Figure 2B-C). Interestingly, while this velocity far exceeded that of cells lacking Msps, it was not statistically distinct from cells depleted of endogenous Msps and rescued with the N-terminal TOGs1-4, which does not localize to microtubule structures(Figure 2C).

Sentin regulates Msps plus end association upstream of EB1 and influences its association with the microtubule lattice.

I next examined the dynamics of Msps-GFP in control and Sentin dsRNA-treated cells. In control cells, Msps-GFP decorated interior comets and the lattice of peripheral microtubules (Figure 3A, left). In Sentin RNAi cells, Msps comets were lost from the cell and instead small punctae of Msps-GFP could be seen decorating the microtubule plus end (Figure 3A, middle). This phenotype was also observed when cells were depleted of EB1 by RNAi, suggesting that Sentin is the upstream regulator of Msps plus end association (Figure 3A, right). Msps-GFP was also mislocalized from the lattice of peripheral microtubules. Fluorescent linescans of microtubule plus ends revealed that Msps-GFP accumulation at plus end was diminished from control cells, which exhibited comets similar in their intensity profile to EB1 (Figure 3B).

The N-terminus of Sentin acts as a dominant negative to displace Msps-GFP from microtubule plus ends

Based on the hypothesis that SLAIN and Sentin have analogous functions in cells to bind TOG proteins through their N-terminus and EB1 at their C-terminus, I wondered if expressing the N-terminus of Sentin would be sufficient to dissociate Msps from plus ends by competing with endogenous Sentin. To do this, I co-transfected S2 cells with the first 237 amino acids of Sentin tagged with mCherry under the constitutive actin promoter and Msps-GFP under an inducible promoter to control the levels of expressed Msps. Using this approach, pAc-Sentin1-237-mCh was able to mislocalize Msps-GFP from the plus end and phenocopy the Sentin RNAi phenotype (Figure 3C).

Sentin influences the ability of Msps-GFP to associate with the lattice of interior microtubules

When examining the localization of Msps-GFP in control and Sentin RNAi cells, I often observed in Sentin RNAi cells where Msps-GFP decorated the lattice of interior microtubules, a phenotype that was not observed for the control cells, where Msps lattice binding was restricted to the periphery (Figure 3D). To quantitate this, I counted the cells observed to exhibit this aberrant localization to the interior microtubule lattice versus cells with a localization of Msps-GFP to small punctate plus end accumulations, with normal wildtype comets, or with an entirely cytosolic pool of fluorescent protein. In control cells and EB1 depleted cells, a small percentage of cells (~15-20%) had lattice-labeled interior microtubules. Upon Sentin RNAi this was elevated to approximately 50-60% of the observed cells (Figure 3E). Double Sentin/EB1 dsRNA treatment did not change this value, suggesting that it is Sentin itself that may normally negatively regulate the association of Msps with the lattice of interior microtubules.

Msps' plus end association domain

Finally, to assess which part of Msps is sufficient to localize to the plus end, we performed a structure function analysis of the C-terminus of Msps from residues 1406-2050. Expression of Msps1406-2050-GFP was sufficient to localize to microtubule plus ends and displayed a localization similar to EB1 rather than wildtype Msps-GFP. This might be expected since this fragment of

Msps does not contain any microtubule lattice-binding domains. Further dissection of Msps' C-terminus lead us to find a 150 amino acid region of Msps, amino acids 1707-1852, that was sufficient when co-expressed with EB1-tRFP to decorate the plus end of microtubules in S2 cells (Figure 4). This suggests that this region maybe necessary for binding to the adaptor protein, Sentin. Further study will determine if this is the case.

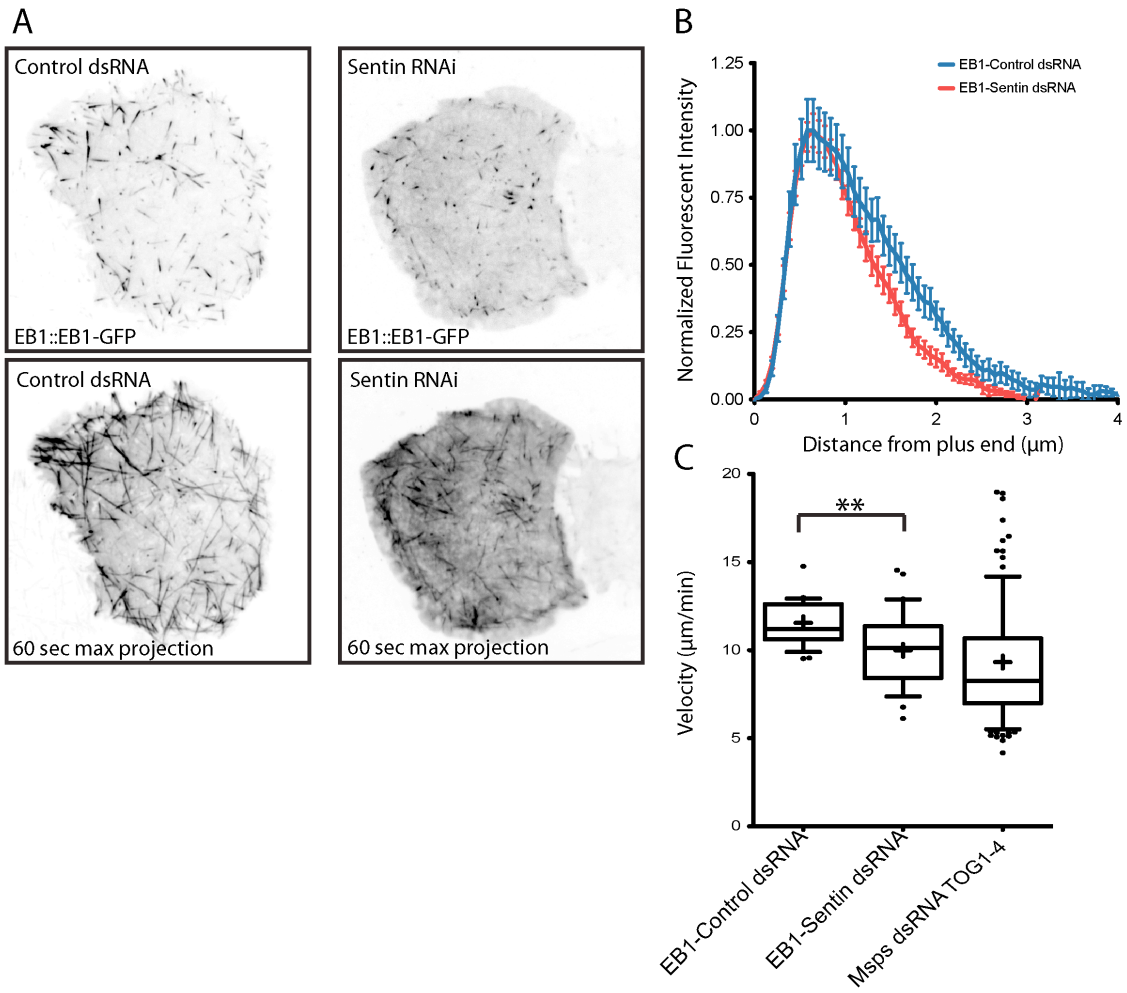

Figure 4-2. Sentin RNAi affects the velocity and lifetime of EB1-GFP comets

(A) S2 cell expressing EB1-GFP driven from its endogenous promoter treated with either control dsRNA (left) or Sentin dsRNA (right). Below are maximum projections of the timelapses for 60 seconds. (B) Fluorescent intensity profiles of EB1-GFP comets in control and Sentin RNAi treated cells. (C) Mean velocities of EB1-GFP comets from either control treated, Sentin RNAi treated, or Msps RNAi treated expressing Msps-TOG1-4. Asterisks denote p = < 0.005.

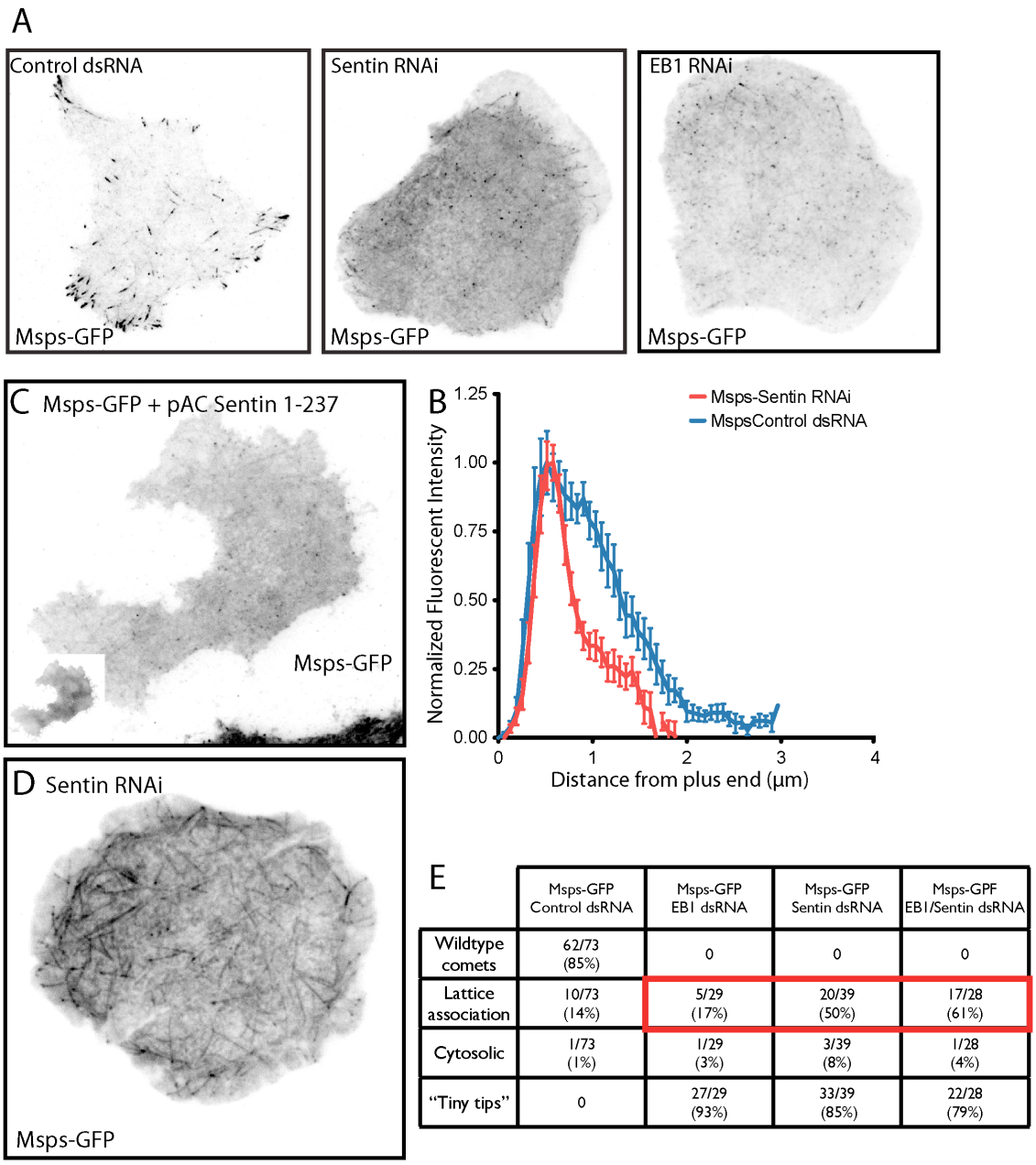

E

	Msps-GFP Control dsRNA	Msps-GFP EB1 dsRNA	Msps-GFP Sentin dsRNA	Msps-GPF EB1/Sentin dsRNA
Wildtype comets	62/73 (85%)	0	0	0
Lattice association	10/73 (14%)	5/29 (17%)	20/39 (50%)	17/28 (61%)
Cytosolic	1/73 (1%)	1/29 (3%)	3/39 (8%)	1/28 (4%)
"Tiny tips"	0	27/29 (93%)	33/39 (85%)	22/28 (79%)

Figure 4-3. Sentin is responsible for the plus end accumulation of Msps-GFP and negatively regulates the microtubule lattice association Msps-GFP for interior microtubules

(A) Msps-GFP in control treated (left), Sentin dsRNA treated (middle), or EB1 dsRNA treated (right). Fluorescent intensity linescans of Msps-GFP in control or

Sentin dsRNA-treated cells. (C) Cell co-expressing Msps-GFP and pAC-Sentin1-237-mCh (inset). (D) Msps-GFP decorating the lattice of interior microtubules in a Sentin RNAi background. (E) Phenotypic counts of cells expressing Msps-GFP under various dsRNA treatment backgrounds. Counts are not cumulative and represent overlapping phenotypes, specifically between “tiny tips” and lattice association.

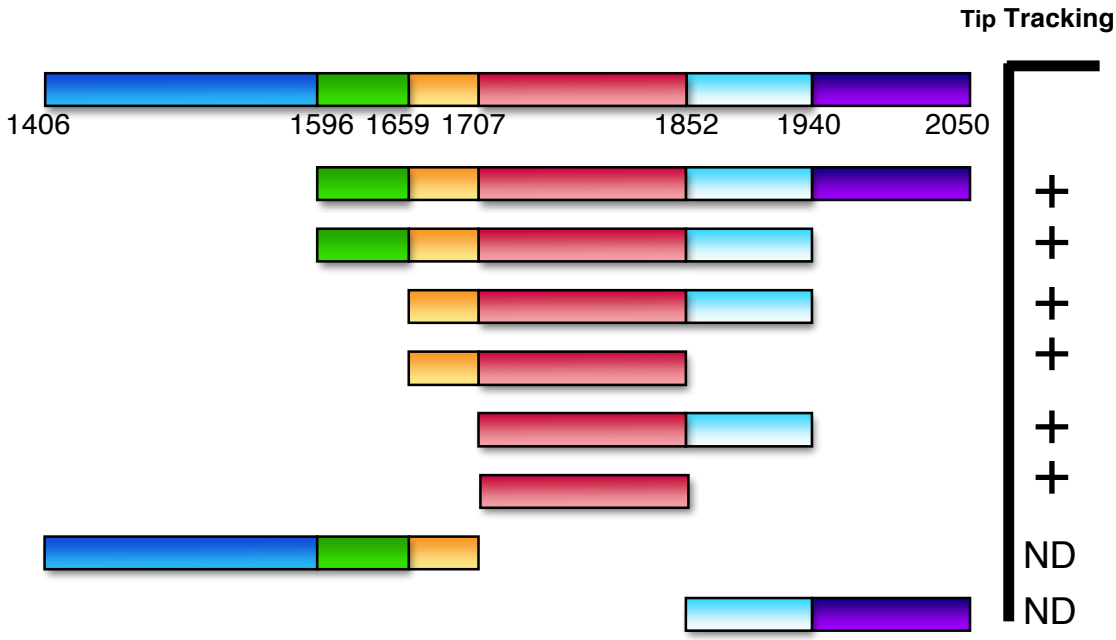

Figure 4-4. Msps 1707-1852 is the minimal plus end association domain of Msps.

Cartoon schematic demonstrating constructs used to assay the plus end association domain of Msps. Constructs were C-terminally tagged with GFP and co-expressed with EB1::EB1-tRFP in S2 cells.

Chapter 5

CONCLUSION AND FUTURE DIRECTIONS

Although microtubules are inherently dynamic polymers, cells have evolved a host of microtubule associated proteins (MAPs) to regulate their assembly, disassembly, and dynamicity. Specifically, Plus end proteins (+TIPs) are important regulators that recognize and control microtubules at their growing end (Akhmanova and Steinmetz, 2008). Despite having identified a large number of +TIP molecules, we lack a full understanding of how they regulate one another and function together to regulate microtubule dynamics. Below, I will outline some of the unanswered questions essential to understanding +TIP, and specifically, TOG protein function.

In Vivo Study of Interphase TOG Dynamics

Since their first characterization in the late 1980's (Gard and Kirschner, 1987), studies of TOG proteins have benefited from the conserved nature of the protein super family (Kinoshita et al., 2002) and established in vitro and in vivo experimental systems that are extremely amenable to studying MAP function. While these have two key attributes have yielded numerous studies of TOG proteins, they have primarily focused on a narrow subset of experimental approaches and phenotypic functions. Specifically, the bulk of research has focus on XMAP215 phenotypes in mitosis (Hyman et al., 1999; Cullen et al., 1999; Wang and Huffaker, 1997) with functional approaches often performed

using vitro systems of either purified components (Brouhard et al., 2008) or *Xenopus* extracts (Hyman et al., 1999). Based on the phenotypes of inhibited spindle and astral microtubule growth, many of these studies have described the sole function of TOG proteins as that of microtubule polymerases. Past studies have also neglected or been unable to study the realtime dynamics of TOG proteins and have instead used bulk microtubule assays (Spittle et al., 2000) or fixed samples (Basto et al., 2007) to assay protein localization and behavior. These studies have been extremely valuable, however, in identifying important binding partners for TOG proteins such as the conserved TACC family proteins (Lee et al., 2001). Additionally, in vitro Xenopus extract experiments previously described a potent microtubule disassembly property of TOG proteins (Shirasu-Hiza, 2003). In 2005, Ohkura and Brittle were the first to describe an interphase function for the *Drosophila* TOG protein Mini spindles (Msps). They found that depletion of Msps lead to an increase in microtubule pause, suggesting that TOG proteins may have a more complex function in vivo (Brittle and Ohkura, 2005). Recent work examining single XMAP215-GFP molecules interacting with microtubules, became the first study of realtime dynamics of any animal TOG protein (Brouhard et al., 2008). This revealed behaviors for XMAP215 that were unique compared to other +TIPs. While XMAP215 plus end tracked in vitro similarly to EB1, instead of transiently associating and dissociating with the plus end like other +TIPs, XMAP215 stayed associated with the plus end for several seconds and “surfed” processively along the growing end. In addition, XMAP215 was able to diffuse along the lattice of in vitro microtubules and could associate

with soluble tubulin while diffusing along the microtubule lattice. The use of purified components unequivocally identified a number of ways that XMAP215 can autonomously interact with microtubules. But how do these in vitro behaviors translate to explain the function and behavior of TOG domain proteins in cells? This has been the goal of my research; to examine TOG protein function and behavior in cells and relate this information to the structure and information revealed from in vitro studies.

The Spatial Regulation of Msps Localization

One of the most surprising revelations about the behavior of *Drosophila* Mini spindles is that the plus end and lattice association, both behaviors previously described in vitro, are spatially segregated localizations in S2 cells. In the cell interior, Msps localizes to the plus end, much like EB1, while in the peripheral lamella, Msps associates along the lattice and plus end of growing and shrinking microtubules. This suggests that the nature of this bimodal localization is a regulated process. I do not yet know the exact mechanism of this switch, but I can hypothesize based on my structure-function analysis of Msps.

Expression of Msps' first five TOG domains (TOG1-5), which encodes two lattice-binding domains, constitutively associates with the microtubule lattice. Unlike the wildtype protein, this fragment does not discriminate between interior or peripheral microtubules. This suggests that the regulation of microtubule lattice association is conferred by or requires a more C-terminal portion of the protein. Additionally, plus end tracking seems to be a function of the C-terminus

of Msps, as no fragment lacking this region was observed to plus end track. Most studies of TOG proteins have focused on the more clearly defined N-terminal TOG domains, but our work puts an unexpected emphasis on the C-terminus of Msps for the protein's behavior in cells. I speculate that it is an interplay between the microtubule plus end localization domain and the microtubule lattice binding domain that regulates this spatial switch in S2 cells. Based on this hypothesis there are two key questions that will be critical in future research of Msps. Firstly, is this a direct intra-molecular interplay between two the Msps domains or is it mediated through an adaptor such as EB1 or Sentin. Secondly, if this is true, what is the molecular mechanism to initiate this switch?

RNAi treatments against candidate adaptors such as Sentin should begin to address the question concerning how this regulated switch is achieved. In vitro microtubule cosedimentation assays using fragments of Msps that encode both lattice binding domains and the C-terminus should also help reveal if this inter-molecular regulation exists and how it is maintained.

The Molecular Switch Between the Plus End and Microtubule Lattice

Identifying the molecular mechanism of this switch will likely be more challenging. Post-translational modification seems a likely mechanism, since this switch in localization is spatial coincidental with the cell lamella. This cellular subcompartment is established and identifiable by the activity of several cell signaling cascades. Most notably, the small GTPase Rac1 is responsible for orchestrating the assembling and remodeling of the dendritic array of actin at the

lamellipodia and lamella. Rac activity itself is often downstream of phosphatidylinositol signaling via PI3K. Coincidentally, the PI3K pathway has been shown to down-regulate the activity of GSK3β, a kinase that regulates the microtubule lattice and plus end association of mammalian CLASP in epithelial cells (Wittmann and Waterman-Storer, 2005). If post-translational phosphorylation is regulating the switch between Msps' ability to plus end track or bind the microtubule lattice, it will be important to identify if this phosphorylation positively or negatively affects lattice binding. In the case of CLASP, CLASP is normally phosphorylated within the cell body and remains solely on plus ends. Dephosphorylation of CLASP and deactivation of GSK3β in the lamella leads to lattice association (Kumar et al., 2009). One important caveat to the hypothesis of phosphorylation regulating Msps' spatial localization is that this post-translational modification need not be applied directly to Msps. This phosphorylation of Msps could instead be applied to EB1 or Sentin within the peripheral region of the cell, freeing Msps to associate with the microtubule lattice. In particular, the localization of Msps-GFP in either Sentin or EB1 RNAi when examined by TIRF more closely resembles the localization of Msps in the cell periphery than the plus end comets from the cell interior. This suggests that the peripheral lattice binding constitutes at least a partial dissociation from either a Sentin/EB1 complex or Sentin alone. The ability of a N-terminal portion of Sentin to disrupt plus end tracking, but not lattice association, also suggests that a partial association with Sentin may still be possible while bound to the microtubule lattice.

One alternative mechanism for Msps' peripheral lattice association is that Msps binds to the microtubule lattice based on an alteration of microtubules within the cell periphery. I found that Msps contains two microtubule lattice binding sites within the N-terminal TOG domains. Linker4-TOG5 seemed to be a constitutive microtubule binding domain, meaning it bound microtubules when expressed in any truncated form of Msps. Linker2-TOG3, however, displayed microtubule lattice binding only in configurations where it was the most N-terminal portion expressed. Within TOG1-4, the linker2-TOG3 microtubule binding site was masked and displayed a cytosolic localization in S2 cells. However, using an in vitro cosedimentation assay, I found that TOG1-4 bound taxol-stabilized microtubules with a high avidity (Figure 1A). In cells treated with taxol, TOG1-4 quickly mobilized from the cytosol to the microtubule lattice (Figure 1B). This suggests that this microtubule binding site is unmasked when tubulin is stabilized by taxol. This taxol-stabilized confirmation of tubulin may mimic a GTP-bound or "straight" confirmation of tubulin that would normally exist at the plus end as a cap on untreated peripheral microtubules. The recognition by linker2-TOG3 could cause a cascading confirmation change that activates lattice-binding by linker4-TOG5 and disengages plus end association. We believe that both microtubule binding domains have a large degree of functional overlap, since mutation of just one domain gives a qualitatively similar localization pattern as the wildtype protein.

An alternative to a nucleotide-dependent confirmation might be that of a post translational modification to the microtubule that occurs preferentially in the

cell periphery. Modifications such as acetylation and detyrosination have been associated spatially with peripheral microtubule segments or the leading edge microtubules of fibroblasts at a wound edge (for review see Verhey and Gaertig, 2007; Janke and Kneussel, 2010). Many of these modifications that make up the "tubulin code" are known to stabilize tubulin and

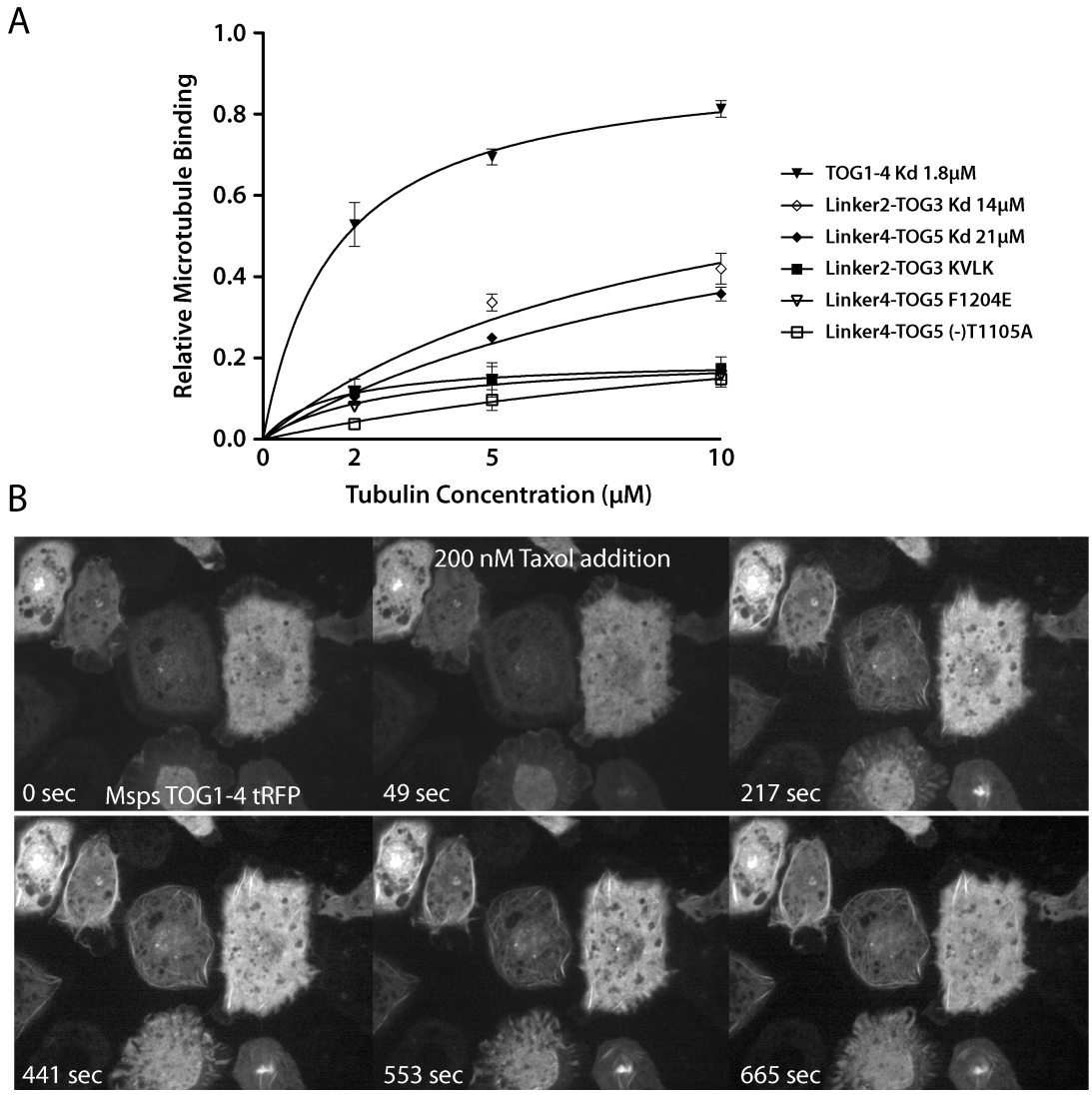

Figure 5-1. TOG1-4 binds with high affinity to taxol-stabilized microtubules.

(A) Microtubule cosedimentation assay of in vitro transcribed/translated proteins incubated with varying concentrations of purified taxol-stabilized microtubules. Apparent Kd is calculated as the concentration of tubulin at which exactly half the concentration of Msps fragment would be expect to bind. (B) S2 cells expressing

Msps TOG1-4tRFP and treated with 200nM taxol at 49 sec. The MspsTOG1-4 quickly mobilizes to the microtubules within ten minutes.

are even increased themselves by taxol-treatment (Piperno et al., 1987). How similar they may be structurally or functionally to taxol-stabilized microtubules is not known. A survey of the modifying enzymes in S2 cells by both RNAi and overexpression would help to determine if these modifications cause changes in +TIP localization.

The Function of Msps' Microtubule Lattice Association

Upon identifying how Msps transitions to the lattice of peripheral microtubules, the next question presented is what function does this transition have on peripheral microtubules and their dynamics? From my work, we can abrogate Msps' microtubule lattice domains by mutating key positively charged residues within the linkers to glutamic acid. By knocking down the endogenous protein, we found that this mutated form of Msps was no longer able to localize to the lattice of peripheral microtubules. This had a strong effect not only on the dynamics of peripheral microtubules, but also their organization at the cell cortex. Instead of microtubules that remain perpendicular to the cortex as they slow and eventually depolymerize, microtubules labeled with the linker mutant Msps continued to grow past the cell cortex and instead began to curve around the cell cortex. Examination of microtubule dynamics revealed that microtubules seemed "locked" into a particular state of growth, pause, or shrinkage. This meant that microtubules that were growing were statistically more likely to continue growing than to transition to shrinkage or pause. This suggested that lattice association is vital for affecting the transition of microtubules to different states in the periphery.

How might lattice association accomplish this? Several mutually inclusive hypotheses might explain how lattice association can help catalyze microtubule transitions.

Specifically in the case of growing microtubules, diverting the pool of Msps onto the microtubule lattice, away from the plus end where it acts as a microtubule polymerase, could act to slow polymerization enough to cause a transition to pause or shrinkage. While the lattice association of most classical MAPs such as Tau has been found to stabilize microtubules, this may not be the case for Msps. Because Msps is thought to specifically enhance the dynamic instability of microtubules, its lattice binding behavior may have a destabilizing effect on microtubules in the periphery. This would not necessarily have the same degree of destabilization as that of a Kin I motor, where ATPase motor activity is used to peel away protofilaments. Instead, Msps' lattice association could slightly perturb lateral interactions between heterodimers and subtly destabilizing protofilaments, priming the microtubule for rapid depolymerization once the MT pauses or the GTP cap is exhausted. This activity could also work in conjunction with Kin I proteins such as MCAK or KLP10A. For microtubules that are already in a state of depolymerization, having a population of Msps that is associated several microns distal from the plus end may also act as a safeguard to "catch" microtubules from excessive depolymerization out of the cell periphery. This safeguard mechanism would also allow severed microtubules to retain Msps on their new plus end. Lattice associated Msps may also diffuse along the lattice toward the plus end of paused microtubules. This lattice diffusion

would allow Msps to efficiently target to paused plus ends in order to catalyze a transition to growth or shrinkage. The lateral diffusion of both Msps as well as Kin I motors to plus ends might also serve as a "timer" function. This would allow microtubules a small temporal window to remain paused at the cell cortex to facilitate the delivery of proteins or cargo attachment to minus end motors. This timer would last until a critical concentration of TOG and Kin I protein was able to target to the plus end and catalyze disassembly.

New Potential Msps Partners

Another unanswered question arising from structure-function analysis of Msps is related to the potential for additional binding partners. Particularly, expression of the inter-TOG linkers 2 and 4, displayed unique localization patterns in mitosis that suggests these regions mediate other protein-protein interactions. Although neither Linker2 or Linker4, when C-terminally tagged with TagRFP, localized to microtubules in interphase, both transgenes localized to the spindle microtubules and centrosomes in mitosis. Additionally, linker2-TOG3 as well as TOG1-4 localized to chromatin specifically in mitosis. Several presumptive and verified binding partners have been established for Msps in *Drosophila* development, primarily through analysis of mutants that caused a loss of Msps from the mitotic and meiotic spindle. These include Hsp90 (Basto et al., 2007), cyclin B (Basto et al., 2007), the mitotic motor Ncd (Cullen and Ohkura, 2001), Augmin components (Bucciarelli et al., 2009), and conserved TACC family member dTACC (Lee et al., 2001). Many of these interactions have only been

tested using bulk extracts or through genetic interactions. Identifying these potential interactors using biochemical or proteomic approaches could seriously progress our understanding of how TOG proteins work with other factors in vivo. This approach has been applied several times to +TIPs such as EB1 (Rogers et al., 2004b) and CLIP170 (Akhmanova et al., 2001), generating novel insights into the +TIP interactome.

Msps' Connections at the Plus End

In addition to identifying new partners of Msps function, it will be essential to understand the molecular mechanism and function of Msps' known interactions with other +TIPs. At the heart of these interactions is Msps' interaction with EB1. Although it seems that molecular mechanism may happen indirectly through the adaptor protein, Sentin, making sense of how these two vital +TIPs coordinate their activities to promote microtubule growth will build a foundation for a "core" +TIP complex. It will be important to understand if the relationship between Msps and EB1 represents a truly cooperative promotion of growth through their unique microtubule interaction domains, or if it is simply a matter of enhancing Msps' localization to the plus end through a connection to EB1. Although either possibility exist, I speculate that the later scenario is more likely, since depletion of Sentin still retains a small population of Msps-GFP on plus ends and only has a minor impact on microtubule growth velocity. The partial rescue EB1-GFP velocities achieved by expression of TOG domain constructs also supports this conclusion. The difference between a partial rescue

and wildtype velocities would represent enhanced polymerization due to EB1-dependent concentration of Msps at the plus end.

The addition of Sentin to a complex between Msps and EB1 adds another layer of complexity that remains to be elucidated. Although there appears to be some similarities between SLAIN and Sentin functionally, the two proteins seem to lack a complete overlap of functions. Their core function as an adaptor seems completely analogous since the TOG and EB1 binding domains are similarly located N- and C-terminally, respectively. It will be interesting to further investigate if the placement of these domains has a functional significance or if they can be switched or shortened. It will also be interesting to determine if a chimeric version of Msps with N-terminal TOG domains and a Sentin EB1-binding C-terminus would be sufficient to rescue wildtype dynamics. In mitosis, the relationship between Msps and Sentin could represent a unique parsing of Msps activity between spindle and astral microtubule activity. In Sentin RNAi, Msps localization to the spindle is diminished and the net spindle length is shorter. Sentin RNAi astral microtubules, however, are long and resemble a KLP10A RNAi treatment, where presumably there is an imbalance between polymerase and depolymerase activity. Sentin-dependent localization of Msps to the spindle may balance the pools of Msps between spindle and dTACC-bound centrosome pools. It will be interesting in the future to probe this interaction through double Sentin/dTACC RNAi conditions.

Finally, Msps' relationship with the Kin I MCAK/KLP10A depolymerases represent an intriguing possibility for coupling Msps' dynamic-enhancing ability

with Kin I depolymerization. Instead of strict antagonism between opposing activity, Msps depletion in S2 cells results in loss of growth and shrinkage at the plus end (Brittle and Ohkura, 2005). Additionally, in mammalian cells, MCAK depolymerization was dependent on the presence of ch-TOG (Holmfeldt et al., 2004). Finally, both Msps and KLP10A exhibit a coincidental localization to the lattice of peripheral microtubules in S2 cells (Mennella et al., 2005). Although, there we have not been able to find a direct interaction between these two +TIPs (data not shown), the possibility remains that they may cooperate to induce microtubule shrinkage.

Concluding Remarks

Dis1/XMAP215 proteins represent important regulators of microtubule dynamics. Understanding the complete spectrum of their functions in cells will increase our insight into how cells control the microtubule plus end. Although, our conception of these molecules has perhaps been oversimplified by protagonist/antagonist views of growth versus shrinkage, slowly the complexity of their function is coming to light. Instead of being simply a family of microtubule polymerases, Dis1/XMAP215 molecules represent molecules that are inexorably tied to promoting and enhancing dynamic growing and shrinking microtubule ends. Hopefully, by understanding their unique domain structure, in vivo behavior, and interactions at the microtubule plus end we can begin to unravel the molecular intricacies of TOG proteins.

REFERENCES

Adams, M.D., S.E. Celniker, R.A. Holt, C.A. Evans, J.D. Gocayne, P.G. Amanatides, S.E. Scherer, P.W. Li, R.A. Hoskins, R.F. Galle, R.A. George, S.E. Lewis, S. Richards, M. Ashburner, S.N. Henderson, G.G. Sutton, J.R. Wortman, M.D. Yandell, Q. Zhang, L.X. Chen, R.C. Brandon, Y.H. Rogers, R.G. Blazej, M. Champe, B.D. Pfeiffer, K.H. Wan, C. Doyle, E.G. Baxter, G. Helt, C.R. Nelson, G.L. Gabor, J.F. Abril, A. Agbayani, H.J. An, C. Andrews-Pfannkoch, D. Baldwin, R.M. Ballew, A. Basu, J. Baxendale, L. Bayraktaroglu, E.M. Beasley, K.Y. Beeson, P.V. Benos, B.P. Berman, D. Bhandari, S. Bolshakov, D. Borkova, M.R. Botchan, J. Bouck, P. Brokstein, P. Brottier, K.C. Burtis, D.A. Busam, H. Butler, E. Cadieu, A. Center, I. Chandra, J.M. Cherry, S. Cawley, C. Dahlke, L.B. Davenport, P. Davies, B. de Pablos, A. Delcher, Z. Deng, A.D. Mays, I. Dew, S.M. Dietz, K. Dodson, L.E. Doup, M. Downes, S. Dugan-Rocha, B.C. Dunkov, P. Dunn, K.J. Durbin, C.C. Evangelista, C. Ferraz, S. Ferriera, W. Fleischmann, C. Fosler, A.E. Gabrielian, N.S. Garg, W.M. Gelbart, K. Glasser, A. Glodek, F. Gong, J.H. Gorrell, Z. Gu, P. Guan, M. Harris, N.L. Harris, D. Harvey, T.J. Heiman, J.R. Hernandez, J. Houck, D. Hostin, K.A. Houston, T.J. Howland, M.H. Wei, et al. 2000. The genome sequence of Drosophila melanogaster *Science*. 287:2185–2195.

Akhmanova, A., C.C. Hoogenraad, K. Drabek, T. Stepanova, B. Dortland, T. Verkerk, W. Vermeulen, B.M. Burgering, C.I. de Zeeuw, F. Grosveld, and N. Galjart. 2001. Clasps are CLIP-115 and -170 associating proteins involved in the regional regulation of microtubule dynamics in motile fibroblasts *Cell*. 104:923–935.

Akhmanova, A., and C.C. Hoogenraad. 2005. Microtubule plus-end-tracking proteins: mechanisms and functions. *Curr Opin Cell Biol*. 17:47–54.

Akhmanova, A., and M. Steinmetz. 2008. Tracking the ends: a dynamic protein network controls the fate of microtubule tips. *Nat Rev Mol Cell Biol*.

Al-Bassam, J., N.A. Larsen, A.A. Hyman, and S.C. Harrison. 2007. Crystal structure of a TOG domain: conserved features of XMAP215/Dis1-family TOG domains and implications for tubulin binding. *Structure*. 15:355–362.

Al-Bassam, J., H. Kim, G. Brouhard, A. van Oijen, S.C. Harrison, and F. Chang. 2010. CLASP promotes microtubule rescue by recruiting tubulin dimers to the microtubule. *Dev Cell*. 19:245–258.

Allen, C., and G.G. Borisy. 1974. Structural polarity and directional growth of microtubules of Chlamydomonas flagella *J Mol Biol*. 90:381–402.

Amos, L., and A. Klug. 1974. Arrangement of subunits in flagellar microtubules *J Cell Sci*. 14:523–549.

Applewhite, D.A., K.D. Grode, D. Keller, A. Zadeh, K.C. Slep, and S.L. Rogers. 2010. The Spectraplakin Short Stop Is an Actin-Microtubule Crosslinker that Contributes to Organization of the Microtubule Network. *Mol Biol Cell*.

Asbury, C.L. 2008. XMAP215: a tip tracker that really moves. *Cell*. 132:19–20.

Basto, R., F. Gergely, V.M. Draviam, H. Ohkura, K. Liley, and J.W. Raff. 2007. Hsp90 is required to localise cyclin B and Msps/ch-TOG to the mitotic spindle in Drosophila and humans. *J Cell Sci*. 120:1278–1287.

Batchelder, E.M., and D. Yarar. 2010. Differential requirements for clathrin-dependent endocytosis at sites of cell-substrate adhesion *Mol Biol Cell*. 21:3070–3079.

Bieling, P., L. Laan, H. Schek, E.L. Munteanu, L. Sandblad, M. Dogterom, D. Brunner, and T. Surrey. 2007. Reconstitution of a microtubule plus-end tracking system in vitro *Nature*. 450:1100–1105.

Bieling, P., S. Kandels-Lewis, I.A. Telley, J. van Dijk, C. Janke, and T. Surrey. 2008. CLIP-170 tracks growing microtubule ends by dynamically recognizing composite EB1/tubulin-binding sites *J Cell Biol*. 183:1223–1233.

Brittle, A.L., and H. Ohkura. 2005. Mini spindles, the XMAP215 homologue, suppresses pausing of interphase microtubules in Drosophila. *EMBO J*. 24:1387–1396.

Brouhard, G.J., J.H. Stear, T.L. Noetzel, J. Al-Bassam, K. Kinoshita, S.C. Harrison, J. Howard, and A.A. Hyman. 2008. XMAP215 is a processive microtubule polymerase. *Cell*. 132:79–88.

Bucciarelli, E., C. Pellacani, V. Naim, A. Palena, M. Gatti, and M.P. Somma. 2009. Drosophila Dgt6 interacts with Ndc80, Msps/XMAP215, and gamma-tubulin to promote kinetochore-driven MT formation *Curr Biol*. 19:1839–1845.

Caplow, M., and J. Shanks. 1996. Evidence that a single monolayer tubulin-GTP cap is both necessary and sufficient to stabilize microtubules. *Mol Biol Cell*. 7:663–675.

Caplow, M., and R. Reid. 1985. Directed elongation model for microtubule GTP hydrolysis *Proc Natl Acad Sci USA*. 82:3267–3271.

Cau, J., and A. Hall. 2005. Cdc42 controls the polarity of the actin and microtubule cytoskeletons through two distinct signal transduction pathways *J Cell Sci*. 118:2579–2587.

Celniker, S.E., L.A.L. Dillon, M.B. Gerstein, K.C. Gunsalus, S. Henikoff, G.H. Karpen, M. Kellis, E.C. Lai, J.D. Lieb, D.M. MacAlpine, G. Micklem, F. Piano, M. Snyder, L. Stein, K.P. White, R.H. Waterston, and modENCODE Consortium. 2009. Unlocking the secrets of the genome. *Nature*. 459:927–930.

Charrasse, S., M. Mazel, S. Taviaux, P. Berta, T. Chow, and C. Larroque. 1995. Characterization of the cDNA and pattern of expression of a new gene over-expressed in human hepatomas and colonic tumors. *Eur J Biochem*. 234:406–413.

Charrasse, S., M. Schroeder, C. Gauthier-Rouviere, F. Ango, L. Cassimeris, D.L. Gard, and C. Larroque. 1998. The TOGp protein is a new human microtubule-associated protein homologous to the Xenopus XMAP215. *J Cell Sci*. 111 (Pt 10):1371–1383.

Cherbas, L., A. Willingham, D. Zhang, L. Yang, Y. Zou, B.D. Eads, J.W. Carlson, J.M. Landolin, P. Kapranov, J. Dumais, A. Samsonova, J.-H. Choi, J. Roberts, C.A. Davis, H. Tang, M.J. van Baren, S. Ghosh, A. Dobin, K. Bell, W. Lin, L. Langton, M.O. Duff, A.E. Tenney, C. Zaleski, M.R. Brent, R.A. Hoskins, T.C. Kaufman, J. Andrews, B.R. Graveley, N. Perrimon, S.E. Celniker, T.R. Gingeras, and P. Cherbas. 2011. The transcriptional diversity of 25 Drosophila cell lines *Genome Res* 21:301–314.

Clemens, J.C., C.A. Worby, N. Simonson-Leff, M. Muda, T. Maehama, B.A. Hemmings, and J.E. Dixon. 2000. Use of double-stranded RNA interference in Drosophila cell lines to dissect signal transduction pathways. *Proc Natl Acad Sci USA*. 97:6499–6503.

Cooper, J.R., M. Wagenbach, C.L. Asbury, and L. Wordeman. 2010. Catalysis of the microtubule on-rate is the major parameter regulating the depolymerase activity of MCAK *Nat Struct Mol Biol*. 17:77–82.

Cooper, J.R., and L. Wordeman. 2009. The diffusive interaction of microtubule binding proteins *Curr Opin Cell Biol*. 21:68–73.

Coquelle, F.M., M. Caspi, F.P. Cordelières, J.P. Dompierre, D.L. Dujardin, C. Koifman, P. Martin, C.C. Hoogenraad, A. Akhmanova, N. Galjart, J.R. de Mey, and O. Reiner. 2002. LIS1, CLIP-170's key to the dynein/dynactin pathway *Mol Cell Biol*. 22:3089–3102.

Cullen, C.F., P. Deák, D.M. Glover, and H. Ohkura. 1999. mini spindles: A gene encoding a conserved microtubule-associated protein required for the integrity of the mitotic spindle in Drosophila. *J Cell Biol*. 146:1005–1018.

Cullen, C.F., and H. Ohkura. 2001. Msps protein is localized to acentrosomal poles to ensure bipolarity of Drosophila meiotic spindles. *Nat Cell Biol*. 3:637–642.

D'Ambrosio, M.V., and R.D. Vale. 2010. A whole genome RNAi screen of Drosophila S2 cell spreading performed using automated computational image analysis *J Cell Biol*. 191:471–478.

Desai, A., S. Verma, T.J. Mitchison, and C.E. Walczak. 1999. Kin I kinesins are microtubule-destabilizing enzymes *Cell*. 96:69–78.

Dixit, R., B. Barnett, J.E. Lazarus, M. Tokito, Y.E. Goldman, and E.L.F. Holzbaur. 2009. Microtubule plus-end tracking by CLIP-170 requires EB1. *Proc Natl Acad Sci USA*. 106:492–497.

Dorer, M.S., D. Kirton, J.S. Bader, and R.R. Isberg. 2006. RNA interference analysis of Legionella in Drosophila cells: exploitation of early secretory apparatus dynamics *PLoS Pathog* 2:e34.

Drabek, K., M. van Ham, T. Stepanova, K. Draegestein, R. van Horssen, C.L. Sayas, A. Akhmanova, T. ten Hagen, R. Smits, R. Fodde, F. Grosveld, and N. Galjart. 2006. Role of CLASP2 in microtubule stabilization and the regulation of persistent motility *Curr Biol*. 16:2259–2264.

Drechsel, D.N., A.A. Hyman, A. Hall, and M. Glotzer. 1997. A requirement for Rho and Cdc42 during cytokinesis in Xenopus embryos. *Curr Biol*. 7:12–23.

Du, Y., C.A. English, and R. Ohi. 2010. The kinesin-8 Kif18A dampens microtubule plus-end dynamics *Curr Biol*. 20:374–380.

Dzhindzhev, N.S., S.L. Rogers, R.D. Vale, and H. Ohkura. 2005. Distinct mechanisms govern the localisation of Drosophila CLIP-190 to unattached kinetochores and microtubule plus-ends. *J Cell Sci*. 118:3781–3790.

Dziadek, M.A., and L.S. Johnstone. 2007. Biochemical properties and cellular localisation of STIM proteins *Cell Calcium*. 42:123–132.

Enke, C., N. Zekert, D. Veith, C. Schaaf, S. Konzack, and R. Fischer. 2007. Aspergillus nidulans Dis1/XMAP215 protein AlpA localizes to spindle pole bodies and microtubule plus ends and contributes to growth directionality. *Eukaryotic Cell*. 6:555–562.

Etienne-Manneville, S., and A. Hall. 2003. Cdc42 regulates GSK-3beta and adenomatous polyposis coli to control cell polarity. *Nature*. 421:753–756.

Fasano, L., L. Röder, N. Coré, E. Alexandre, C. Vola, B. Jacq, and S. Kerridge. 1991. The gene teashirt is required for the development of Drosophila embryonic trunk segments and encodes a protein with widely spaced zinc finger motifs *Cell*. 64:63–79.

Fessler, J.H., R.E. Nelson, and L.I. Fessler. 1994. Preparation of extracellular matrix. *Methods Cell Biol*. 44:303–328.

Fukata, M., T. Watanabe, J. Noritake, M. Nakagawa, M. Yamaga, S. Kuroda, Y. Matsuura, A. Iwamatsu, F. Perez, and K. Kaibuchi. 2002. Rac1 and Cdc42 capture microtubules through IQGAP1 and CLIP-170. *Cell*. 109:873–885.

Garcia, M.A. 2001. Fission yeast ch-TOG/XMAP215 homologue Alp14 connects mitotic spindles with the kinetochore and is a component of the Mad2-dependent spindle checkpoint. *EMBO J*. 20:3389–3401.

Gard, D.L., B.E. Becker, and S. Josh Romney. 2004. MAPping the eukaryotic tree of life: structure, function, and evolution of the MAP215/Dis1 family of microtubule-associated proteins. *Int Rev Cytol*. 239:179–272.

Gard, D.L., and M.W. Kirschner. 1987. A microtubule-associated protein from Xenopus eggs that specifically promotes assembly at the plus-end. *J Cell Biol*. 105:2203–2215.

Gardner, M.K., A.J. Hunt, H.V. Goodson, and D.J. Odde. 2008. Microtubule assembly dynamics: new insights at the nanoscale *Curr Opin Cell Biol*. 20:64–70.

Gennerich, A., and R.D. Vale. 2009. Walking the walk: how kinesin and dynein coordinate their steps *Curr Opin Cell Biol*. 21:59–67.

Gergely, F., V.M. Draviam, and J.W. Raff. 2003. The ch-TOG/XMAP215 protein is essential for spindle pole organization in human somatic cells. *Genes Dev*. 17:336–341.

Goode, B.L., D.G. Drubin, and G. Barnes. 2000. Functional cooperation between the microtubule and actin cytoskeletons *Curr Opin Cell Biol*. 12:63–71.

Gräf, R., U. Euteneuer, T.-H. Ho, and M. Rehberg. 2003. Regulated expression of the centrosomal protein DdCP224 affects microtubule dynamics and reveals mechanisms for the control of supernumerary centrosome number. *Mol Biol Cell*. 14:4067–4074.

Grigoriev, I., S.M. Gouveia, B. van der Vaart, J. Demmers, J.T. Smyth, S. Honnappa, D. Splinter, M.O. Steinmetz, J.W. Putney, C.C. Hoogenraad, and A. Akhmanova. 2008. STIM1 Is a MT-Plus-End-Tracking Protein Involved in Remodeling of the ER. *Curr Biol*. 18:177–182.

Guimaraes, G.J., Y. Dong, B.F. McEwen, and J.G. Deluca. 2008. Kinetochore-microtubule attachment relies on the disordered N-terminal tail domain of Hec1 *Curr Biol*. 18:1778–1784.

Gupta, K.K., M.V. Joyce, A.R. Slabbekoorn, Z.C. Zhu, B.A. Paulson, B. Boggess, and H.V. Goodson. 2010. Probing interactions between CLIP-170, EB1, and microtubules *J Mol Biol*. 395:1049–1062.

Hall, A. 2005. Rho GTPases and the control of cell behaviour *Biochem Soc Trans*. 33:891–895.

Hayashi, I., M.J. Plevin, and M. Ikura. 2007. CLIP170 autoinhibition mimics intermolecular interactions with p150Glued or EB1 *Nat Struct Mol Biol*. 14:980–981.

Hayashi, I., and M. Ikura. 2003. Crystal structure of the amino-terminal microtubule-binding domain of end-binding protein 1 (EB1) *J Biol Chem*. 278:36430–36434.

He, X., D.R. Rines, C.W. Espelin, and P.K. Sorger. 2001. Molecular analysis of kinetochore-microtubule attachment in budding yeast. *Cell*. 106:195–206.

Hertzer, K.M., S.C. Ems-McClung, S.L. Kline-Smith, T.G. Lipkin, S.P. Gilbert, and C.E. Walczak. 2006. Full-length dimeric MCAK is a more efficient microtubule depolymerase than minimal domain monomeric MCAK *Mol Biol Cell*. 17:700–710.

Holmfeldt, P., S. Stenmark, and M. Gullberg. 2004. Differential functional interplay of TOGp/XMAP215 and the KinI kinesin MCAK during interphase and mitosis. *EMBO J*. 23:627–637.

Honnappa, S., O. Okhrimenko, R. Jaussi, H. Jawhari, I. Jelesarov, F.K. Winkler, and M.O. Steinmetz. 2006. Key interaction modes of dynamic +TIP networks. *Mol Cell*. 23:663–671.

Honnappa, S., S.M. Gouveia, A. Weisbrich, F.F. Damberger, N.S. Bhavesh, H. Jawhari, I. Grigoriev, F.J.A. van Rijssel, R.M. Buey, A. Lawera, I. Jelesarov, F.K. Winkler, K. Wüthrich, A. Akhmanova, and M.O. Steinmetz. 2009. An EB1-binding motif acts as a microtubule tip localization signal *Cell*. 138:366–376.

Hoogenraad, C.C., A. Akhmanova, F. Grosveld, C.I. de Zeeuw, and N. Galjart. 2000. Functional analysis of CLIP-115 and its binding to microtubules *J Cell Sci*. 113 (Pt 12):2285–2297.

Howard, J., and A.A. Hyman. 2003. Dynamics and mechanics of the microtubule plus end. *Nature*. 422:753–758.

Howard, J., and A.A. Hyman. 2009. Growth, fluctuation and switching at microtubule plus ends. *Nat Rev Mol Cell Biol*. 10:569–574.

Hyman, A.A., R. Tournebize, A. Popov, K. Kinoshita, A.J. Ashford, S. Rybina, A. Pozniakovsky, T.U. Mayer, C.E. Walczak, and E. Karsenti. 1999. Control of microtubule dynamics by the antagonistic activities of XMAP215

and XKCM1 in Xenopus egg extracts. *Nat Cell Biol*. 2:13–19.

Inoue, Y.H., M. Do Carmo Avides, M. Shiraki, P. Deak, M. Yamaguchi, Y. Nishimoto, A. Matsukage, and D.M. Glover. 2000. Orbit, a novel microtubule-associated protein essential for mitosis in Drosophila melanogaster. *J Cell Biol*. 149:153–166.

Iwasa, J.H., and R.D. Mullins. 2007. Spatial and temporal relationships between actin-filament nucleation, capping, and disassembly. *Curr Biol*. 17:395–406.

Janke, C., and M. Kneussel. 2010. Tubulin post-translational modifications: encoding functions on the neuronal microtubule cytoskeleton *Trends Neurosci* 33:362–372.

Jiang, K., J. Wang, J. Liu, T. Ward, L. Wordeman, A. Davidson, F. Wang, and X. Yao. 2009. TIP150 interacts with and targets MCAK at the microtubule plus ends *EMBO Rep*. 10:857–865.

Jiang, L., S.L. Rogers, and S.T. Crews. 2007. The Drosophila Dead end Arf-like3 GTPase controls vesicle trafficking during tracheal fusion cell morphogenesis *Dev Biol*. 311:487–499.

Johnston, C.A., K. Hirono, K.E. Prehoda, and C.Q. Doe. 2009. Identification of an Aurora-A/PinsLINKER/Dlg spindle orientation pathway using induced cell polarity in S2 cells. *Cell*. 138:1150–1163.

Kaverina, I., K. Rottner, and J.V. Small. 1998. Targeting, capture, and stabilization of microtubules at early focal adhesions. *J Cell Biol*. 142:181–190.

Kawamura, E., and G.O. Wasteneys. 2008. MOR1, the Arabidopsis thaliana homologue of Xenopus MAP215, promotes rapid growth and shrinkage, and suppresses the pausing of microtubules in vivo. *J Cell Sci*. 121:4114–4123.

Kerssemakers, J.W.J., E.L. Munteanu, L. Laan, T.L. Noetzel, M.E. Janson, and M. Dogterom. 2006. Assembly dynamics of microtubules at molecular resolution. *Nature*. 442:709–712.

Kinoshita, K. 2001. Reconstitution of Physiological Microtubule Dynamics Using Purified Components. *Science*. 294:1340–1343.

Kinoshita, K., B. Habermann, and A.A. Hyman. 2002. XMAP215: a key component of the dynamic microtubule cytoskeleton. *Trends Cell Biol*. 12:267–273.

Kodama, A., I. Karakesisoglou, E. Wong, A. Vaezi, and E. Fuchs. 2003. ACF7: an essential integrator of microtubule dynamics *Cell*. 115:343–354.

Komarova, Y., G. Lansbergen, N. Galjart, F. Grosveld, G.G. Borisy, and A. Akhmanova. 2005. EB1 and EB3 control CLIP dissociation from the ends of growing microtubules *Mol Biol Cell*. 16:5334–5345.

Komarova, Y., C.O. de Groot, I. Grigoriev, S.M. Gouveia, E.L. Munteanu, J.M. Schober, S. Honnappa, R.M. Buey, C.C. Hoogenraad, M. Dogterom, G.G. Borisy, M.O. Steinmetz, and A. Akhmanova. 2009. Mammalian end binding proteins control persistent microtubule growth *J Cell Biol*. 184:691–706.

Komarova, Y.A., A.S. Akhmanova, S.-I. Kojima, N. Galjart, and G.G. Borisy. 2002. Cytoplasmic linker proteins promote microtubule rescue in vivo *J Cell Biol*. 159:589–599.

Kosco, K.A., C.G. Pearson, P.S. Maddox, P.J. Wang, I.R. Adams, E.D. Salmon, K. Bloom, and T.C. Huffaker. 2001. Control of microtubule dynamics by Stu2p is essential for spindle orientation and metaphase chromosome alignment in yeast. *Mol Biol Cell*. 12:2870–2880.

Krebs, A., K.N. Goldie, and A. Hoenger. 2005. Structural rearrangements in tubulin following microtubule formation *EMBO Rep*. 6:227–232.

Kumar, P., K.S. Lyle, S. Gierke, A. Matov, G. Danuser, and T. Wittmann. 2009. GSK3beta phosphorylation modulates CLASP-microtubule association and lamella microtubule attachment. *J Cell Biol*. 184:895–908.

Lansbergen, G., Y. Komarova, M. Modesti, C. Wyman, C.C. Hoogenraad, H.V. Goodson, R.P. Lemaitre, D.N. Drechsel, E. van Munster, T.W.J. Gadella, F. Grosveld, N. Galjart, G.G. Borisy, and A. Akhmanova. 2004. Conformational changes in CLIP-170 regulate its binding to microtubules and dynactin localization *J Cell Biol*. 166:1003–1014.

Lansbergen, G., I. Grigoriev, Y. Mimori-Kiyosue, T. Ohtsuka, S. Higa, I. Kitajima, J. Demmers, N. Galjart, A.B. Houtsmuller, F. Grosveld, and A. Akhmanova. 2006. CLASPs attach microtubule plus ends to the cell cortex through a complex with LL5beta *Dev Cell*. 11:21–32.

Lansbergen, G., and A. Akhmanova. 2006. Microtubule plus end: a hub of cellular activities. *Traffic*. 7:499–507.

Laycock, J.E., M.S. Savoian, and D.M. Glover. 2006. Antagonistic activities of Klp10A and Orbit regulate spindle length, bipolarity and function in vivo. *J Cell Sci*. 119:2354–2361.

Lee, M.J., F. Gergely, K. Jeffers, S.Y. Peak-Chew, and J.W. Raff. 2001. Msps/XMAP215 interacts with the centrosomal protein D-TACC to regulate microtubule behaviour. *Nature a - z index*. 3:643–649.

Lemos, C.L., P. Sampaio, H. Maiato, M. Costa, L.V. Omel'yanchuk, V. Liberal, and C.E. Sunkel. 2000. Mast, a conserved microtubule-associated protein required for bipolar mitotic spindle organization. *EMBO J*. 19:3668–3682.

Liang, C.-C., A.Y. Park, and J.-L. Guan. 2007. In vitro scratch assay: a convenient and inexpensive method for analysis of cell migration in vitro. *Nat Protoc*. 2:329–333.

Lomakin, A.J., I. Semenova, I. Zaliapin, P. Kraikivski, E. Nadezhdina, B.M. Slepchenko, A. Akhmanova, and V. Rodionov. 2009. CLIP-170-dependent capture of membrane organelles by microtubules initiates minus-end directed transport. *Dev Cell*. 17:323–333.

Mandelkow, E.M., and E. Mandelkow. 1985. Unstained microtubules studied by cryo-electron microscopy. Substructure, supertwist and disassembly *J Mol Biol*. 181:123–135.

Maurer, S.P., P. Bieling, J. Cope, A. Hoenger, and T. Surrey. 2011. GTPgammaS microtubules mimic the growing microtubule end structure

recognized by end-binding proteins (EBs) *Proc Natl Acad Sci USA*. 108:3988–3993.

Mennella, V., G.C. Rogers, S.L. Rogers, D.W. Buster, R.D. Vale, and D.J. Sharp. 2005. Functionally distinct kinesin-13 family members cooperate to regulate microtubule dynamics during interphase. *Nat Cell Biol*. 7:235–245.

Mimori-Kiyosue, Y., I. Grigoriev, G. Lansbergen, H. Sasaki, C. Matsui, F. Severin, N. Galjart, F. Grosveld, I. Vorobjev, S. Tsukita, and A. Akhmanova. 2005. CLASP1 and CLASP2 bind to EB1 and regulate microtubule plus-end dynamics at the cell cortex *J Cell Biol*. 168:141–153.

Mitchison, T., and M. Kirschner. 1984. Dynamic instability of microtubule growth. *Nature*. 312:237–242.

Moore, A.T., K.E. Rankin, G. von Dassow, L. Peris, M. Wagenbach, Y. Ovechkina, A. Andrieux, D. Job, and L. Wordeman. 2005. MCAK associates with the tips of polymerizing microtubules *J Cell Biol*. 169:391–397.

Moores, C.A., M. Hekmat-Nejad, R. Sakowicz, and R.A. Milligan. 2003. Regulation of KinI kinesin ATPase activity by binding to the microtubule lattice *J Cell Biol*. 163:963–971.

Moores, C.A., and R.A. Milligan. 2006. Lucky 13-microtubule depolymerisation by kinesin-13 motors. *J Cell Sci*. 119:3905–3913.

Morrison, E.E., B.N. Wardleworth, J.M. Askham, A.F. Markham, and D.M. Meredith. 1998. EB1, a protein which interacts with the APC tumour suppressor, is associated with the microtubule cytoskeleton throughout the cell cycle *Oncogene*. 17:3471–3477.

Mulder, A.M., A. Glavis-Bloom, C.A. Moores, M. Wagenbach, B. Carragher, L. Wordeman, and R.A. Milligan. 2009. A new model for binding of kinesin 13 to curved microtubule protofilaments *J Cell Biol*. 185:51–57.

Nabeshima, K., H. Kurooka, M. Takeuchi, K. Kinoshita, Y. Nakaseko, and M. Yanagida. 1995. p93dis1, which is required for sister chromatid separation, is a novel microtubule and spindle pole body-associating protein phosphorylated at the Cdc2 target sites. *Genes Dev*. 9:1572–1585.

Nakaseko, Y., G. Goshima, J. Morishita, and M. Yanagida. 2001. M phase-specific kinetochore proteins in fission yeast: microtubule-associating Dis1 and Mtc1 display rapid separation and segregation during anaphase. *Curr Biol*. 11:537–549.

Niederstrasser, H., H. Salehi-Had, E.C. Gan, C. Walczak, and E. Nogales. 2002. XKCM1 acts on a single protofilament and requires the C terminus of tubulin *J Mol Biol*. 316:817–828.

Niethammer, P., I. Kronja, S. Kandels-Lewis, S. Rybina, P. Bastiaens, and E. Karsenti. 2007. Discrete states of a protein interaction network govern interphase and mitotic microtubule dynamics. *PLoS Biol*. 5:e29.

Nunez, J., and I. Fischer. 1997. Microtubule-associated proteins (MAPs) in the peripheral nervous system during development and regeneration *J. Mol. Neurosci* 8:207–222.

Odde, D.J. 2005. Chromosome capture: take me to your kinetochore *Curr Biol*. 15:R328–30.

Ogawa, T., R. Nitta, Y. Okada, and N. Hirokawa. 2004. A common mechanism for microtubule destabilizers-M type kinesins stabilize curling of the protofilament using the class-specific neck and loops. *Cell*. 116:591–602.

Paladi, M., and U. Tepass. 2004. Function of Rho GTPases in embryonic blood cell migration in Drosophila. *J Cell Sci*. 117:6313–6326.

Palazzo, A.F., C.H. Eng, D.D. Schlaepfer, E.E. Marcantonio, and G.G. Gundersen. 2004. Localized stabilization of microtubules by integrin- and FAK-facilitated Rho signaling. *Science*. 303:836–839.

Parks, S., and E. Wieschaus. 1991. The Drosophila gastrulation gene concertina encodes a G alpha-like protein *Cell*. 64:447–458.

Pegtel, D.M., S.I.J. Ellenbroek, A.E.E. Mertens, R.A. van der Kammen, J. de Rooij, and J.G. Collard. 2007. The Par-Tiam1 complex controls persistent migration by stabilizing microtubule-dependent front-rear polarity *Curr Biol*. 17:1623–1634.

Perez, F., G.S. Diamantopoulos, R. Stalder, and T.E. Kreis. 1999. CLIP-170 highlights growing microtubule ends in vivo. *Cell*. 96:517–527.

Peris, L., M. Thery, J. Fauré, Y. Saoudi, L. Lafanechère, J.K. Chilton, P. Gordon-Weeks, N. Galjart, M. Bornens, L. Wordeman, J. Wehland, A. Andrieux, and D. Job. 2006. Tubulin tyrosination is a major factor affecting the recruitment of CAP-Gly proteins at microtubule plus ends *J Cell Biol*. 174:839–849.

Pierre, P., J. Scheel, J.E. Rickard, and T.E. Kreis. 1992. CLIP-170 links endocytic vesicles to microtubules. *Cell*. 70:887–900.

Piperno, G., M. LeDizet, and X.J. Chang. 1987. Microtubules containing acetylated alpha-tubulin in mammalian cells in culture *J Cell Biol*. 104:289–302.

Popov, A.V., A. Pozniakovsky, I. Arnal, C. Antony, A.J. Ashford, K. Kinoshita, R. Tournebize, A.A. Hyman, and E. Karsenti. 2001. XMAP215 regulates microtubule dynamics through two distinct domains. *EMBO J*. 20:397–410.

Popov, A.V., F. Severin, and E. Karsenti. 2002. XMAP215 is required for the microtubule-nucleating activity of centrosomes. *Curr Biol*. 12:1326–1330.

Popov, A.V., and E. Karsenti. 2003. Stu2p and XMAP215: turncoat microtubule-associated proteins *Trends Cell Biol*. 13:547–550.

Ramadan, N., I. Flockhart, M. Booker, N. Perrimon, and B. Mathey-Prevot. 2007. Design and implementation of high-throughput RNAi screens in cultured Drosophila cells. *Nat Protoc*. 2:2245–2264.

Rehorn, K.P., H. Thelen, A.M. Michelson, and R. Reuter. 1996. A molecular aspect of hematopoiesis and endoderm development common to vertebrates and Drosophila. *Development*. 122:4023–4031.

Ridley, A.J., M.A. Schwartz, K. Burridge, R.A. Firtel, M.H. Ginsberg, G. Borisy, J.T. Parsons, and A.R. Horwitz. 2003. Cell migration: integrating signals from front to back *Science*. 302:1704–1709.

Rodionov, V.I., F.K. Gyoeva, A.S. Kashina, S.A. Kuznetsov, and V.I. Gelfand. 1990. Microtubule-associated proteins and microtubule-based translocators have different binding sites on tubulin molecule. *J Biol Chem*. 265:5702–5707.

Rodriguez, O.C., A.W. Schaefer, C.A. Mandato, P. Forscher, W.M. Bement, and C.M. Waterman-Storer. 2003. Conserved microtubule-actin interactions in cell movement and morphogenesis *Nat Cell Biol*. 5:599–609.

Rogers, G.C., S.L. Rogers, T.A. Schwimmer, S.C. Ems-McClung, C.E. Walczak, R.D. Vale, J.M. Scholey, and D.J. Sharp. 2004a. Two mitotic kinesins cooperate to drive sister chromatid separation during anaphase. *Nature*. 427:364–370.

Rogers, G.C., N.M. Rusan, M. Peifer, and S.L. Rogers. 2008. A multicomponent assembly pathway contributes to the formation of acentrosomal microtubule arrays in interphase Drosophila cells. *Mol Biol Cell*. 19:3163–3178.

Rogers, G.C., N.M. Rusan, D.M. Roberts, M. Peifer, and S.L. Rogers. 2009. The SCF Slimb ubiquitin ligase regulates Plk4/Sak levels to block centriole reduplication. *J Cell Biol*. 184:225–239.

Rogers, S.L. 2002. Drosophila EB1 is important for proper assembly, dynamics, and positioning of the mitotic spindle. *J Cell Biol*. 158:873–884.

Rogers, S.L., U. Wiedemann, N. Stuurman, and R.D. Vale. 2003. Molecular requirements for actin-based lamella formation in Drosophila S2 cells *J Cell Biol*. 162:1079–1088.

Rogers, S.L., U. Wiedemann, U. Häcker, C. Turck, and R.D. Vale. 2004b. Drosophila RhoGEF2 associates with microtubule plus ends in an EB1-dependent manner *Curr Biol*. 14:1827–1833.

Rogers, S.L., and G.C. Rogers. 2008. Culture of Drosophila S2 cells and their use for RNAi-mediated loss-of-function studies and immunofluorescence microscopy. *Nat Protoc*. 3:606–611.

Sato, M., L. Vardy, M. Angel Garcia, N. Koonrugsa, and T. Toda. 2004. Interdependency of Fission Yeast Alp14/TOG and Coiled Coil Protein Alp7 in Microtubule Localization and Bipolar Spindle Formation. *Mol Biol Cell*. 15:1609–1622.

Schneider, I. 1972. Cell lines derived from late embryonic stages of Drosophila melanogaster. *J Embryol Exp Morphol*. 27:353–365.

Shaner, N.C., M.Z. Lin, M.R. McKeown, P.A. Steinbach, K.L. Hazelwood, M.W. Davidson, and R.Y. Tsien. 2008. Improving the photostability of bright monomeric orange and red fluorescent proteins. *Nat Methods*. 5:545–551.

Shelden, E., and P. Wadsworth. 1993. Observation and quantification of individual microtubule behavior in vivo: microtubule dynamics are cell-type specific *J Cell Biol*. 120:935–945.

Shirasu-Hiza, M. 2003. Identification of XMAP215 as a microtubule-destabilizing factor in Xenopus egg extract by biochemical purification. *J Cell Biol*. 161:349–358.

Slep, K.C. 2009. The role of TOG domains in microtubule plus end dynamics. *Biochem Soc Trans*. 37:1002–1006.

Slep, K.C., S.L. Rogers, S.L. Elliott, H. Ohkura, P.A. Kolodziej, and R.D. Vale. 2005. Structural determinants for EB1-mediated recruitment of APC and spectraplakins to the microtubule plus end. *J Cell Biol*. 168:587–598.

Slep, K.C., and R.D. Vale. 2007. Structural Basis of Microtubule Plus End Tracking by XMAP215, CLIP-170, and EB1. *Mol Cell*. 27:976–991.

Small, J.V., and I. Kaverina. 2003. Microtubules meet substrate adhesions to arrange cell polarity. *Curr Opin Cell Biol*. 15:40–47.

Sousa, A., R. Reis, P. Sampaio, and C.E. Sunkel. 2007. The Drosophila CLASP homologue, Mast/Orbit regulates the dynamic behaviour of interphase microtubules by promoting the pause state. *Cell Motil Cytoskeleton*. 64:605–620.

Spittle, C., S. Charrasse, C. Larroque, and L. Cassimeris. 2000. The interaction of TOGp with microtubules and tubulin. *J Biol Chem*. 275:20748–20753.

Srayko, M., S. Quintin, A. Schwager, and A.A. Hyman. 2003. Caenorhabditis elegans TAC-1 and ZYG-9 form a complex that is essential for long astral and spindle microtubules. *Curr Biol*. 13:1506–1511.

Steinmetz, M.O., and A. Akhmanova. 2008. Capturing protein tails by CAP-Gly domains. *Trends Biochem Sci*. 33:535–545.

Stone, M.C., F. Roegiers, and M.M. Rolls. 2008. Microtubules have opposite orientation in axons and dendrites of Drosophila neurons. *Mol Biol Cell*. 19:4122–4129.

Stramer, B. 2005. Live imaging of wound inflammation in Drosophila embryos reveals key roles for small GTPases during in vivo cell migration. *J Cell Biol*. 168:567–573.

Su, L.K., M. Burrell, D.E. Hill, J. Gyuris, R. Brent, R. Wiltshire, J. Trent, B. Vogelstein, and K.W. Kinzler. 1995. APC binds to the novel protein EB1 *Cancer Res* 55:2972–2977.

Subramanian, A., A. Prokop, M. Yamamoto, K. Sugimura, T. Uemura, J. Betschinger, J.A. Knoblich, and T. Volk. 2003. Shortstop recruits EB1/APC1 and promotes microtubule assembly at the muscle-tendon junction *Curr Biol*. 13:1086–1095.

Subramanian, R., E.M. Wilson-Kubalek, C.P. Arthur, M.J. Bick, E.A. Campbell, S.A. Darst, R.A. Milligan, and T.M. Kapoor. 2010. Insights into antiparallel microtubule crosslinking by PRC1, a conserved nonmotor microtubule binding protein. *Cell*. 142:433–443.

Tanaka, K., N. Mukae, H. Dewar, M. van Breugel, E.K. James, A.R. Prescott, C. Antony, and T.U. Tanaka. 2005. Molecular mechanisms of kinetochore capture by spindle microtubules *Nature*. 434:987–994.

Tran, P.T., R.A. Walker, and E.D. Salmon. 1997. A metastable intermediate state of microtubule dynamic instability that differs significantly between plus and minus ends. *J Cell Biol*. 138:105–117.

Ui, K., R. Ueda, and T. Miyake. 1987. Cell lines from imaginal discs of Drosophila melanogaster. *In Vitro Cell Dev Biol*. 23:707–711.

Vale, R.D., and R.J. Fletterick. 1997. The design plan of kinesin motors *Annu Rev Cell Dev Biol*. 13:745–777.

van Breugel, M., D. Drechsel, and A. Hyman. 2003. Stu2p, the budding yeast member of the conserved Dis1/XMAP215 family of microtubule-associated proteins is a plus end-binding microtubule destabilizer. *J Cell Biol*. 161:359–369.

van der Vaart, B., A. Akhmanova, and A. Straube. 2009. Regulation of microtubule dynamic instability. *Biochem Soc Trans*. 37:1007–1013.

Varga, V., J. Helenius, K. Tanaka, A.A. Hyman, T.U. Tanaka, and J. Howard. 2006. Yeast kinesin-8 depolymerizes microtubules in a length-dependent manner *Nat Cell Biol*. 8:957–962.

Vasquez, R.J., D.L. Gard, and L. Cassimeris. 1994. XMAP from Xenopus eggs promotes rapid plus end assembly of microtubules and rapid microtubule polymer turnover. *J Cell Biol*. 127:985–993.

Vaughan, K.T. 2005. TIP maker and TIP marker; EB1 as a master controller of microtubule plus ends. *J Cell Biol*. 171:197–200.

Verhey, K.J., and J. Gaertig. 2007. The tubulin code *Cell Cycle*. 6:2152–2160.

Vitorino, P., and T. Meyer. 2008. Modular control of endothelial sheet migration. *Genes Dev*. 22:3268–3281.

Vitre, B., F.M. Coquelle, C. Heichette, C. Garnier, D. Chrétien, and I. Arnal. 2008. EB1 regulates microtubule dynamics and tubulin sheet closure in vitro. *Nat Cell Biol*. 10:415–421.

Wagner, E.J., B.D. Burch, A.C. Godfrey, H.R. Salzler, R.J. Duronio, and W.F. Marzluff. 2007. A genome-wide RNA interference screen reveals that variant histones are necessary for replication-dependent histone pre-mRNA processing *Mol Cell*. 28:692–699.

Wang, P.J., and T.C. Huffaker. 1997. Stu2p: A microtubule-binding protein that is an essential component of the yeast spindle pole body. *J Cell Biol*. 139:1271–1280.

Waterman-Storer, C.M., and E.D. Salmon. 1997. Actomyosin-based retrograde flow of microtubules in the lamella of migrating epithelial cells influences microtubule dynamic instability and turnover and is associated with microtubule breakage and treadmilling. *J Cell Biol*. 139:417–434.

Wei, R.R., J. Al-Bassam, and S.C. Harrison. 2007. The Ndc80/HEC1 complex is a contact point for kinetochore-microtubule attachment *Nat Struct Mol Biol*. 14:54–59.

Weisenberg, R.C., W.J. Deery, and P.J. Dickinson. 1976. Tubulin-nucleotide interactions during the polymerization and depolymerization of microtubules *Biochemistry*. 15:4248–4254.

Wheeler, S.R., S. Banerjee, K. Blauth, S.L. Rogers, M.A. Bhat, and S.T. Crews. 2009. Neurexin IV and Wrapper interactions mediate Drosophila midline glial migration and axonal ensheathment *Development*. 136:1147–1157.

Whittington, A.T., O. Vugrek, K.J. Wei, N.G. Hasenbein, K. Sugimoto, M.C. Rashbrooke, and G.O. Wasteneys. 2001. MOR1 is essential for organizing cortical microtubules in plants. *Nature*. 411:610–613.

Wittmann, T. 2008. EBs clip CLIPs to growing microtubule ends. *J Cell Biol*. 183:1183–1185.

Wittmann, T., G.M. Bokoch, and C.M. Waterman-Storer. 2003. Regulation of leading edge microtubule and actin dynamics downstream of Rac1 *J Cell Biol*. 161:845–851.

Wittmann, T., G.M. Bokoch, and C.M. Waterman-Storer. 2004. Regulation of microtubule destabilizing activity of Op18/stathmin downstream of Rac1. *J Biol Chem*. 279:6196–6203.

Wittmann, T., and C.M. Waterman-Storer. 2005. Spatial regulation of CLASP affinity for microtubules by Rac1 and GSK3beta in migrating epithelial cells. *J Cell Biol*. 169:929–939.

Wolyniak, M.J., K. Blake-Hodek, K. Kosco, E. Hwang, L. You, and T.C. Huffaker. 2006. The regulation of microtubule dynamics in Saccharomyces cerevisiae by three interacting plus-end tracking proteins. *Mol Biol Cell*. 17:2789–2798.

Wood, W., C. Faria, and A. Jacinto. 2006. Distinct mechanisms regulate hemocyte chemotaxis during development and wound healing in Drosophila melanogaster. *J Cell Biol*. 173:405–416.

Wood, W., and A. Jacinto. 2007. Drosophila melanogaster embryonic haemocytes: masters of multitasking. *Nat Rev Mol Cell Biol*. 8:542–551.

Wu, X., A. Kodama, and E. Fuchs. 2008. ACF7 regulates cytoskeletal-focal adhesion dynamics and migration and has ATPase activity *Cell*. 135:137–148.

Yanagawa, S., J.S. Lee, and A. Ishimoto. 1998. Identification and characterization of a novel line of Drosophila Schneider S2 cells that respond to wingless signaling. *J Biol Chem*. 273:32353–32359.

Yarrow, J.C., Z.E. Perlman, N.J. Westwood, and T.J. Mitchison. 2004. A high-throughput cell migration assay using scratch wound healing, a comparison of image-based readout methods. *BMC Biotechnol*. 4:21.

Yin, H., L. You, D. Pasqualone, K.M. Kopski, and T.C. Huffaker. 2002. Stu1p is physically associated with beta-tubulin and is required for structural integrity of the mitotic spindle *Mol Biol Cell*. 13:1881–1892.

Zhang, D., K.D. Grode, S.F. Stewman, J.D. Diaz-Valencia, E. Liebling, U. Rath, T. Riera, J.D. Currie, D.W. Buster, A.B. Asenjo, H.J. Sosa, J.L. Ross, A. Ma, S.L. Rogers, and D.J. Sharp. 2011. Drosophila katanin is a microtubule depolymerase that regulates cortical-microtubule plus-end interactions and cell migration *Nat Cell Biol*.

Zovko, S., J.P. Abrahams, A.J. Koster, N. Galjart, and A.M. Mommaas. 2008. Microtubule plus-end conformations and dynamics in the periphery of interphase mouse fibroblasts *Mol Biol Cell*. 19:3138–3146.